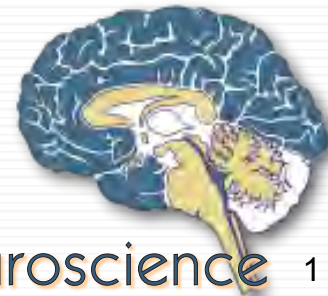


Concurrent Multimodal Imaging

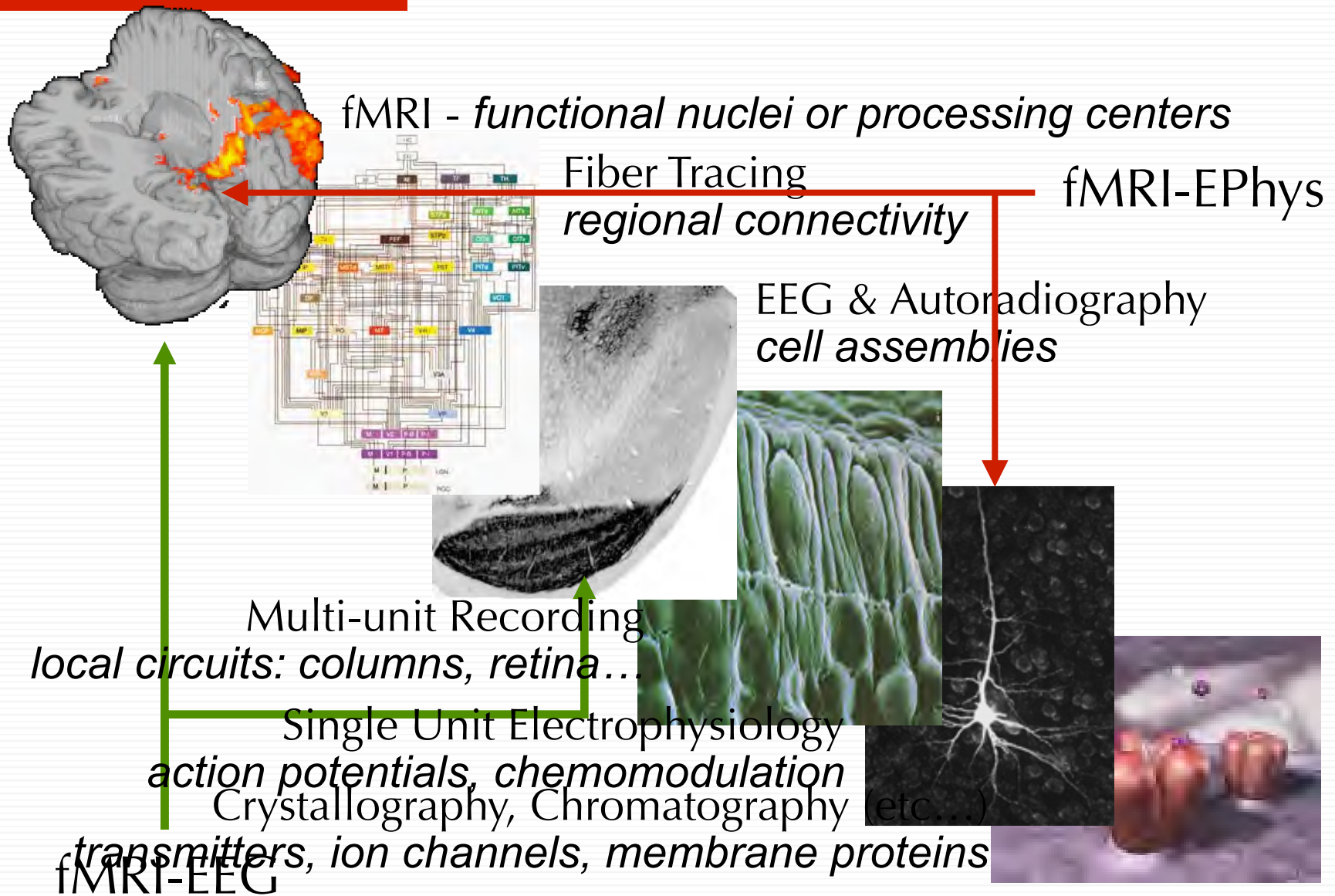


Issues in Multimodal Imaging

- Why Bother? What can we hope to gain?
- General Issues for any multimodal experiment
 - Safety
 - Mutual Interference
 - Signal dependence or independence
 - Joint Analysis
- Some Results
 - PET-MRI
 - PET-CT
 - EEG-PET
 - Optical and E-Phys
 - MRI-EEG
 - MRI and Single Units
 - MRI and Spectroscopy
 - ...

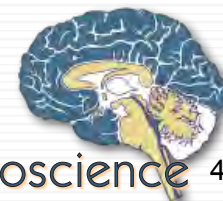


Levels of Understanding



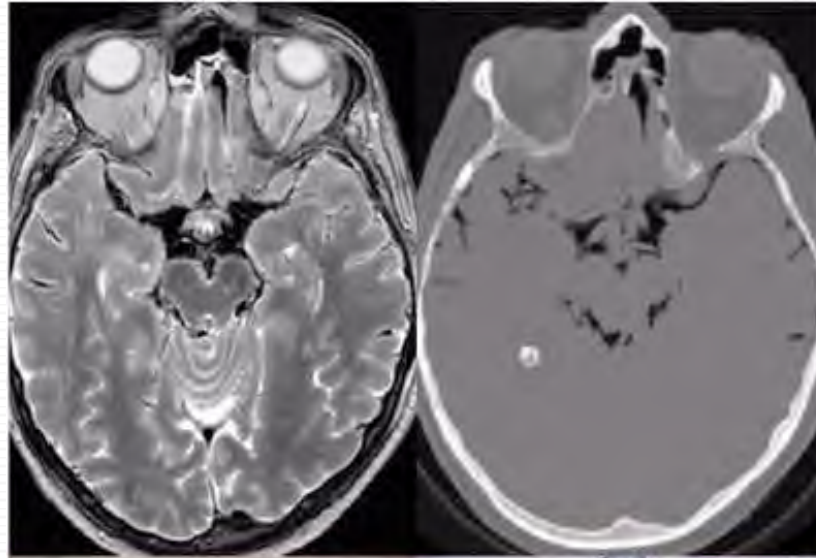
What is to be Gained?

- Many Experiments Can be Performed Separately!
 - *E.g.*, Sensory Processing is more or less time-invariant
- Reduced Study Time
- Spatiotemporal Resolution Sharing
- Registration
 - Shape distortions, poor alignment boundaries, soft tissues
- Transient or Uncontrolled Events
 - Interictal spikes, Response Errors
- Better Detection Power

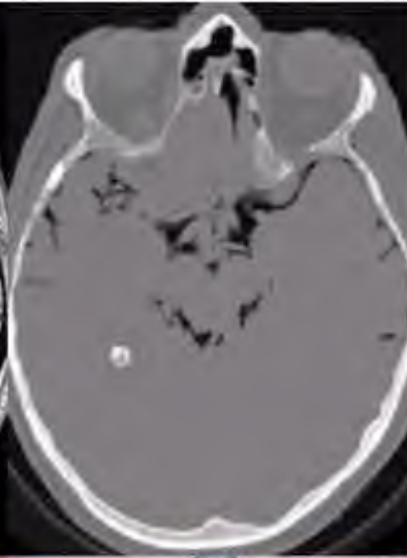


Visible Human

MRI



CT



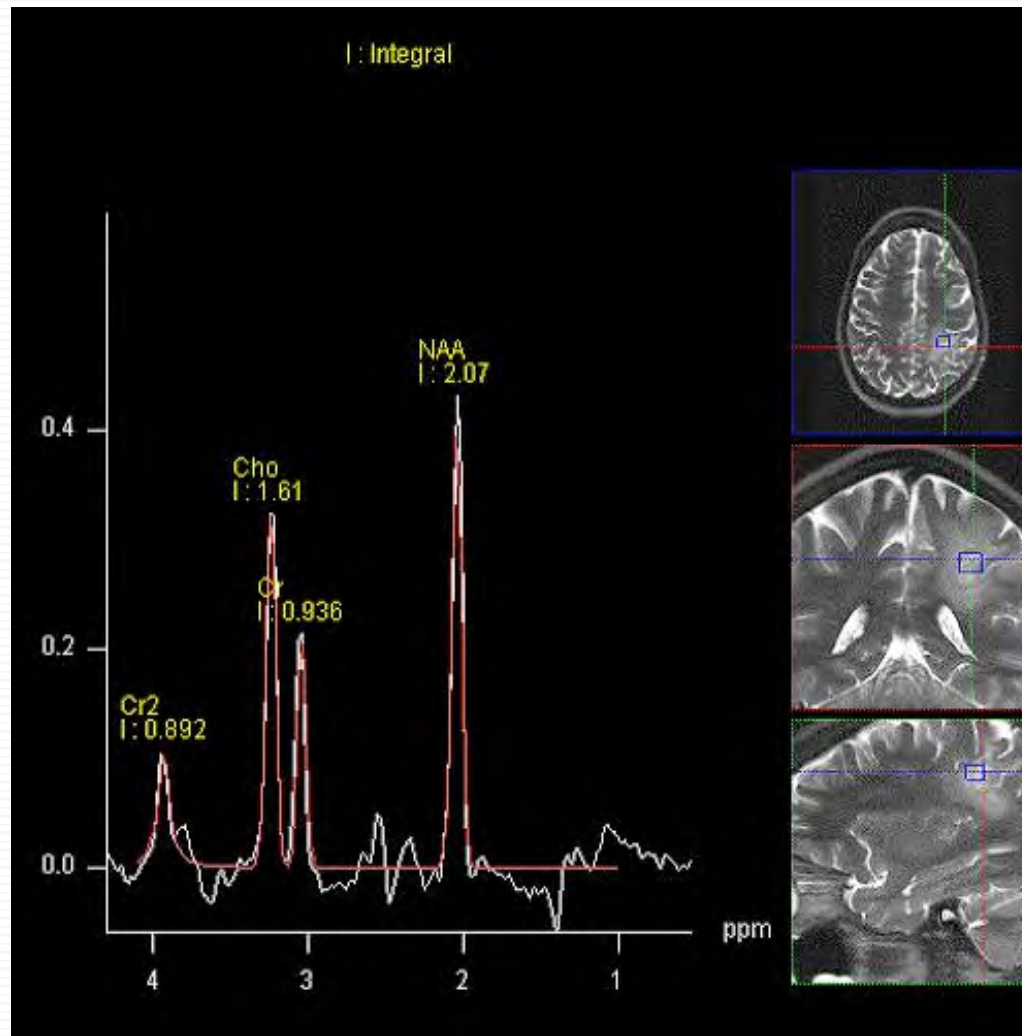
Photograph



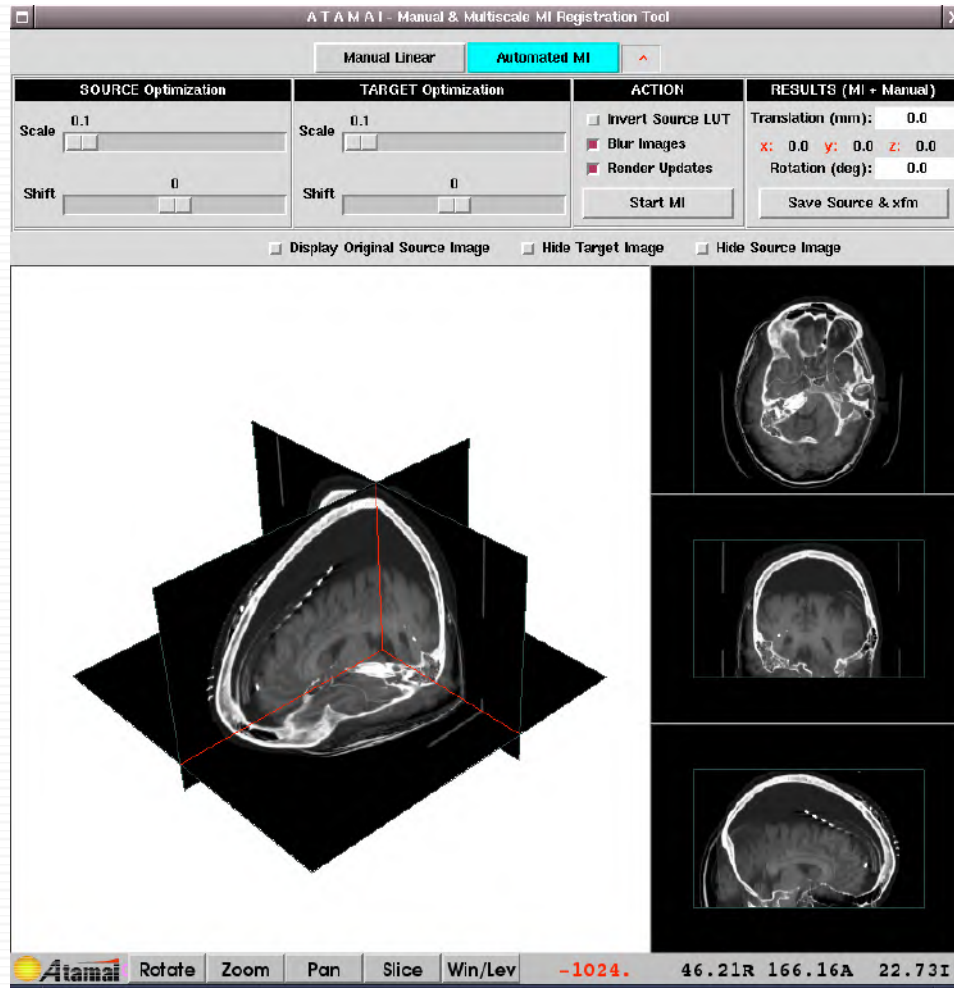
Stained Slice



MR Spectroscopy



Intermodality Registration



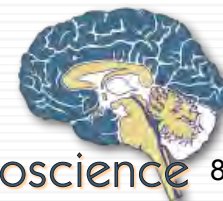
Automated
Image
Registration



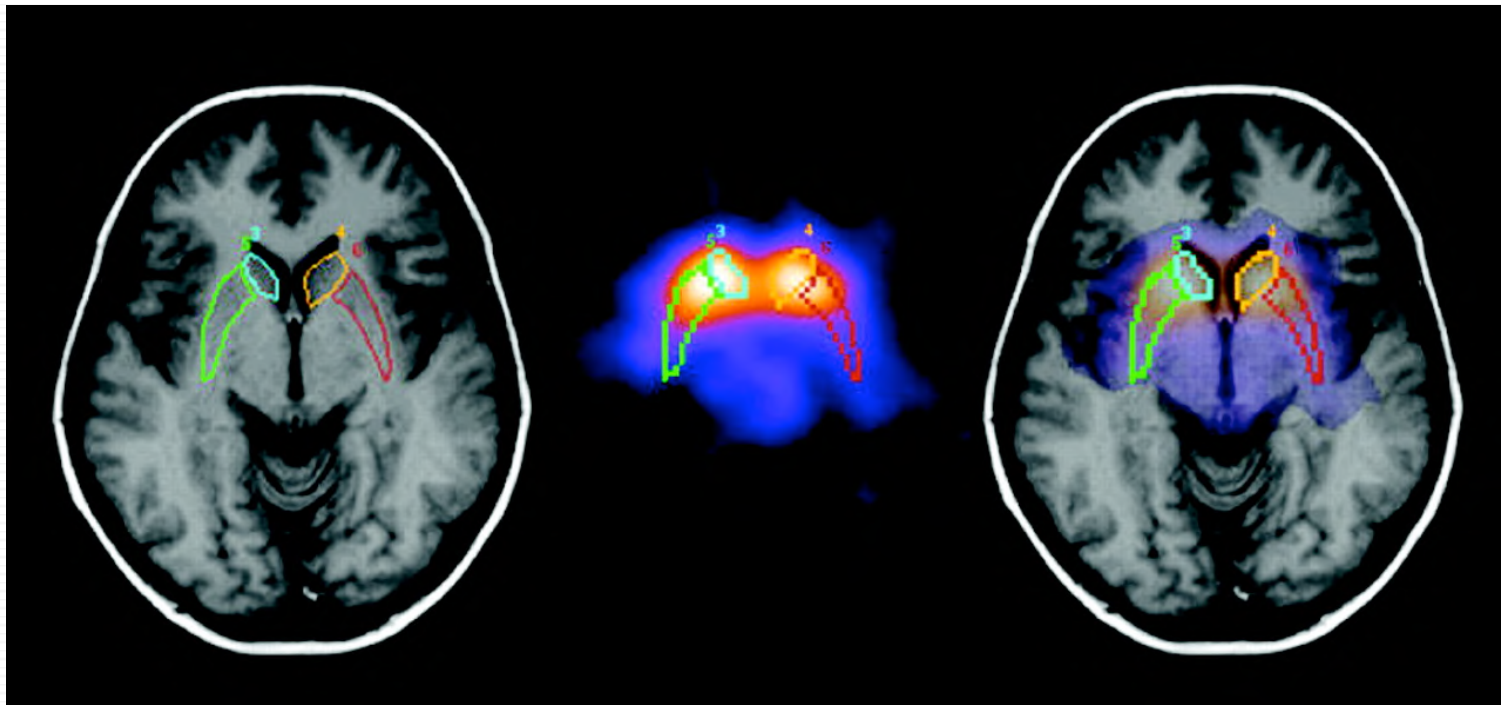
Shape Distortions



Recovery of Change in Brain Tissue due to Post Mortem Effects and Histologic Processing. Warping algorithms based on continuum-mechanical models can recover and compensate for patterns of tissue change which occur in post mortem histologic experiments. A brain section (left), gridded to produce tissue elements for biochemical assays, is reconfigured (middle) into its original position in the cryosection blockface (Mega *et al.*, 1997; algorithm from Thompson and Toga, 1996, 1998). The complexity of the required deformation vector field in a small tissue region (magnified vector map, right) demonstrates that very flexible, high-dimensional transformations are essential (Thompson and Toga, 1996; Schormann *et al.*, 1996). As well as measuring local patterns of mechanical tissue deformations, recovery of deformation fields allows projection of histologic and biochemical data back into the volumetric reference space of the cryosection image. In some cases, these data can also be projected, using additional warping algorithms, onto in vivo MRI and co-registered PET data from the same subject for digital correlation and analysis (Mega *et al.*, 1997).



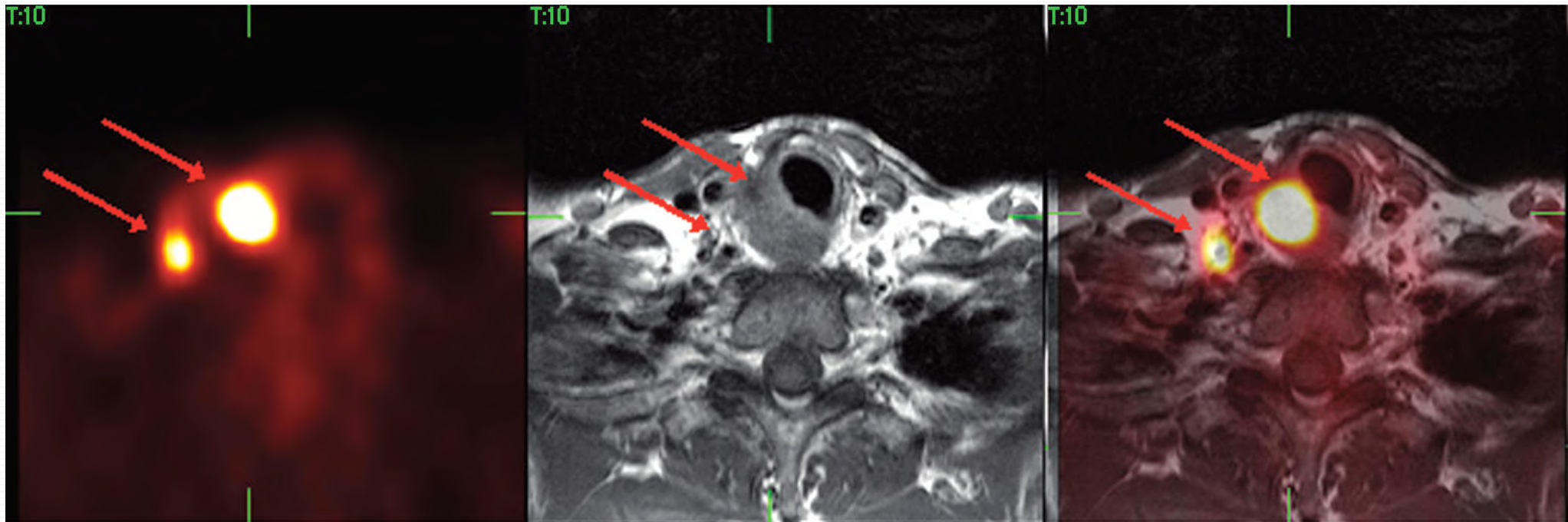
SPECT MRI by Image Fusion



Fusion of ^{123}I - β -carbomethoxyiodophenyl tropane
SPECT neuroreceptor images with MRI



PET MRI by Fusion



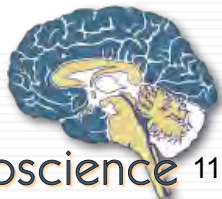
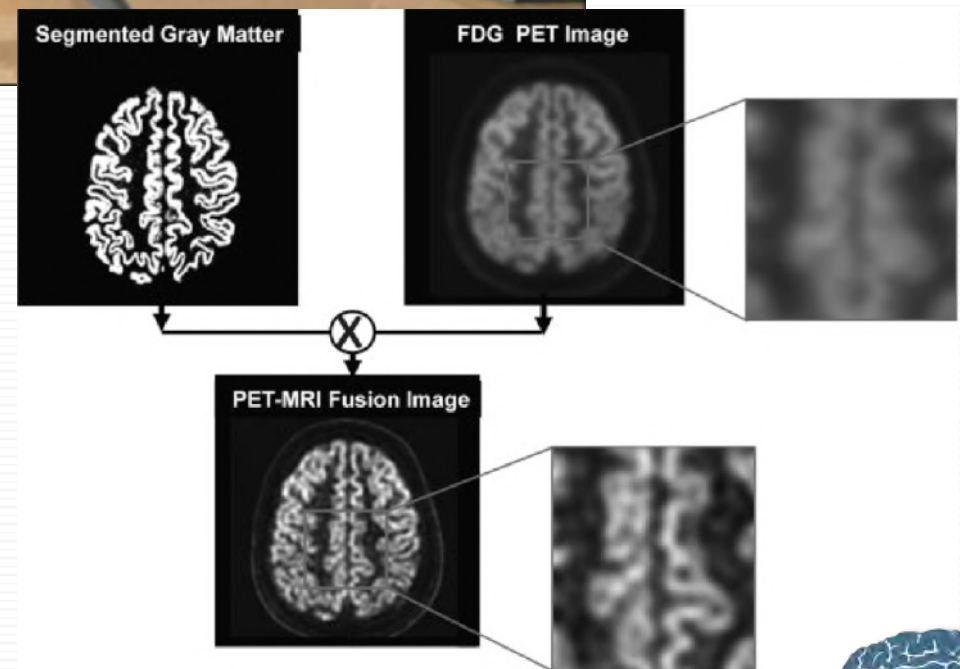
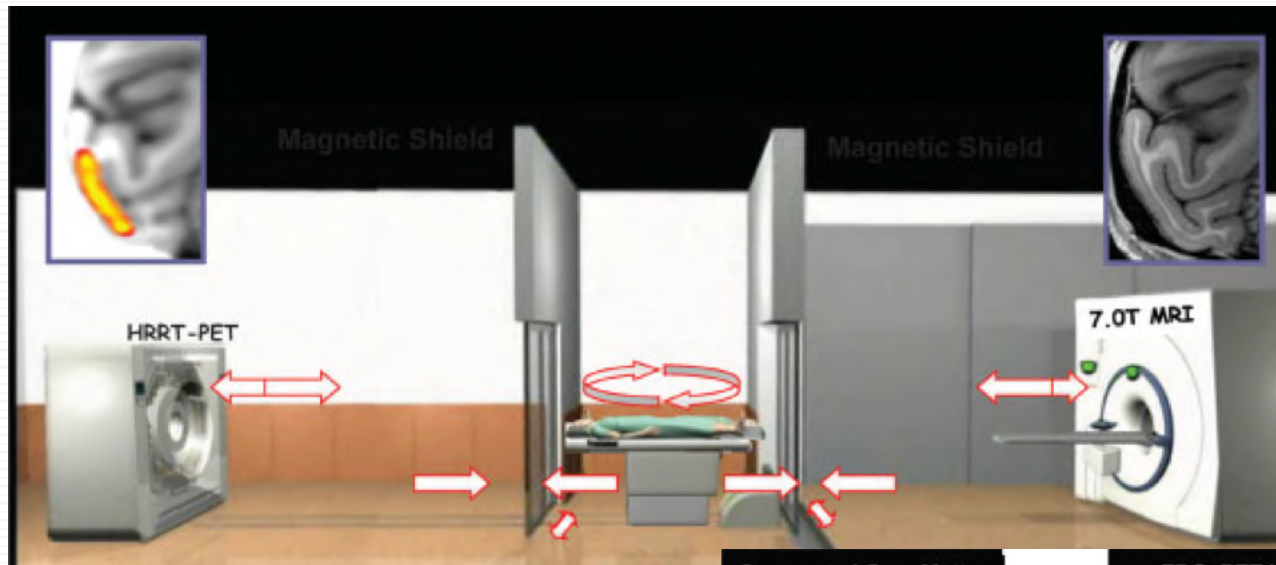
THYROID
Volume 18, Number 2, 2008

Utility of PET/Neck MRI Digital Fusion Images in the Management of Recurrent or Persistent Thyroid Cancer

Laura Seiboth,¹ Douglas Van Nostrand,² Leonard Wartofsky,¹ Yasser Ousman,¹ Jacqueline Jonklaas,³ Calvin Butler,² Frank Atkins,² and Kenneth Burman¹



PET MRI by Fusion

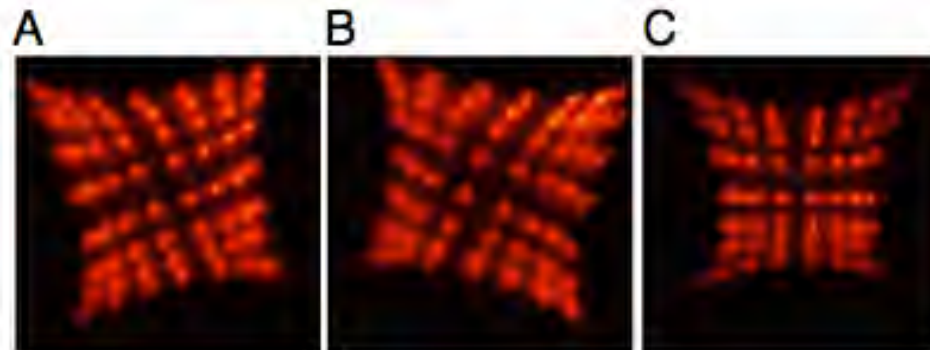


PET-MRI

PNAS

Simultaneous PET and magnetic resonance imaging

Ciprian Catana^{*†}, David J. D. O'Leary[‡], and Simon R. Cherry[‡]



omography

Chler[§], Russell E. Jacobs[‡],

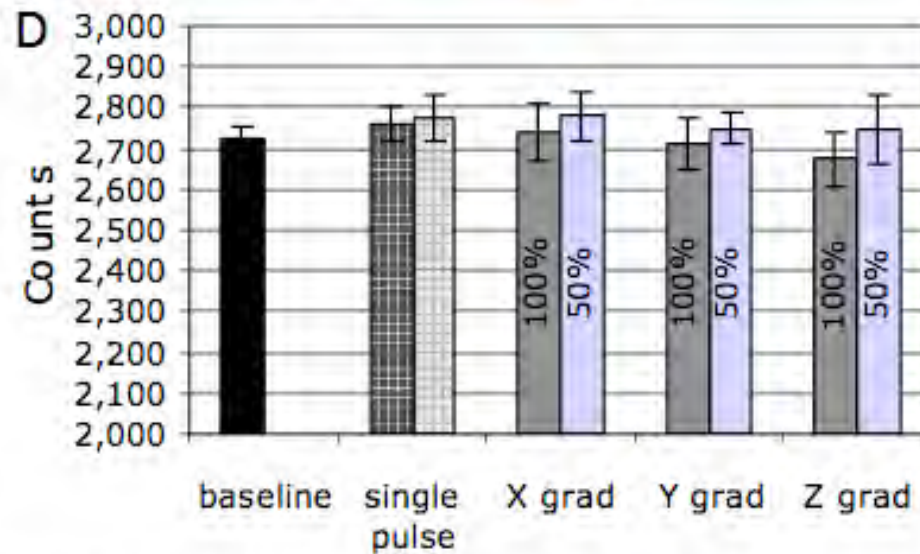
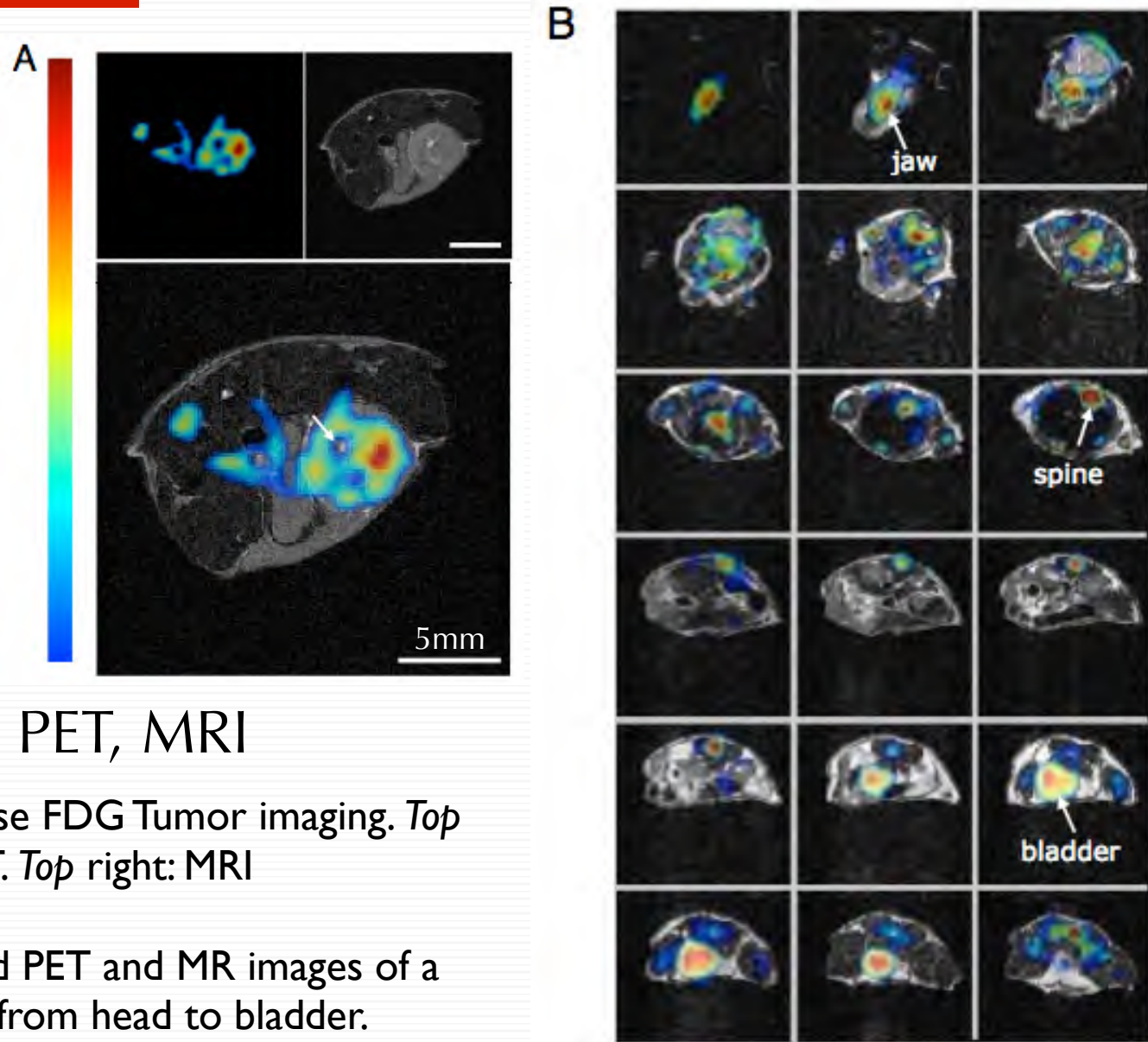


Fig. 1. MR scanner effect on PET system. (A–C) Detector histograms showing the anticlockwise (A) and clockwise (B) rotations of the crystal maps when compared with the data acquired outside of the magnet (C). (D) PET event rate measured under different conditions: (i) while applying only RF power (with 1,000 ms and 500 ms repetition times) and (ii) while switching the x-z gradients independently (at 100% and 50% power; 400 and 200 mT/m, respectively). Baseline represents the event rate recorded without running MR sequences.



PET MRI Results



Simultaneous PET, MRI

A. Mouse FDG Tumor imaging. *Top left: PET. Top right: MRI*

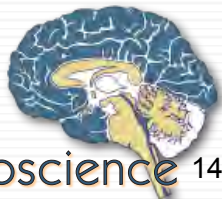
B. Fused PET and MR images of a mouse from head to bladder.



Projectiles



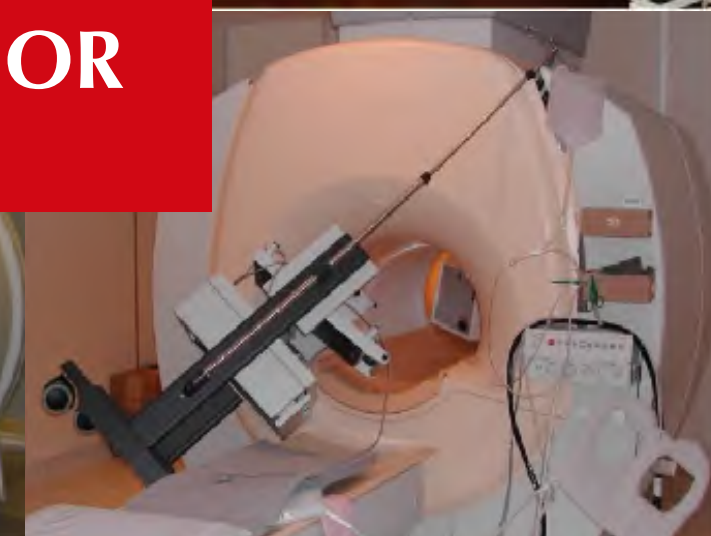
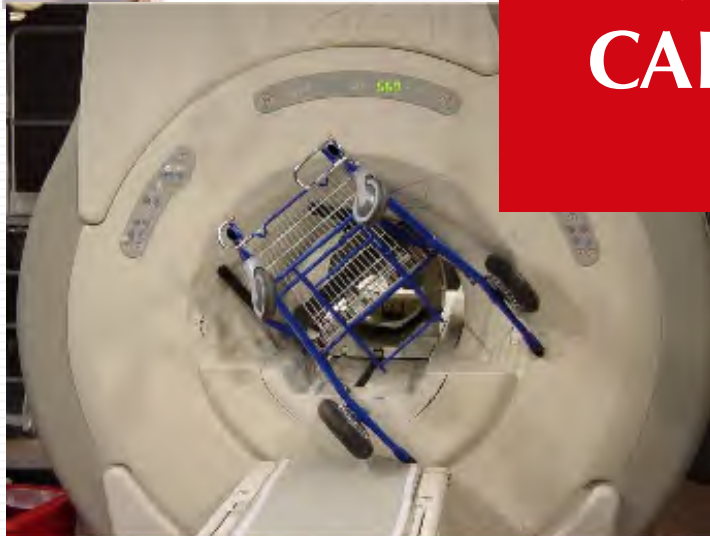
www.SimplyPhysics.com



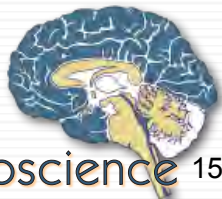
Projectiles



**NEVER TRY TO REMOVE
OBJECTS ON YOUR OWN.
CALL SERVICE or SENIOR
CCN PERSONNEL.**



wwwSimplyPhysics.com



Before you start



Projectiles account for
10% of reported safety
incidents.

10% are from
Implanted Devices

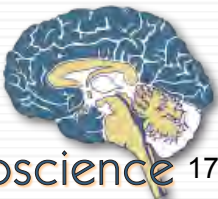
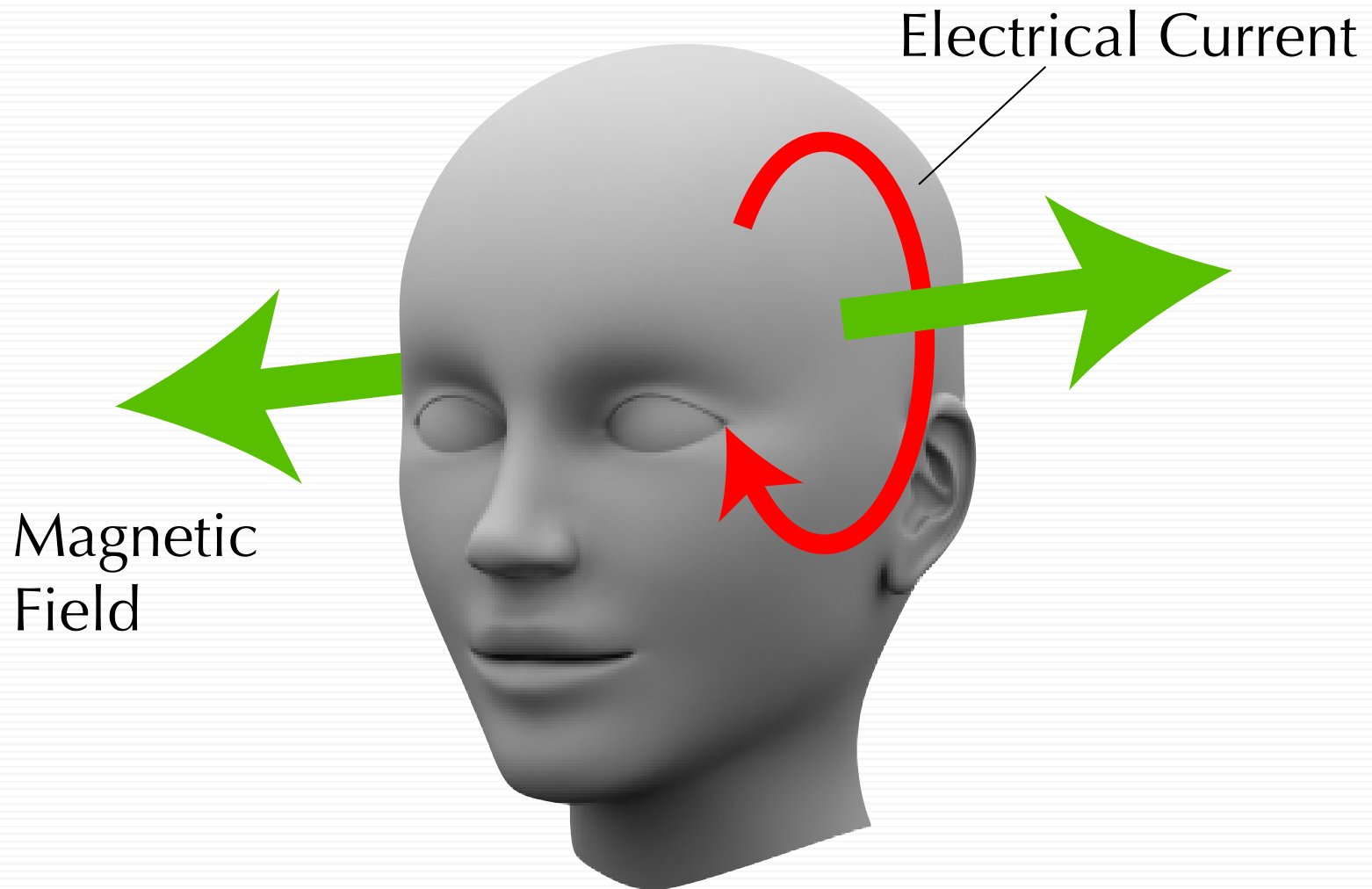
71% are burns!



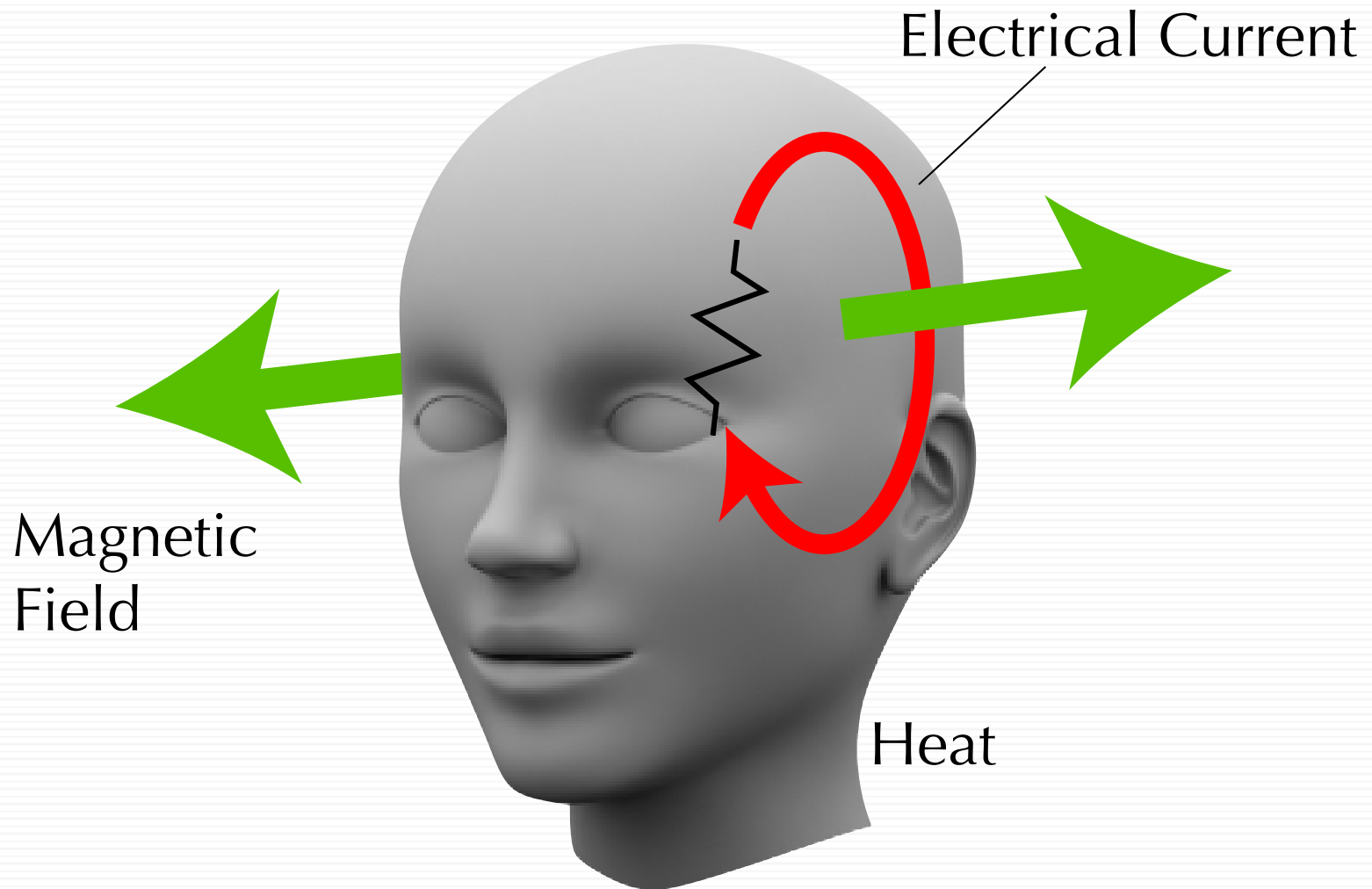
M Mitka, "Safety improvements urged for
MRI facilities." JAMA, 294: 2145. 2005



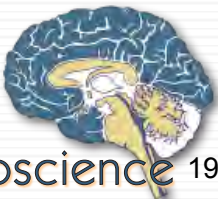
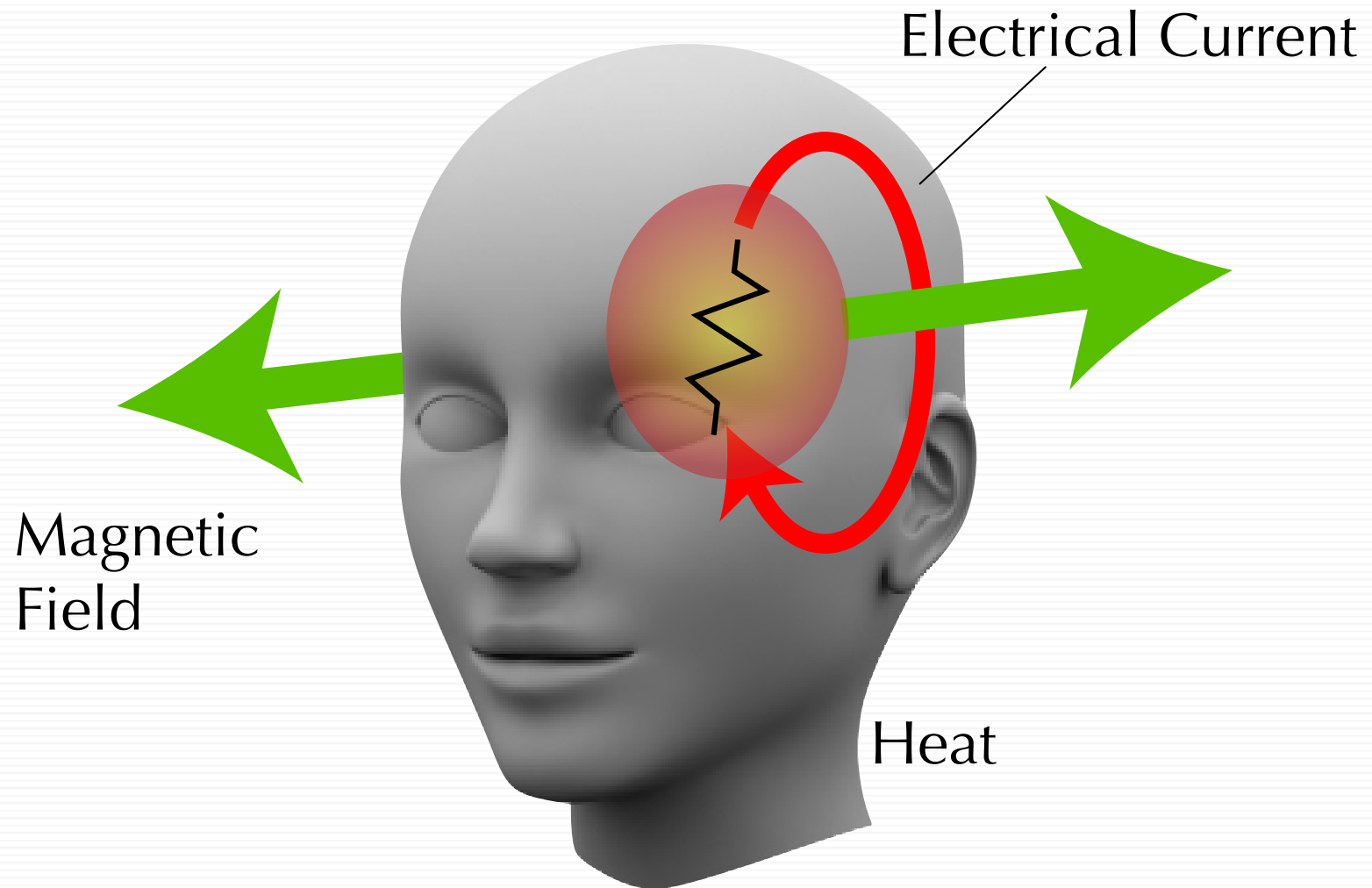
Induced Currents in the Body



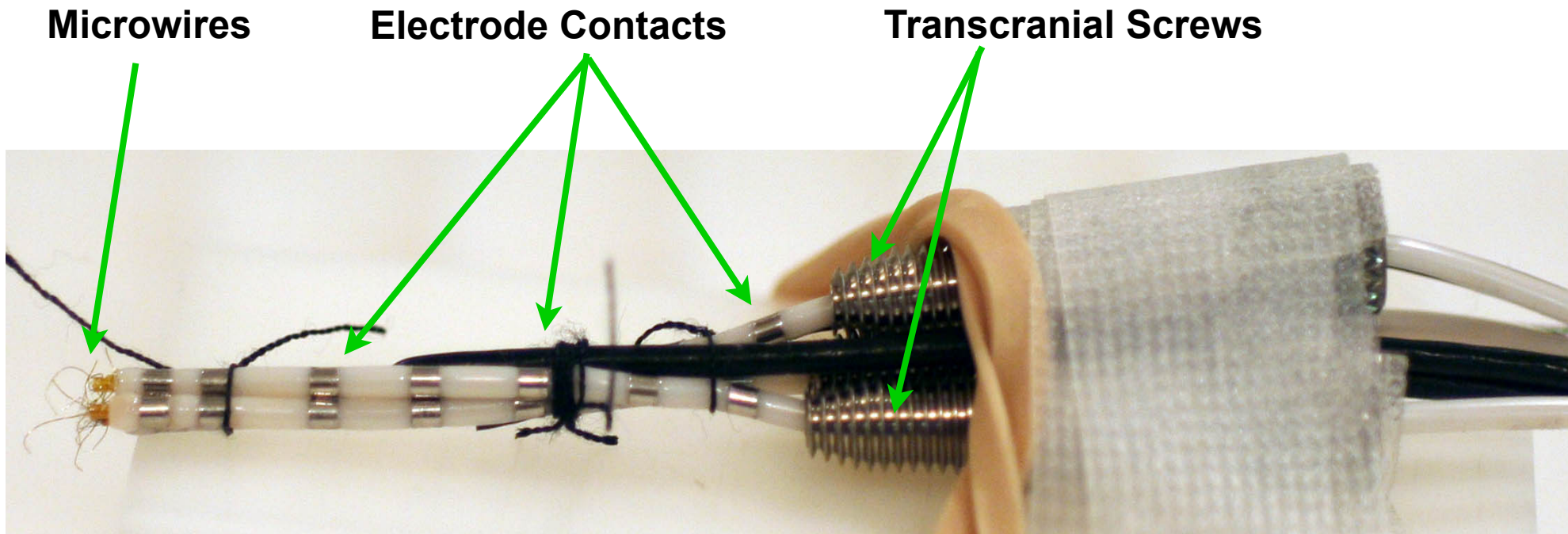
Specific Absorption Rate



Specific Absorption Rate



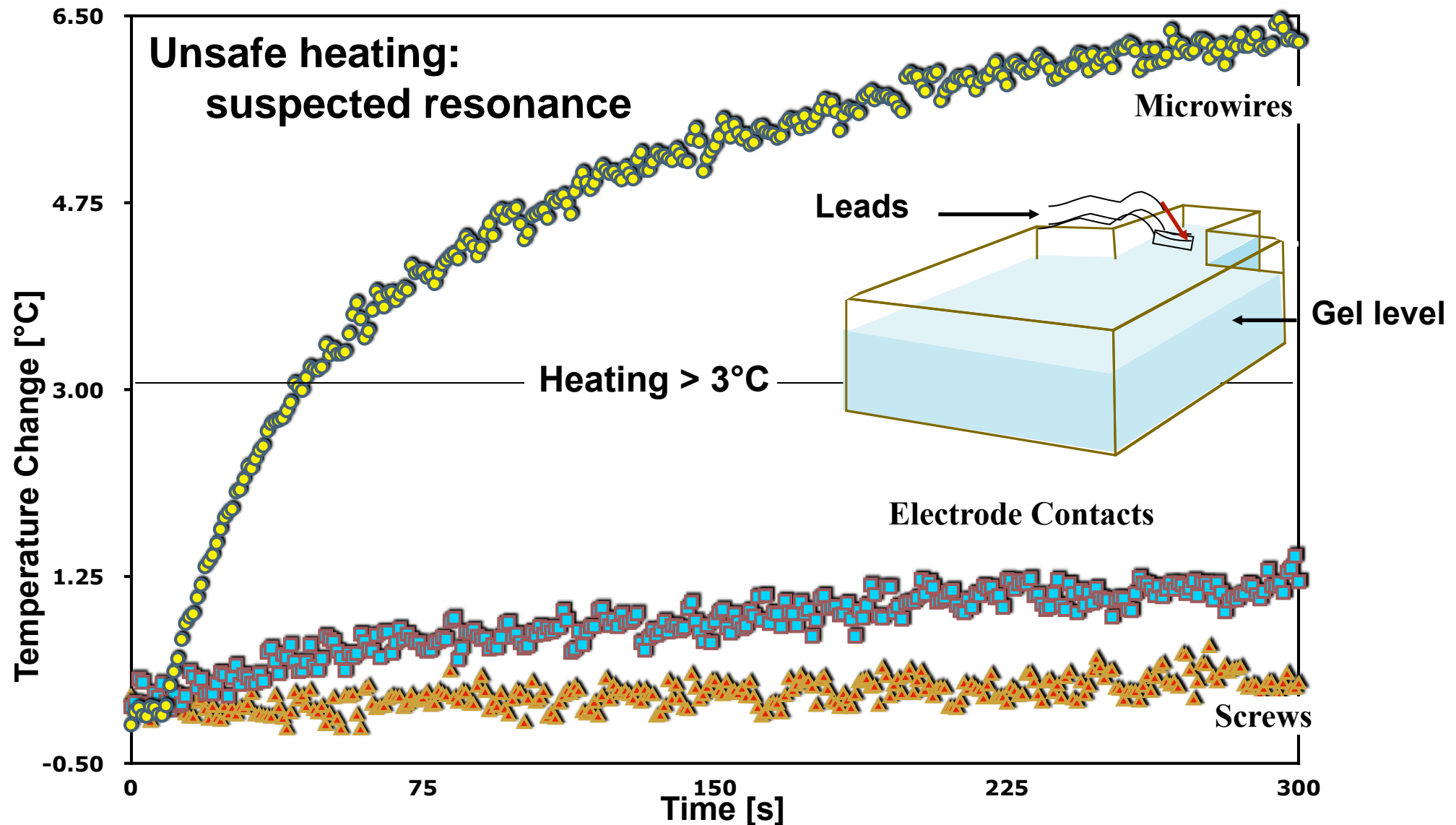
Heating - Experimental Set-up



- **In-vitro study: Semi-solid gel, head and torso phantom**
- **Fluoroptic thermometry system: MRI compatible**
- **High specific absorption rate (SAR) = 3.0 Watts/Kg**

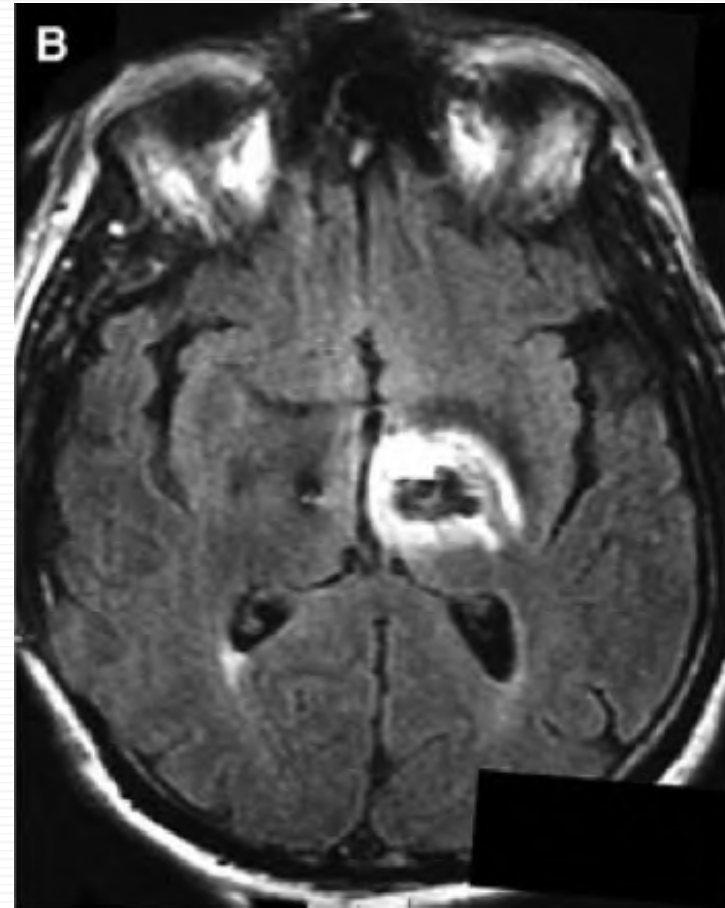
Strick, *et al.*, *Society for Neuroscience*, 2007

Safety Results

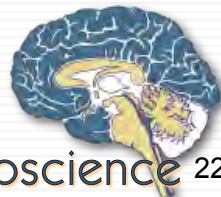


Strick, *et al.*, *Society for Neuroscience*, 2007

Deep Brain Stimulation (DBS) Electrodes



T2-weighted MRI scan of the brain showing edema around the left DBS electrode.



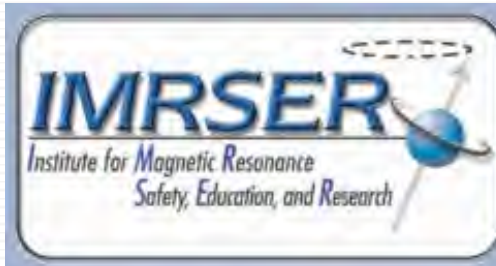
Safety Resources

<http://www.semel.ucla.edu/staglin>

YOUR INFORMATION RESOURCE
FOR MRI SAFETY, BIDEFFECTS,
AND PATIENT MANAGEMENT

MRIsafety.com

THE DEVELOPMENT OF THIS SITE
WAS SUPPORTED BY AN UNRESTRICTED
EDUCATIONAL GRANT PROVIDED BY



Institute for Magnetic Resonance
Safety, Education, and Research

http://users.fmrib.ox.ac.uk/~peterj/safety_docs/index.html



Blobs are not the whole story

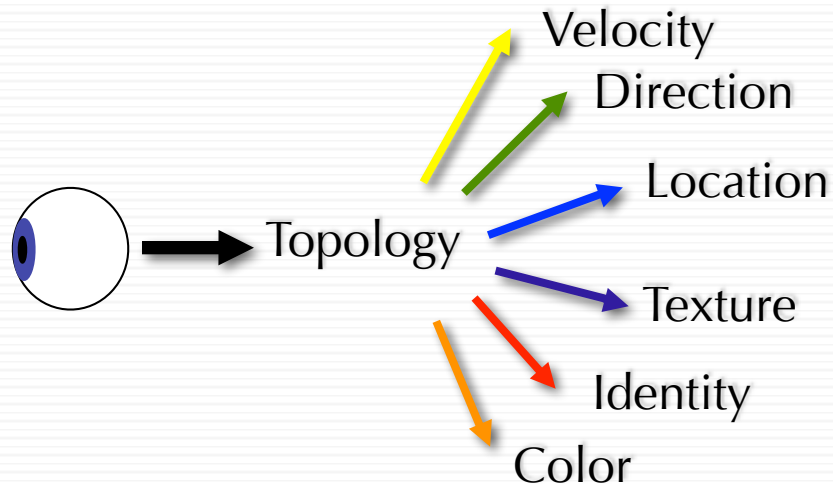


“...the classical concept of cerebral localization is of limited value, because of its static character and its failure to provide any answer to the question of how specialized parts of the cortex interact to produce the integration evident in thought or behavior. The problem here is one of the dynamic relations of the diverse parts of the cortex, whether they be cells or cortical fields.”

--Karl Lashley, 1931



Distinct Visual Pathways



A Simple Question:

If fMRI is so slow, why not record electrical signals to correct the fMRI timing?



Source Localization (Forward Model)

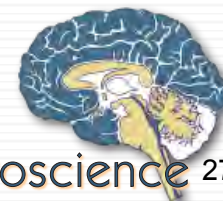
Signal at Sensor j Lead Field Oriented Magnitude

Location

$$\mathbf{x}_j(\mathbf{r}_i, \mathbf{q}_i, t) = \sum_{i=1}^K G(\mathbf{r}_i(t), \mathbf{p}_j) \cdot \mathbf{q}_i(t) + \varepsilon$$

Position of Sensor j

The Lead Field is interpreted as the signal detected by the given electrode from a Unit Dipole at the given location



Inverse Problem

Error model

$$\varepsilon(\mathbf{r}, \mathbf{q}) = \sum_i^K \sum_{t=t_1}^{t_2} \sum_j^M (\mathbf{x}_j(t) - \hat{\mathbf{x}}_j(\mathbf{r}_i, \mathbf{q}_i, t))^2 + \lambda f(\mathbf{r}, \mathbf{q})$$

$f(\mathbf{r}, \mathbf{q}) > 0$ is used to regularize the solution

$\lambda > 0$ trades fit against regularization



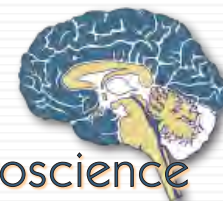
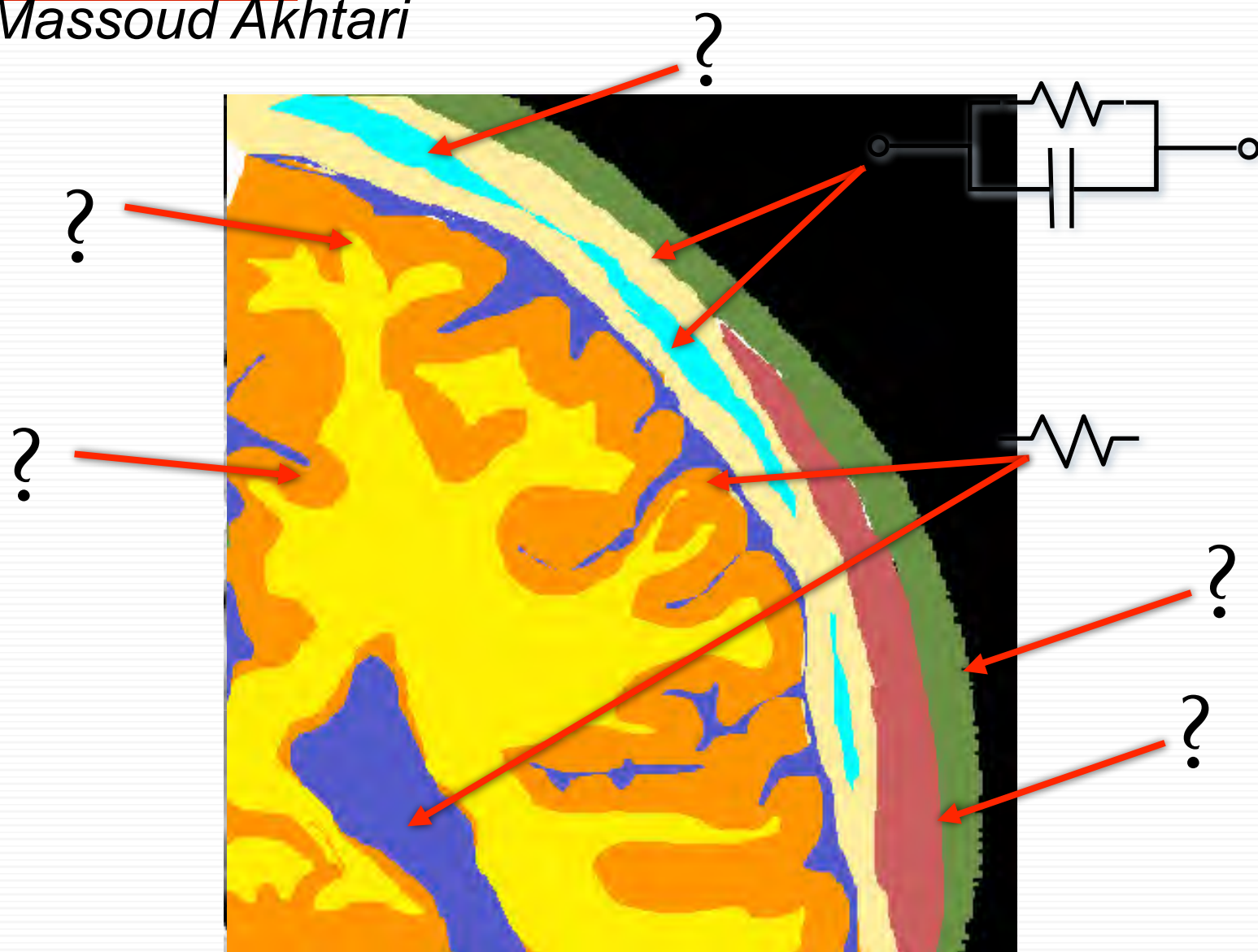
General Limitations in EEG Localization

- Deeper Sources Show Weaker Signals
 - Magnitude Depends on Dipole Orientation
 - Magnitude Depends on Temporal Synchrony
 - Magnitude Depends on Spatial Coherence
 - Conductivity of Body Tissues (CSF, scalp) Blur the Scalp Potentials
- Accuracy is Limited by Knowledge of Electrode Locations Relative to Brain Structures

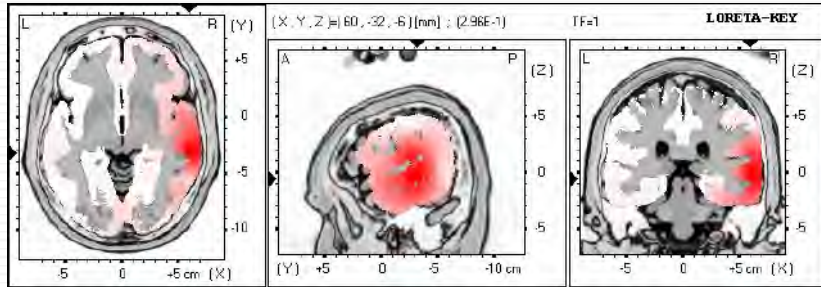


EEG Source Localization

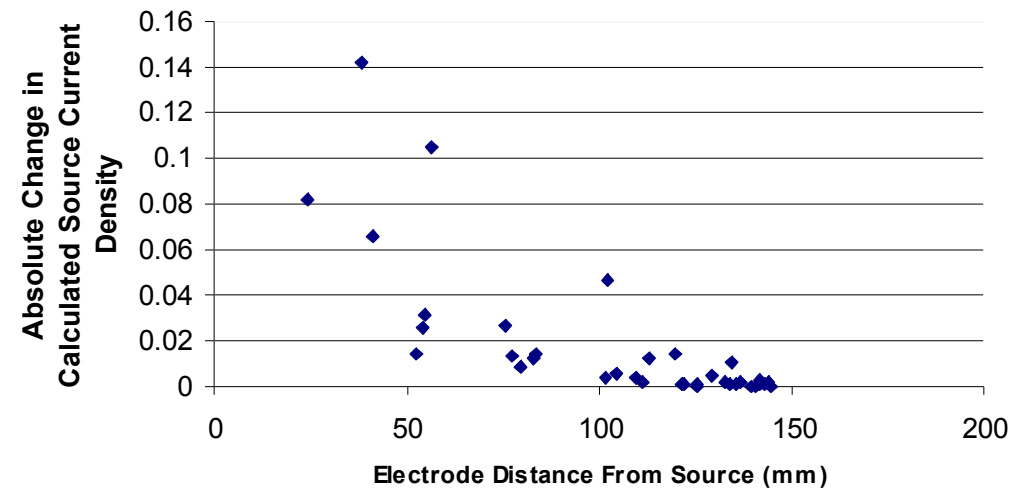
after Massoud Akhtari



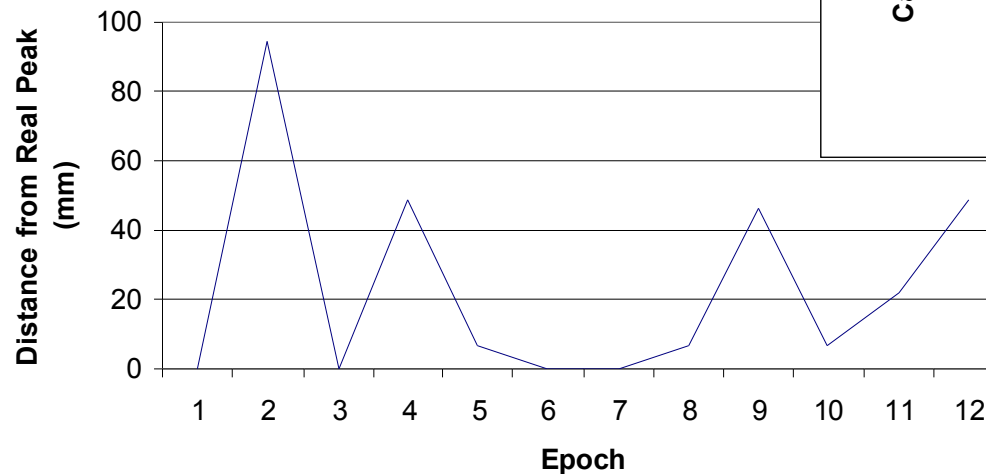
Source Localization Stability (LORETA)



Change in LORETA Calculation When Electrodes are Zeroed

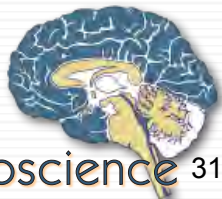


Localization of Peak in Noisy Data



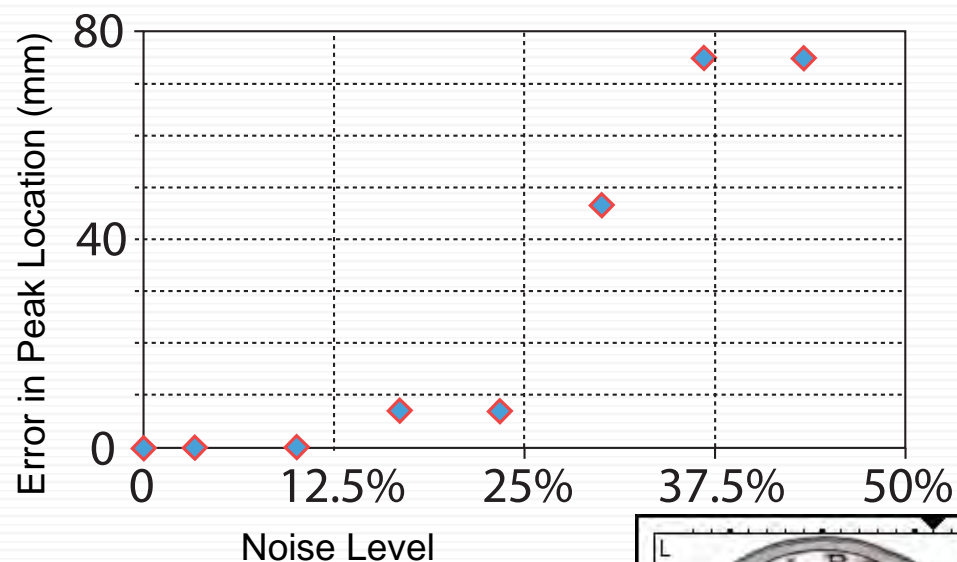
Nominal EEG Amplitude: 18

From Alex Korb (unpublished)

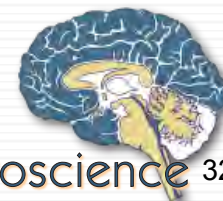
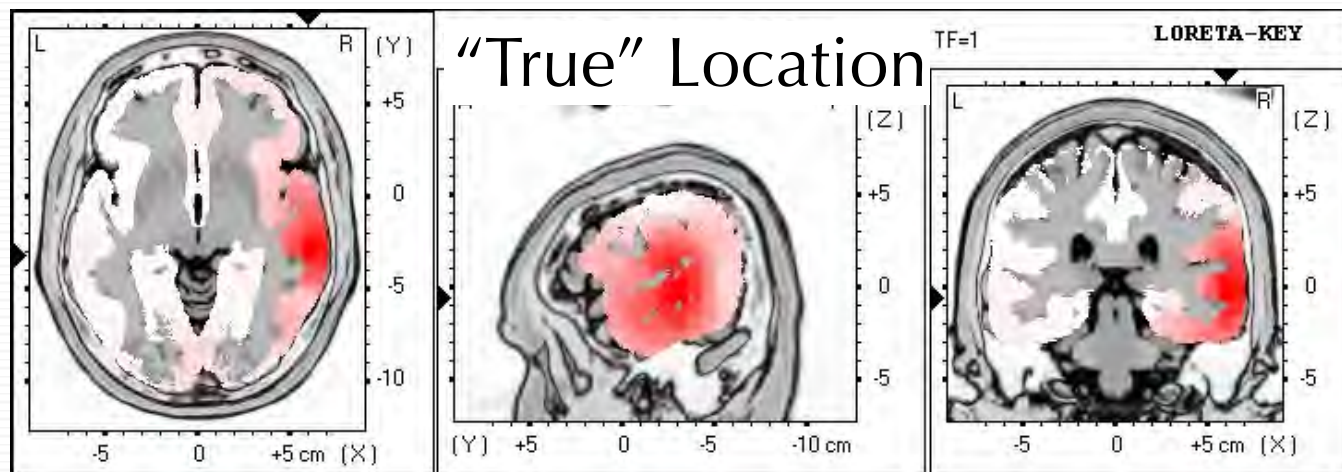


Source Localization Stability (LORETA)

Error in Localization as a function of noise



From Alex Korb (unpublished)



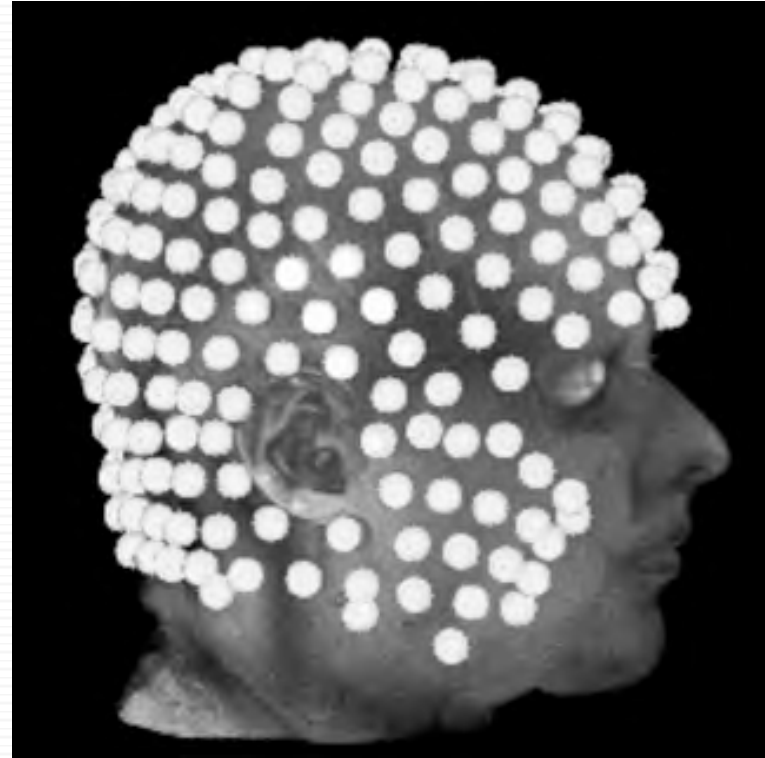
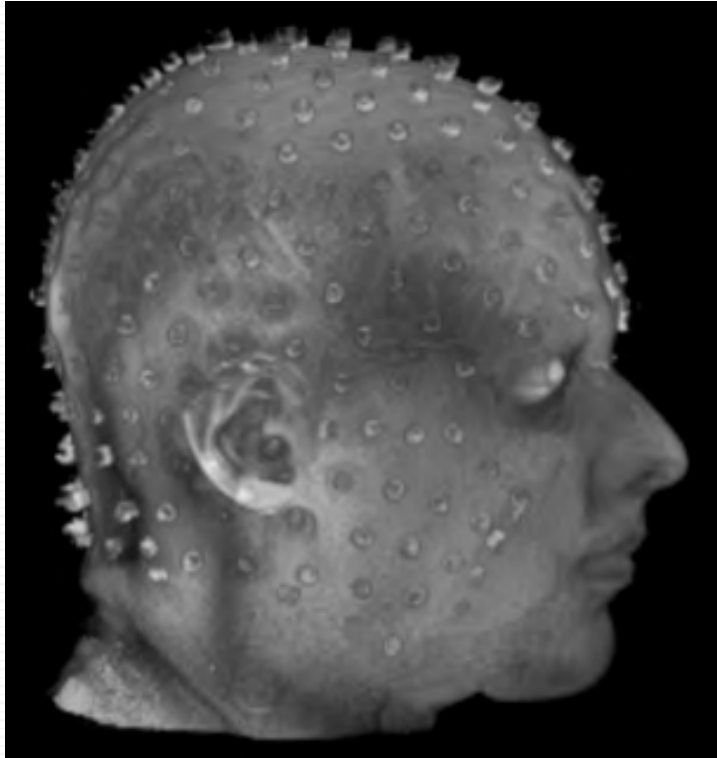
High Density EEG



Courtesy Electrical Geodesics, Inc.



Electrodes Can be Made Visible to MRI



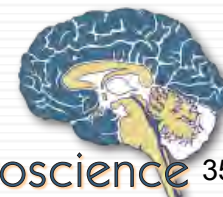
Cameron Rodriguez
Work in Progress



Combining EEG and MRI

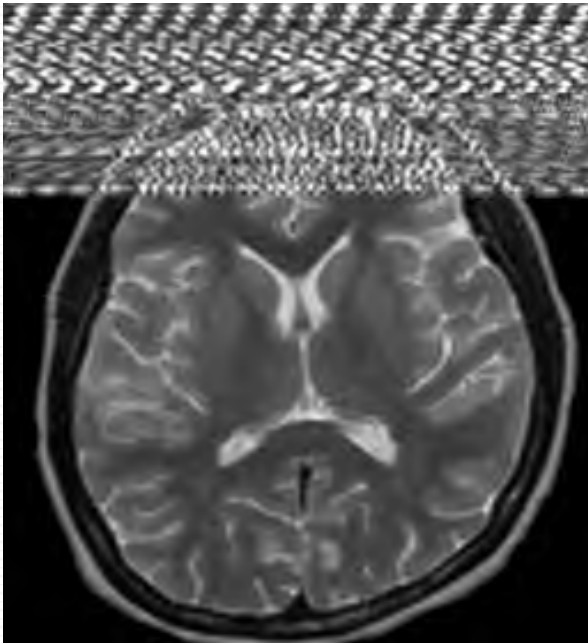
■ Project Goals

- ❑ Unaltered MR Image Quality
- ❑ Diagnostic Quality EEG During functional MRI:
- ❑ Artifact Free
- ❑ Dense Array of Channels
- ❑ Tomographic Correlation of Scalp Electrical Activity
- ❑ [Amplifiers Suitable for Single Units]
- ❑ Subject Safety

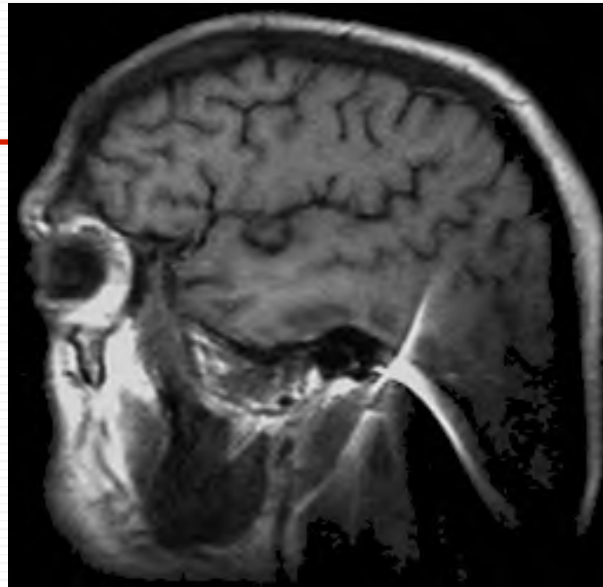


Artifacts - MRI

RF Noise

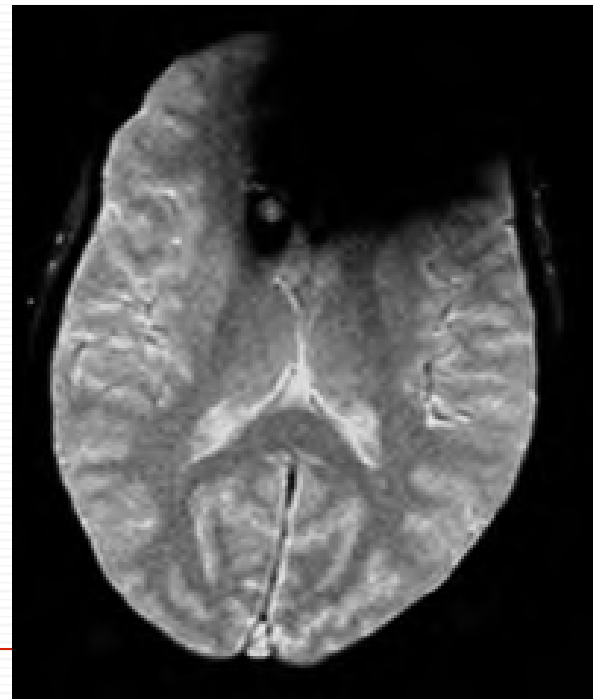


- *Properly-shielded Amplifiers*
- *Softened Logic Pulses*



Magnetic Field Distortion

Non-magnetic material such as Silver

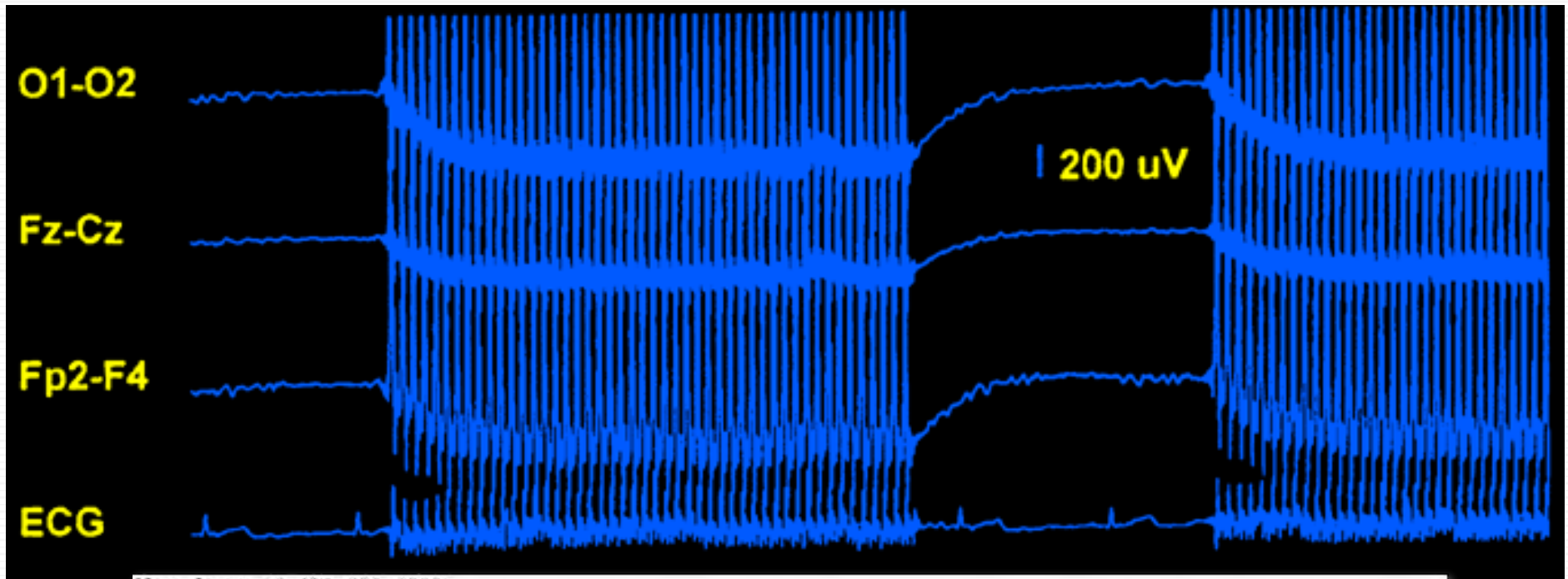


Signal Losses

- *Careful Lead Dress*
- *Eliminate RF Loops*



EEG Amplifier Recovery

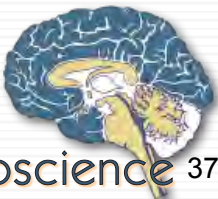


NeuroImage 12, 230–239 (2000)

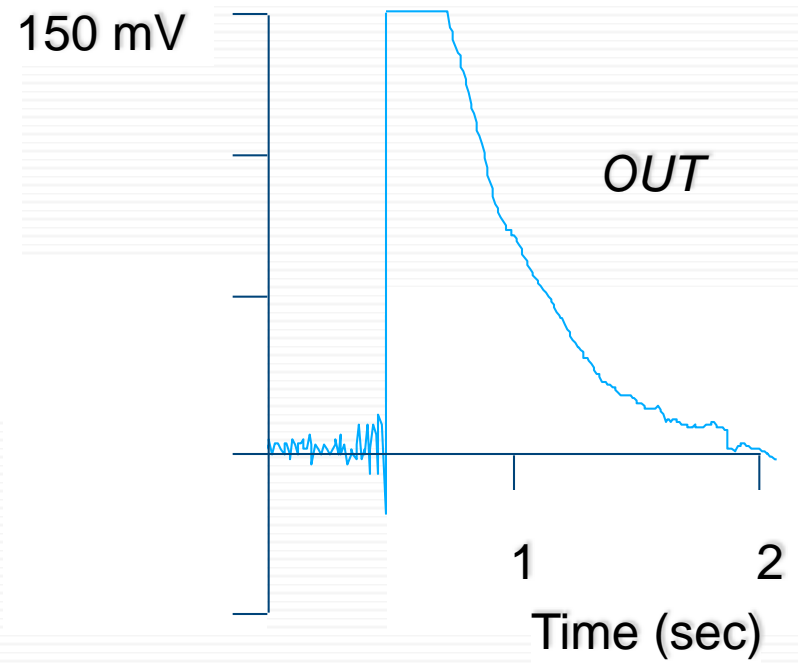
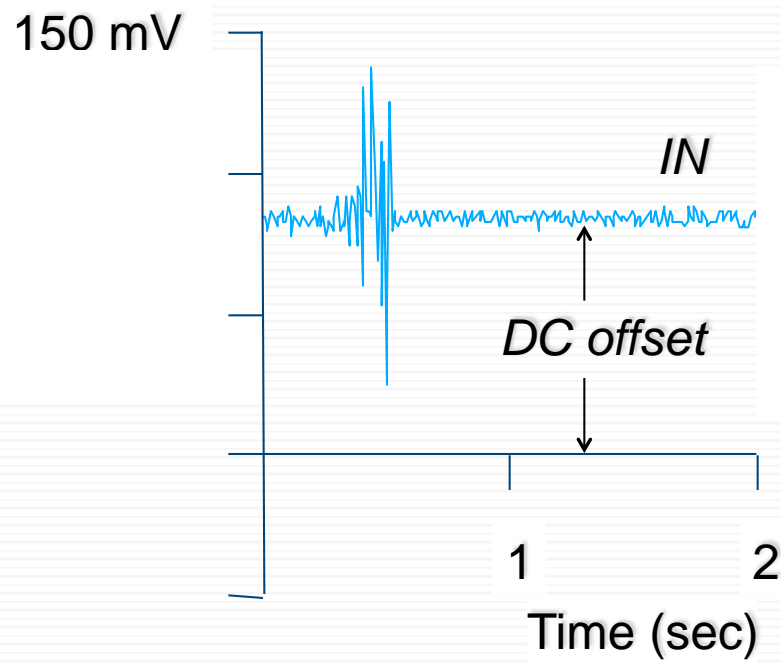
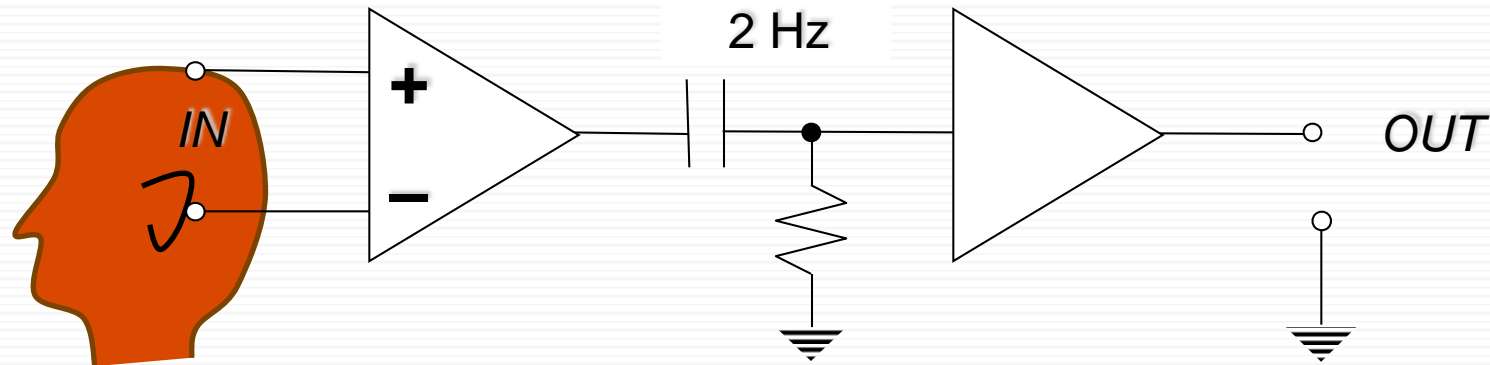
A Method for Removing Imaging Artifact from Continuous EEG Recorded during Functional MRI

Philip J. Allen,^{*} Oliver Josephs,[†] and Robert Turner[†]

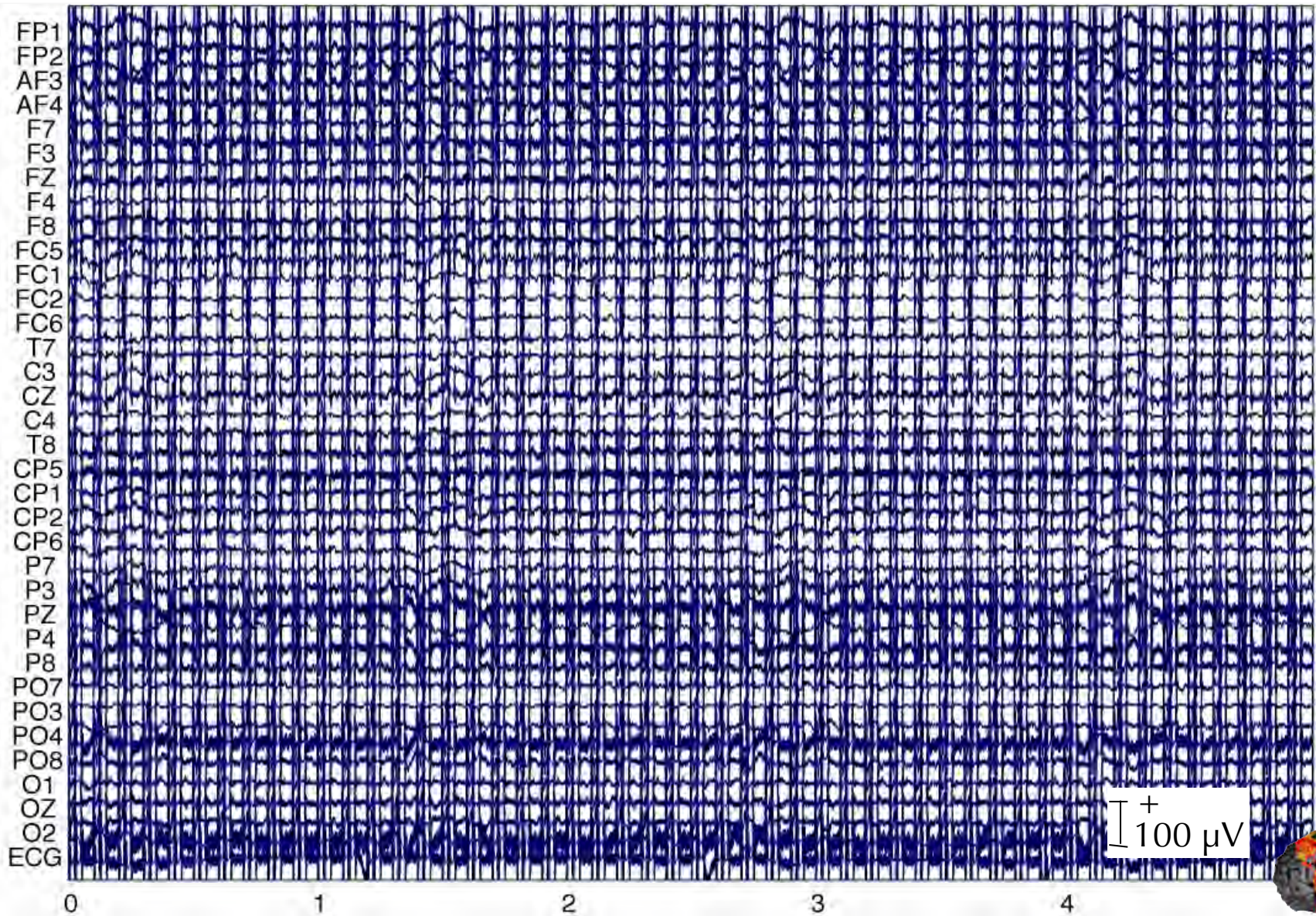
^{*}Department of Clinical Neurophysiology, National Hospital for Neurology and Neurosurgery, University College London Hospitals, Queen Square, London WC1N 3BG, United Kingdom; and [†]The Wellcome Department of Cognitive Neurology, Institute of Neurology, University College London, Queen Square, London, United Kingdom



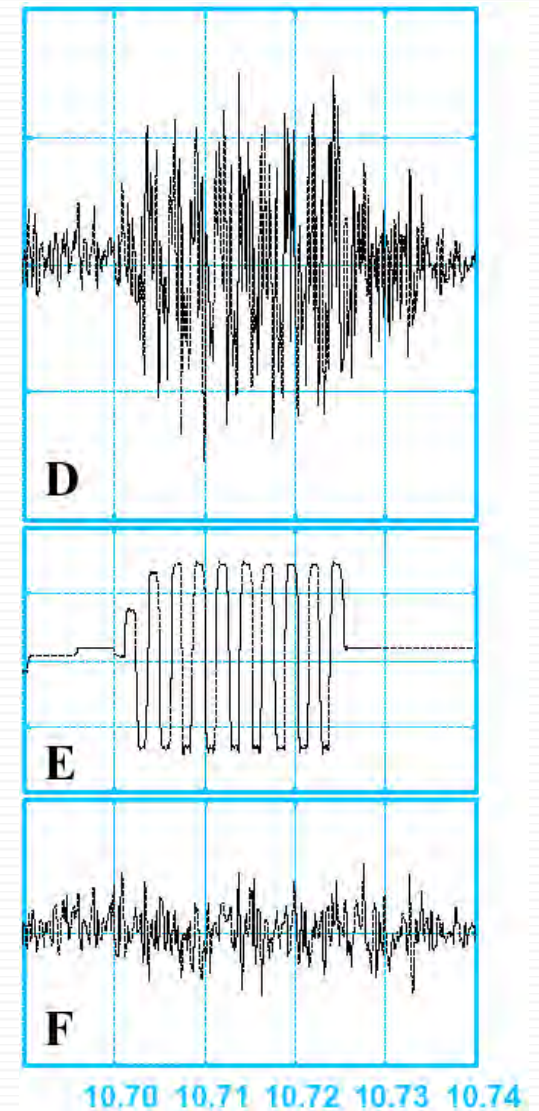
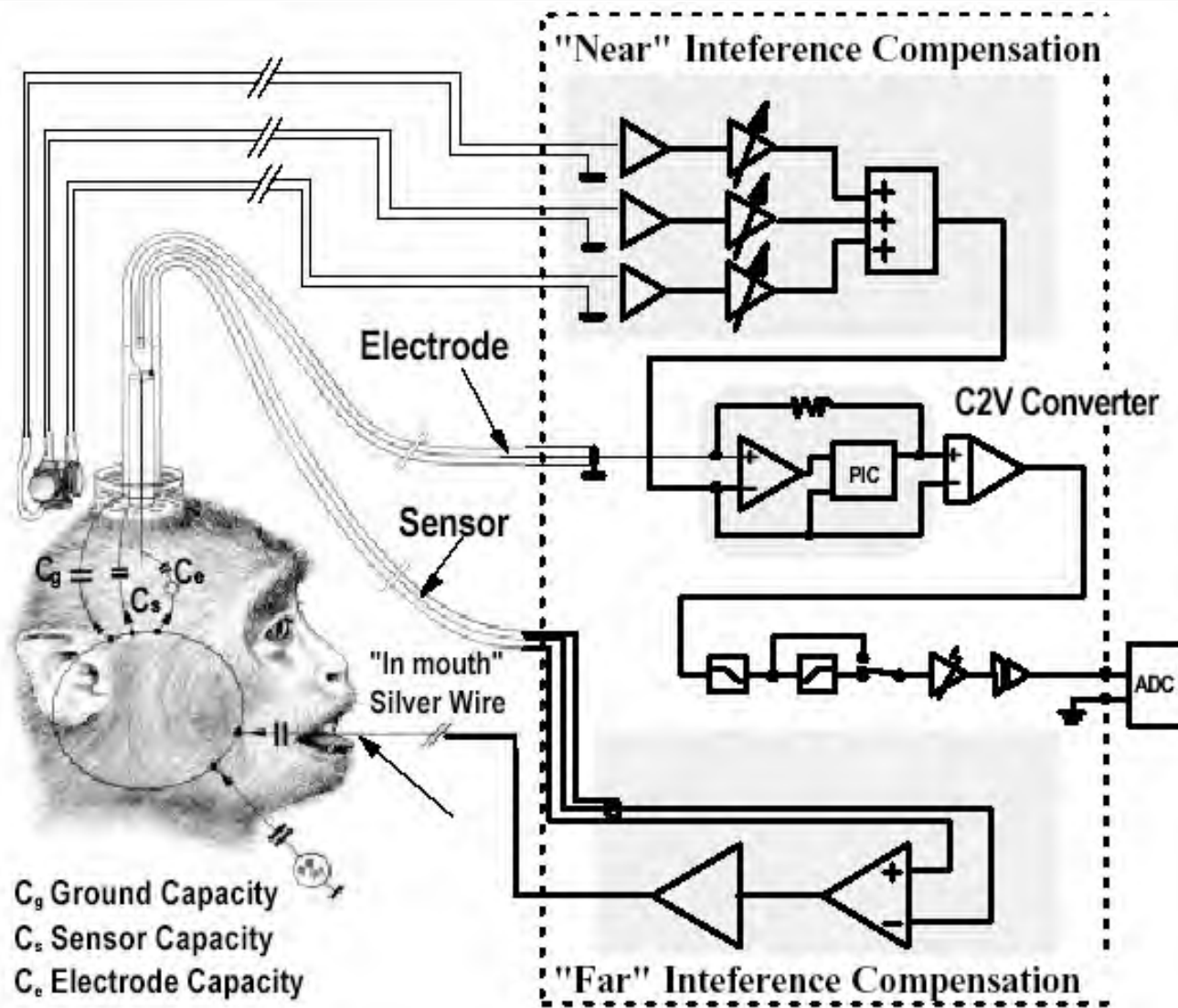
Receiver Saturation



Artifacts During Scanning



Logothetis (recording method)



BOLD response reflects synaptic activity

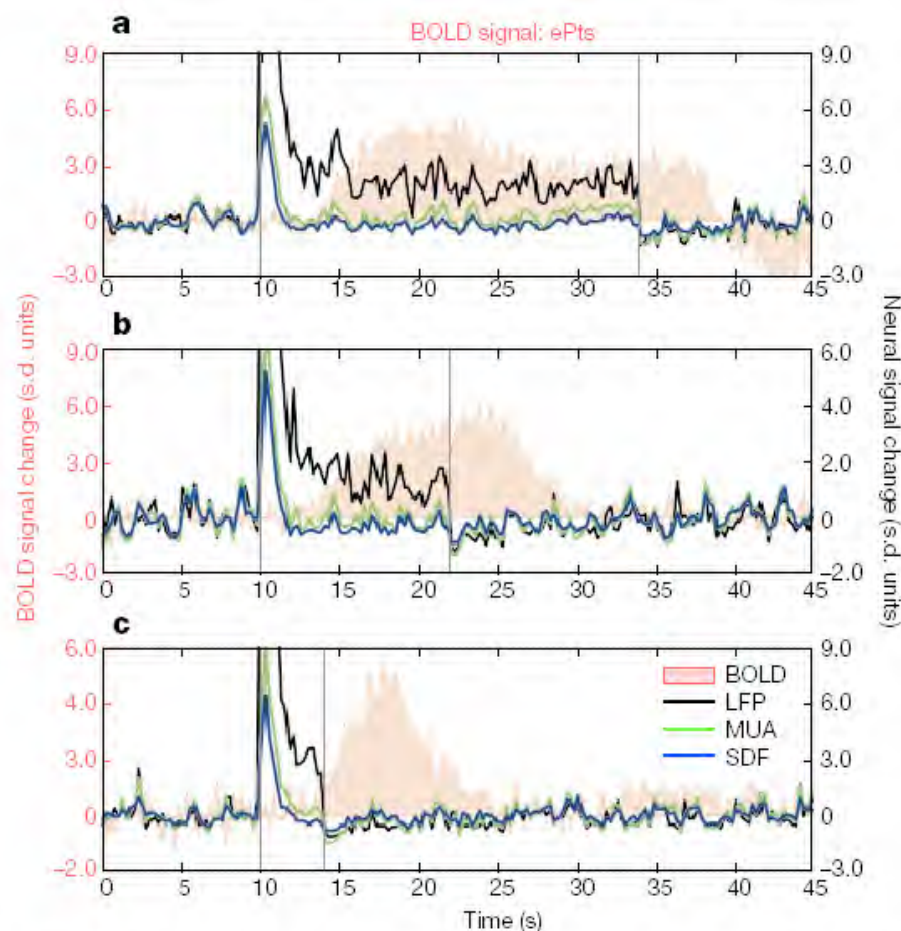
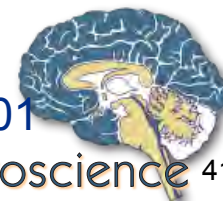


Figure 3 Simultaneous neural and haemodynamic recordings from a cortical site showing transient neural response. **a–c**, Responses to a pulse stimulus of 24, 12 and 4 s. Both single- and multi-unit responses adapt a couple of seconds after stimulus onset, with LFP remaining the only signal correlated with the BOLD response. SDF, spike-density function (see text); ePts, electrode ROI—positive time series.

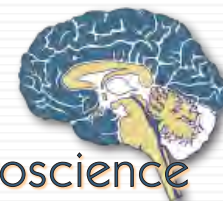
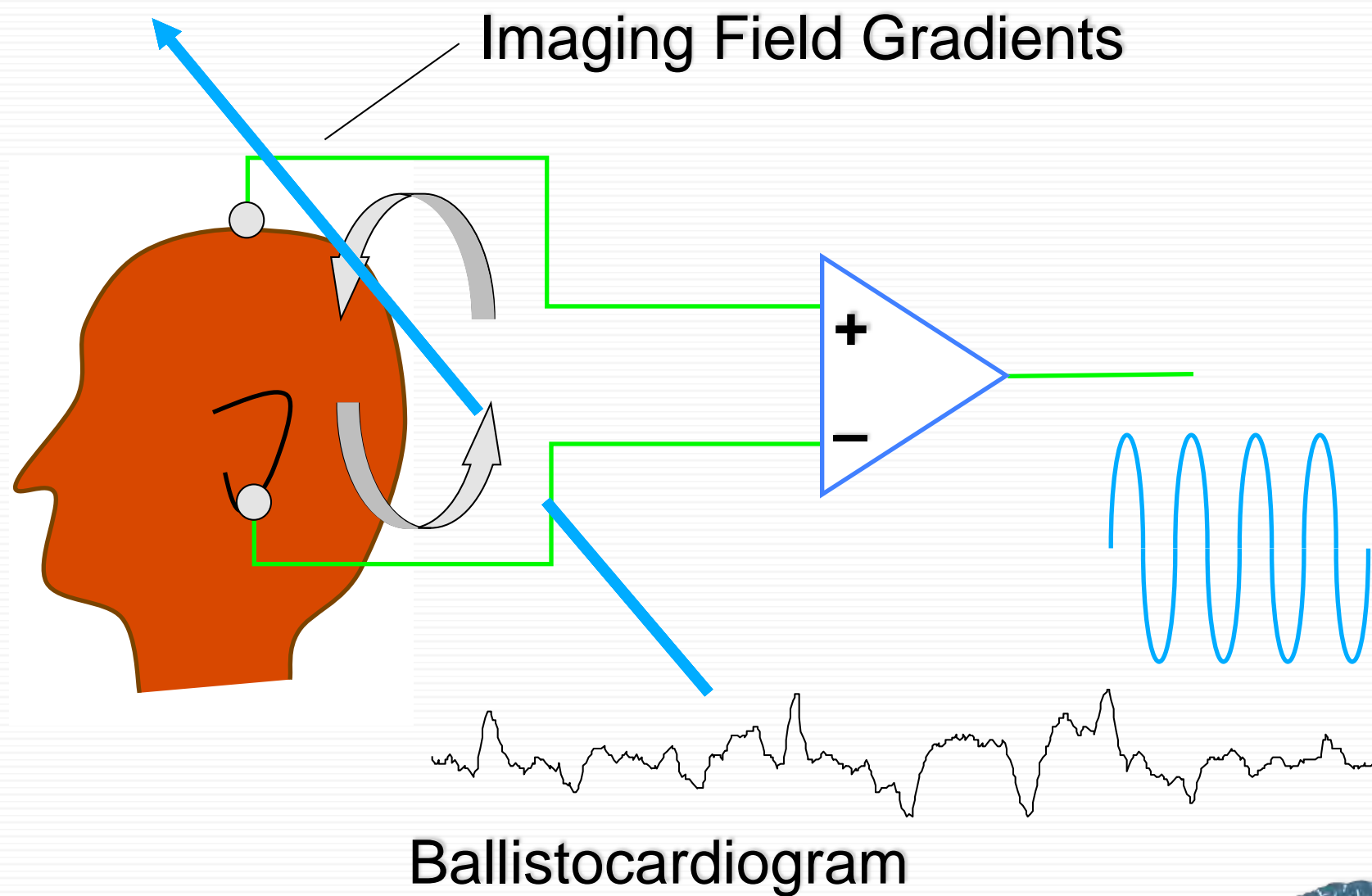
Local field potentials (LFP)
reflect synaptic currents

Multi-unit activity (MUA)
reflects spiking activity

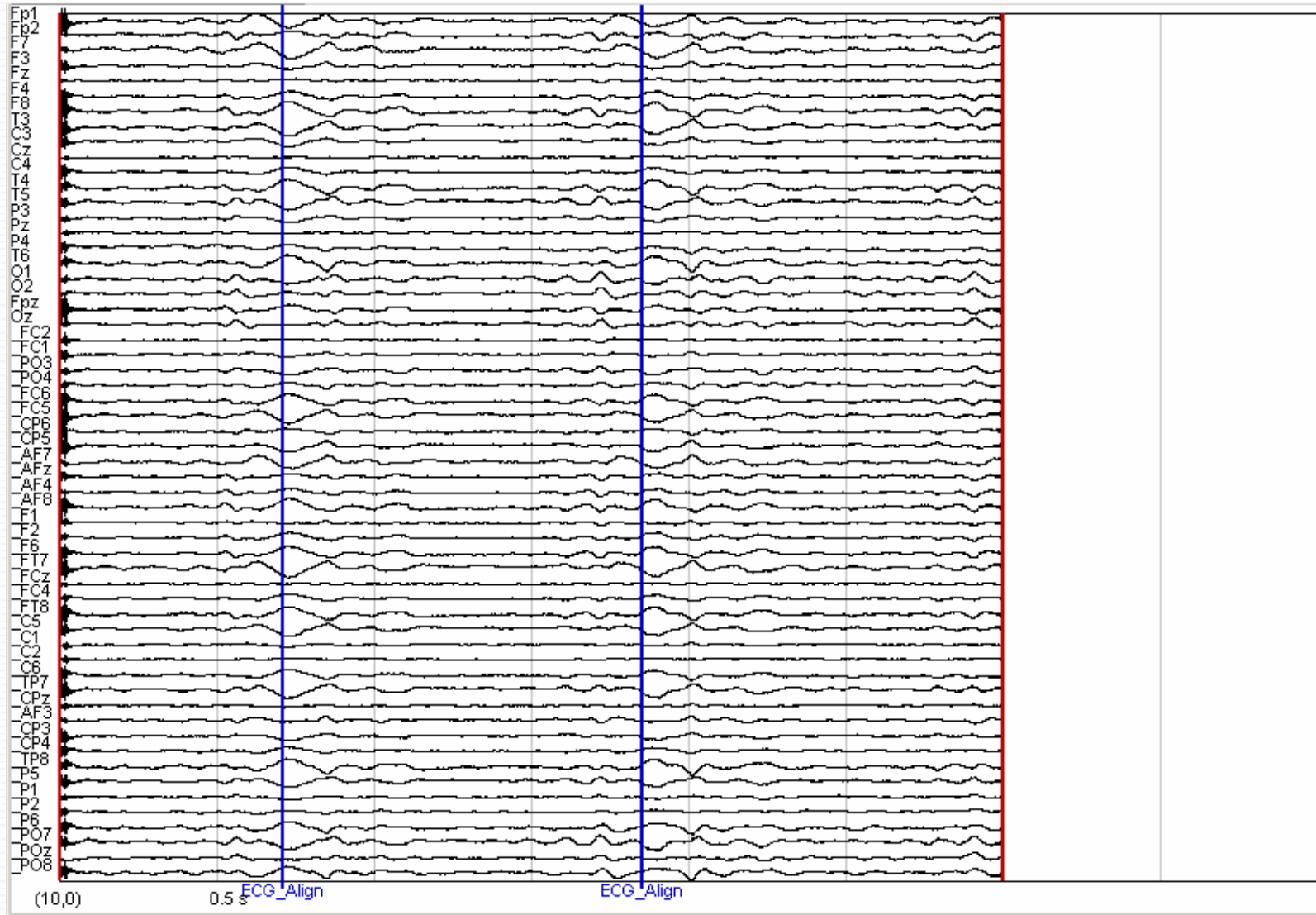
MUA attenuates quickly, while
LFP shows an extended
response that correlates
better with the BOLD
response



Inductive Pickup by EEG leads



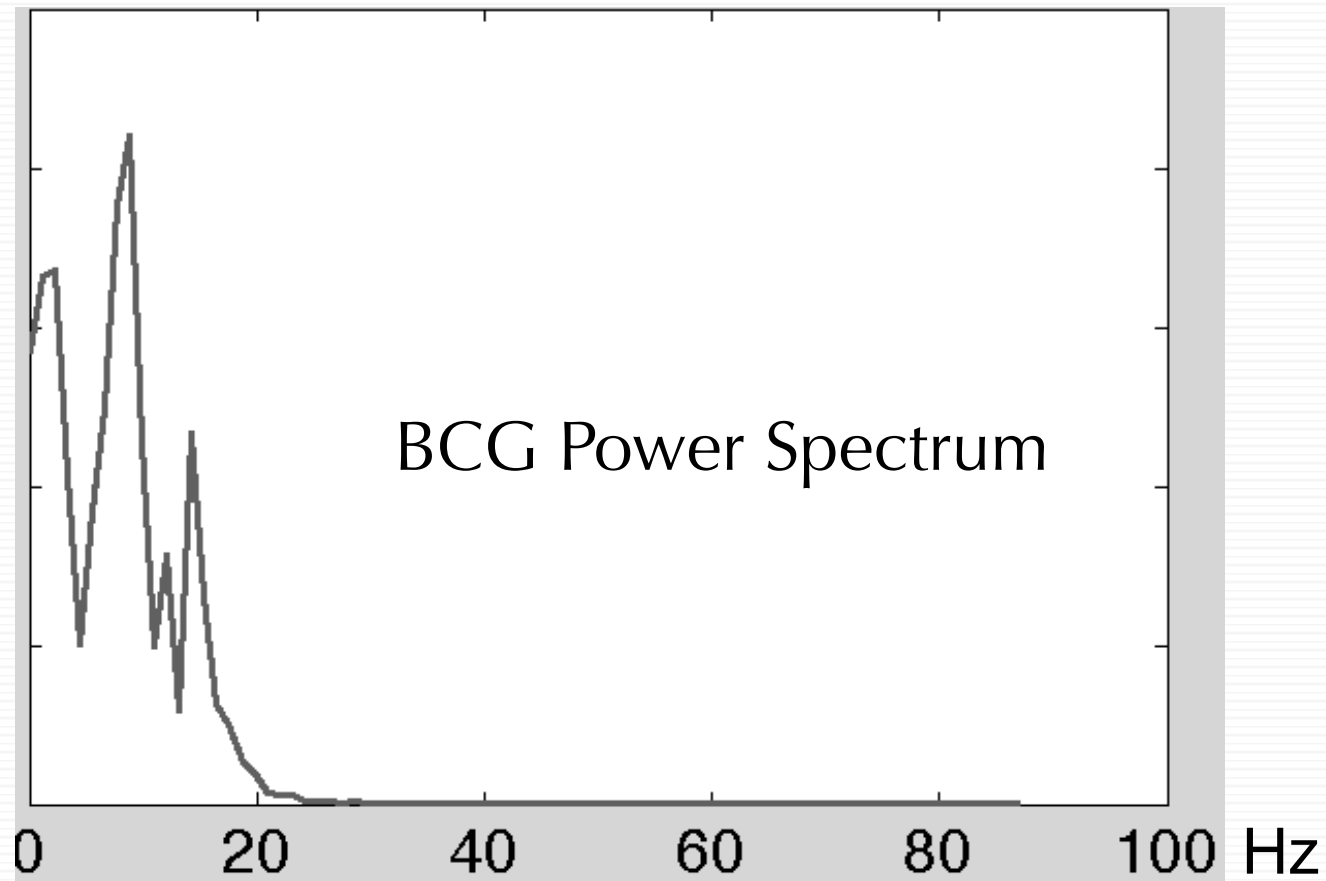
Ballistocardiogram



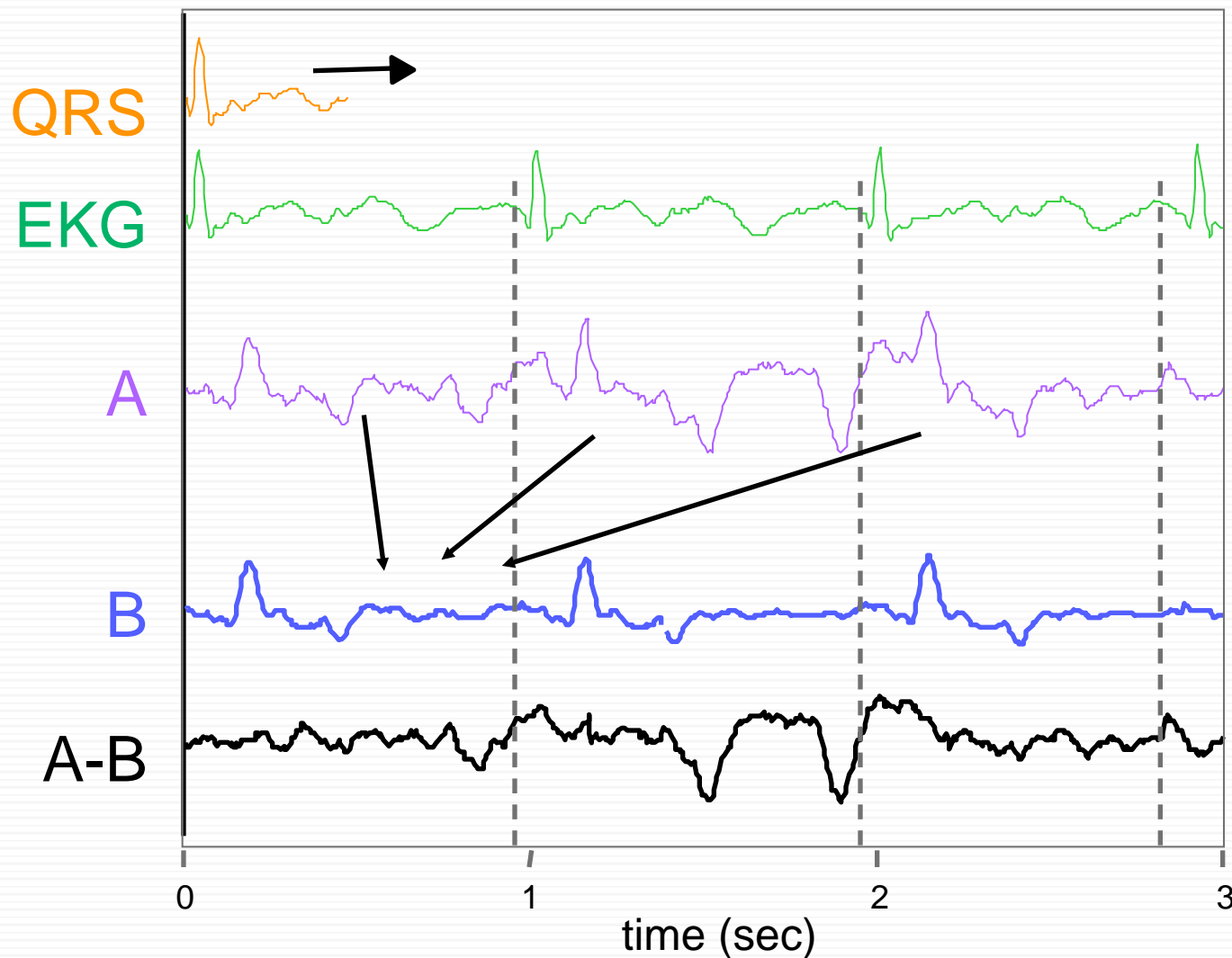
Jan de Munck



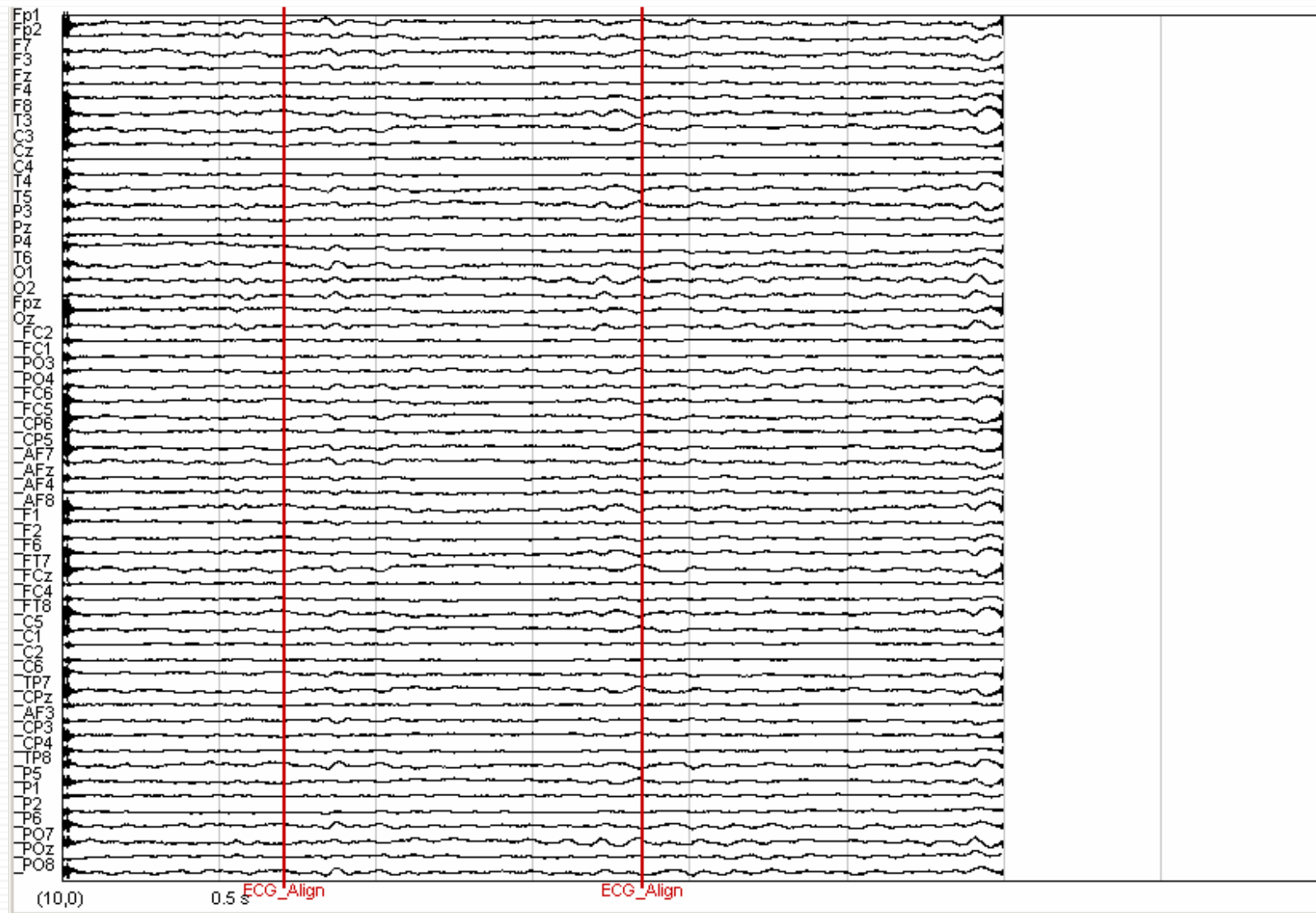
Can We Simply Filter?



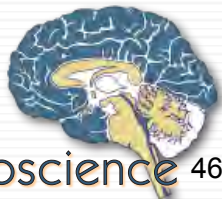
Ballistocardiogram Subtraction



EEG after Ballistocardiogram Averaging

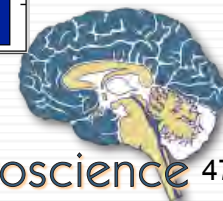
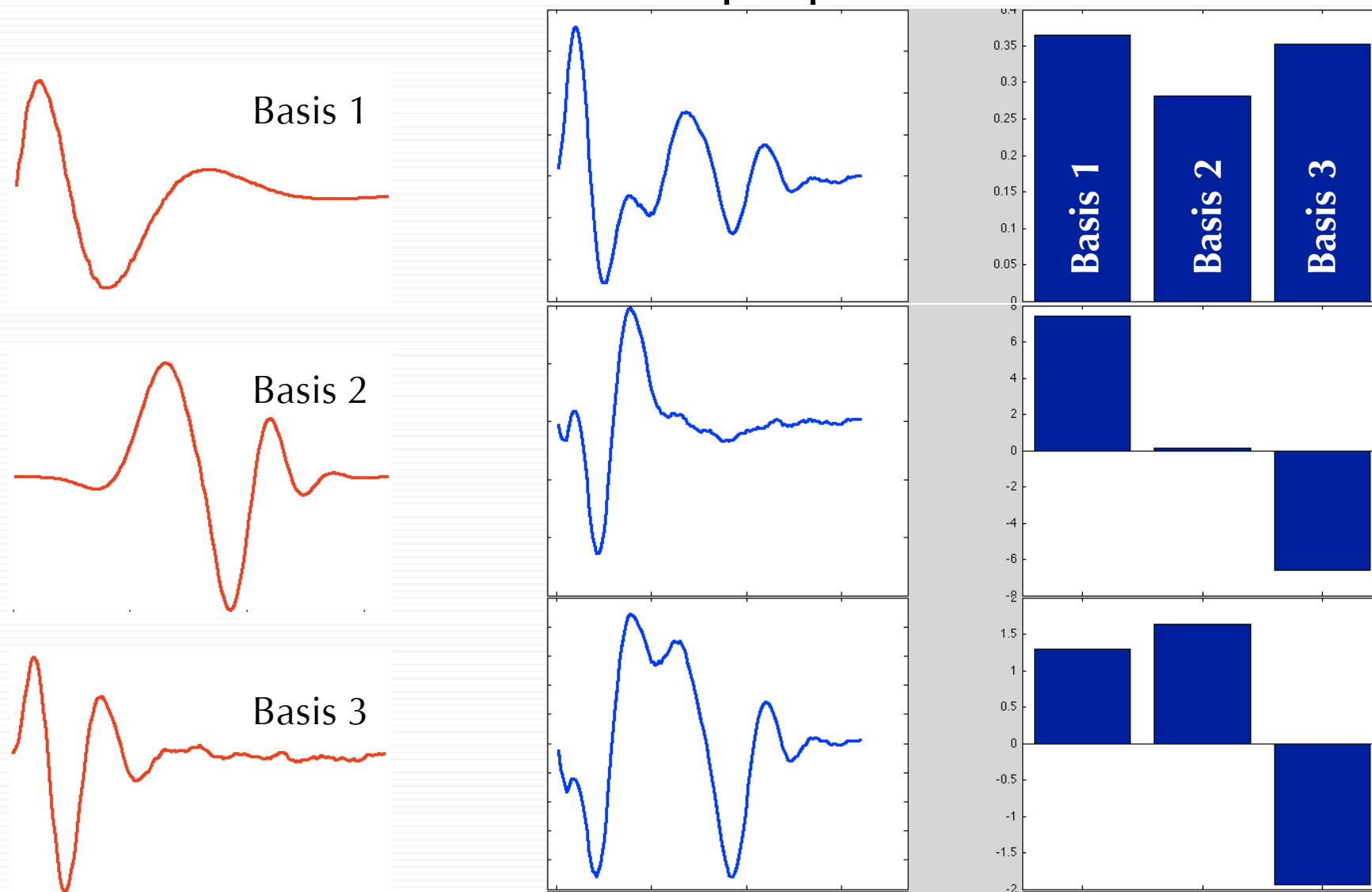


Jan de Munck

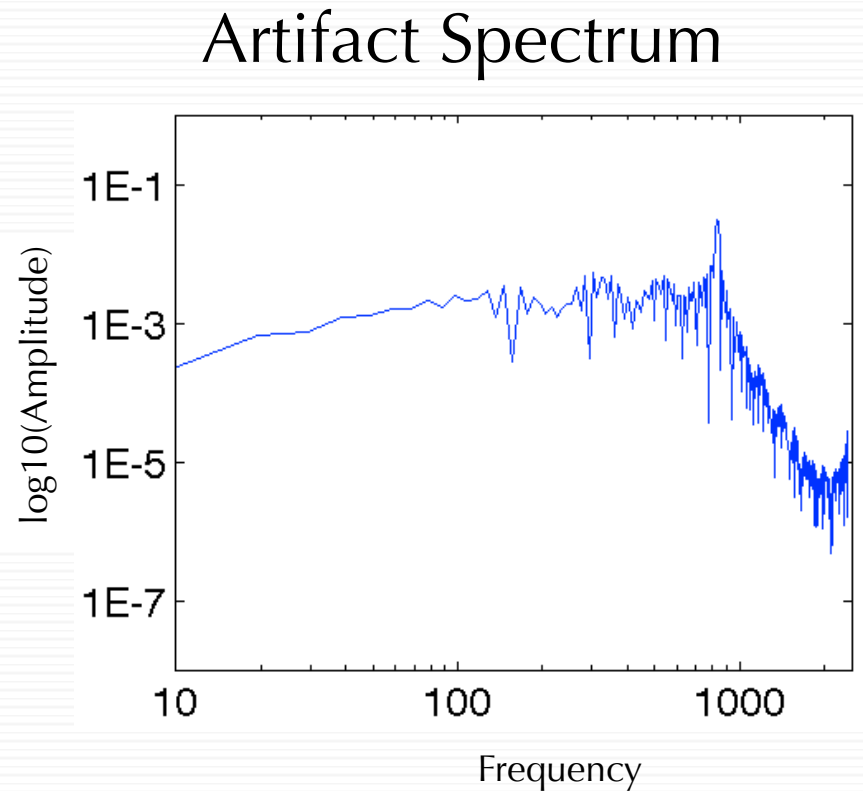
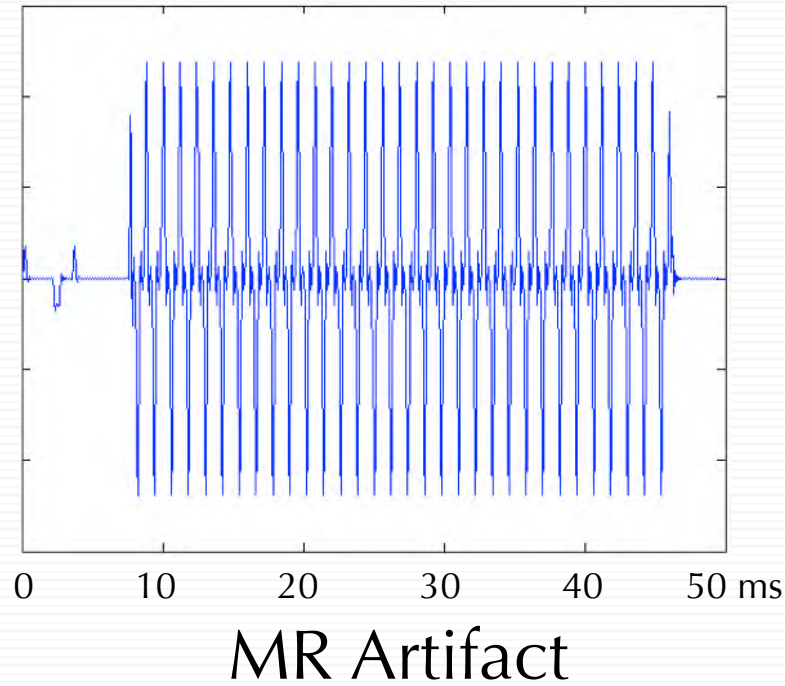


Optimal Basis Functions

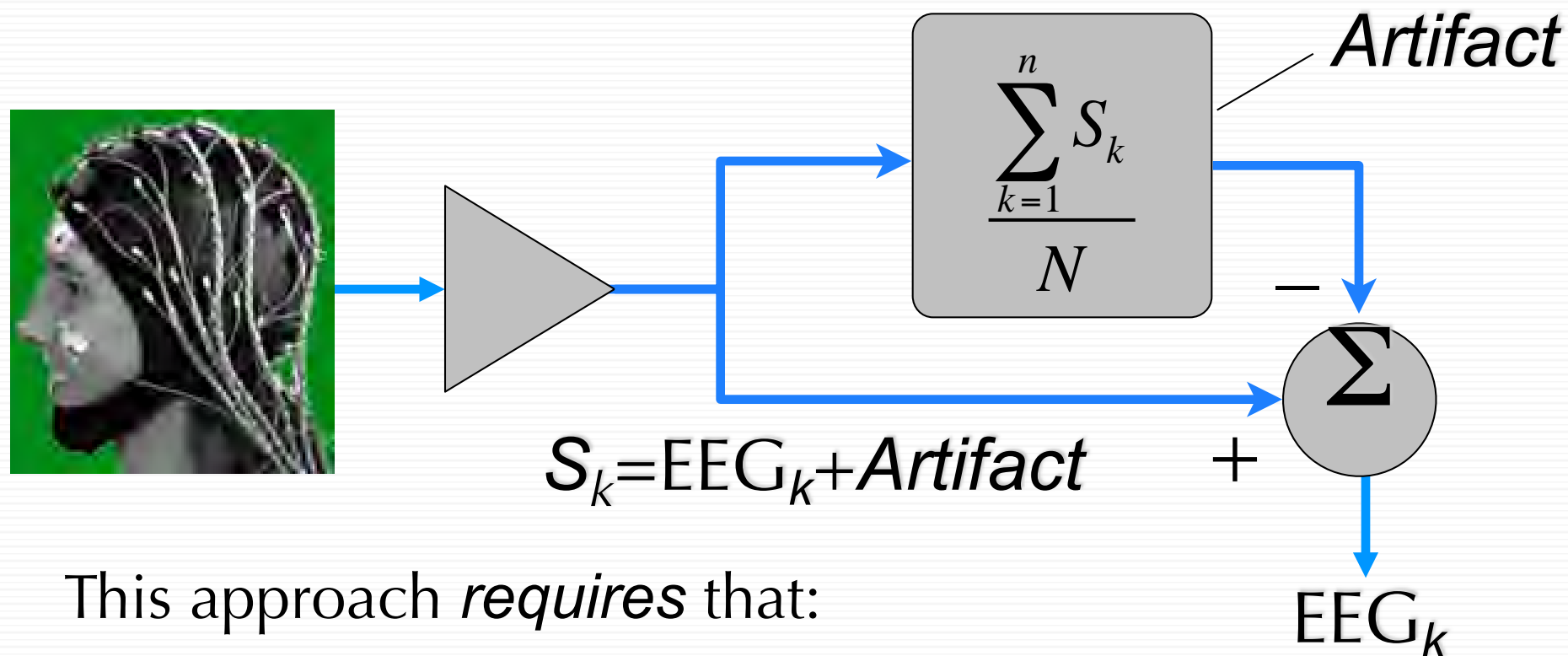
- Model the BCG as the superposition of basis functions



Spectral Suppression

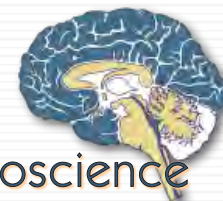


Approach to MR Artifact Removal

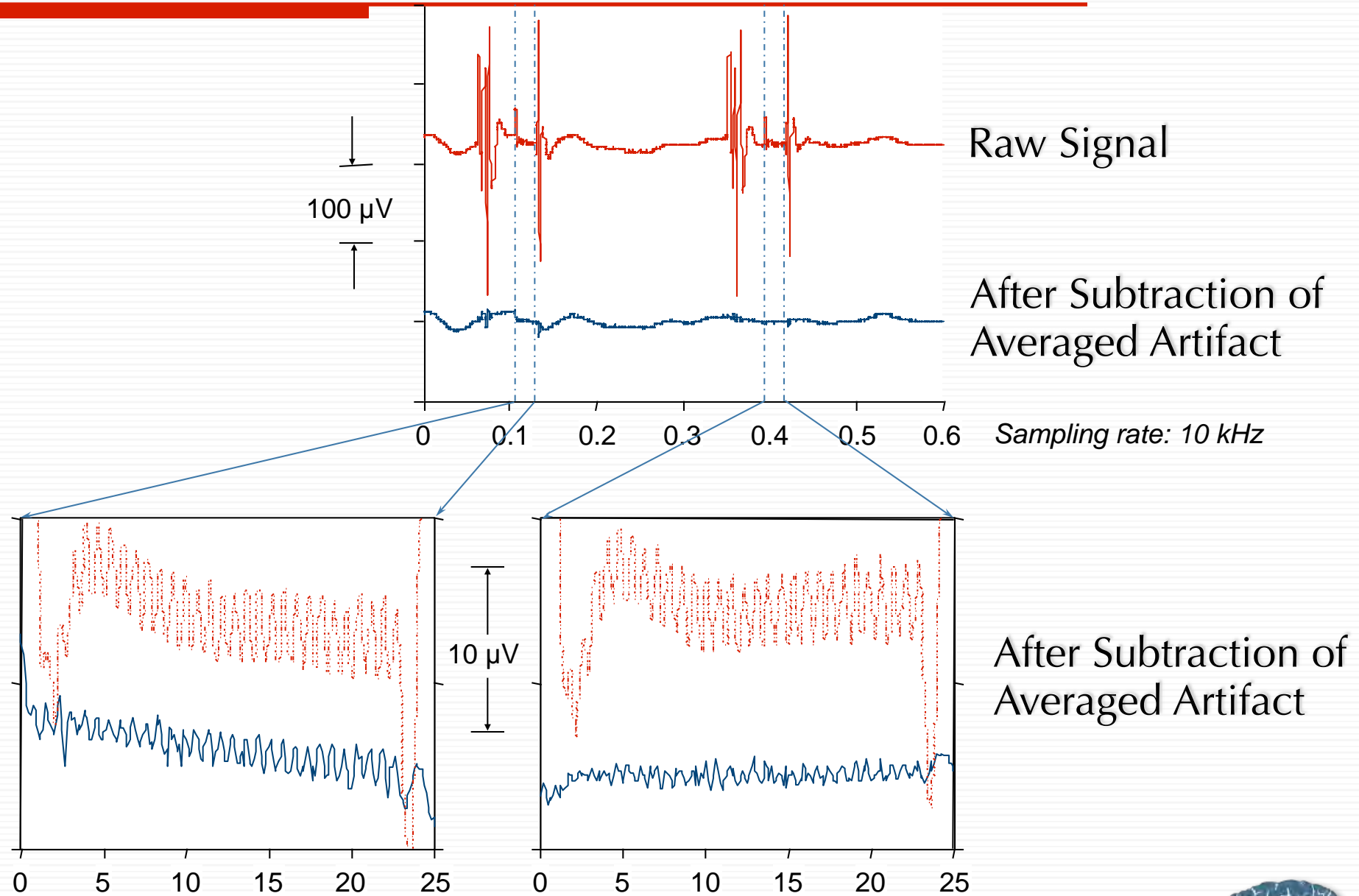


This approach *requires* that:

- EEG_k and *Artifact* are uncorrelated
- EEG_k and *Artifact* add linearly
- *Artifact* is identical at each time (k)



Fast Sampling is NOT enough



Sampling and Nyquist

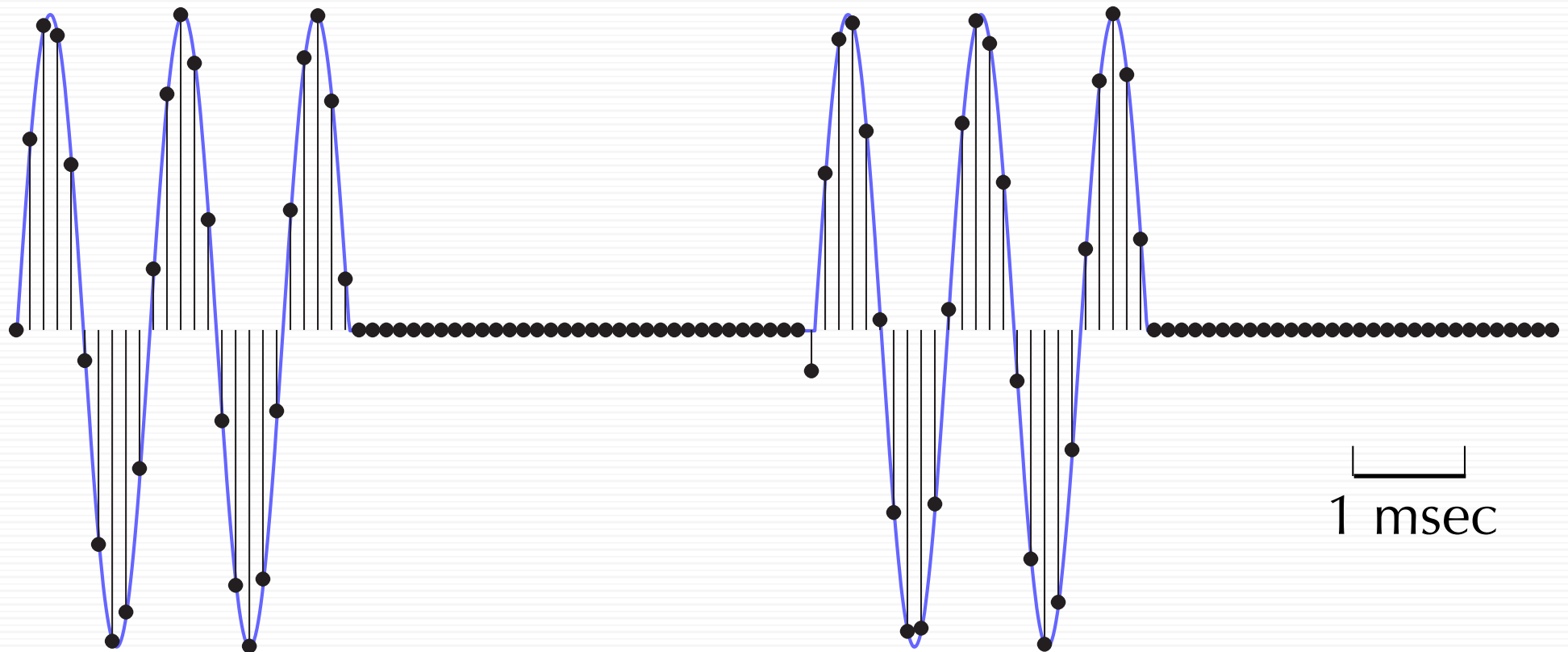


1 msec

Scanner Artifact (simulated)



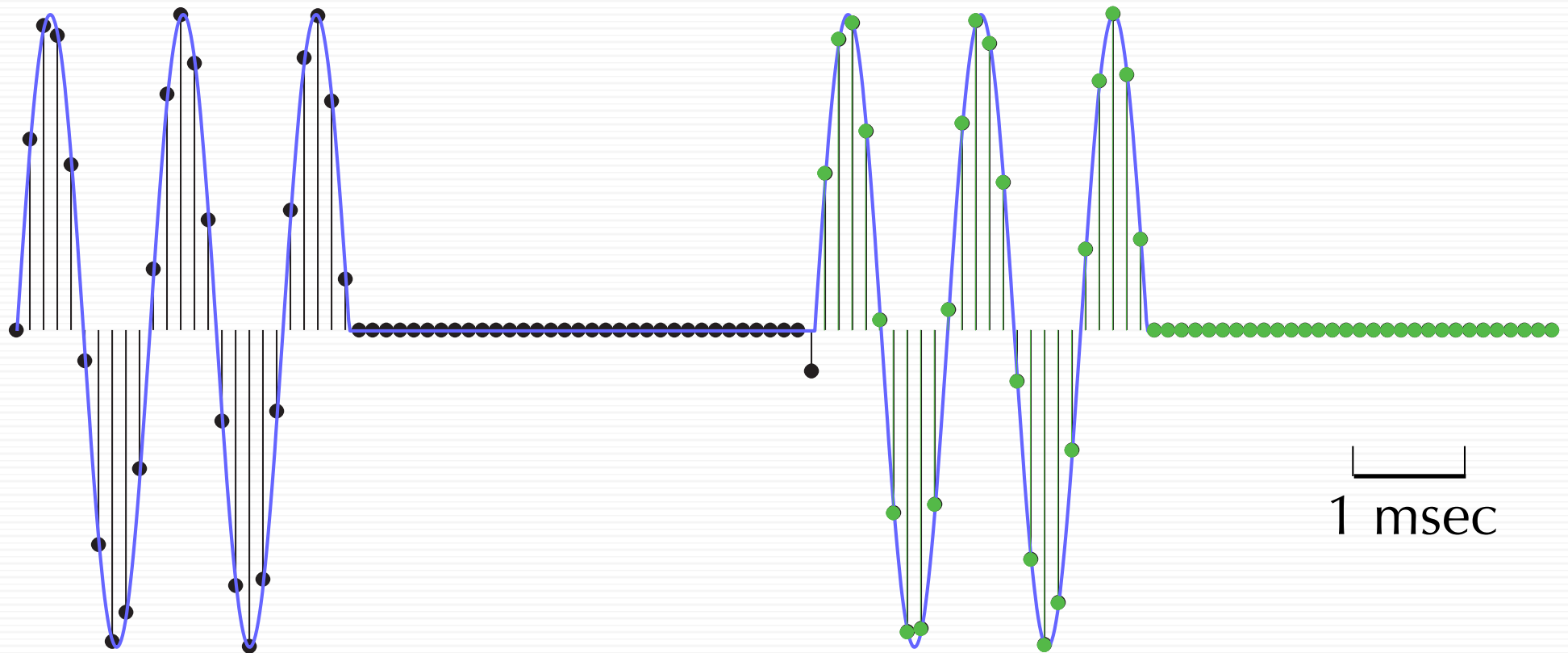
Sampling and Nyquist



Scanner Artifact (simulated)
Digital Sampling $>5X$ Nyquist



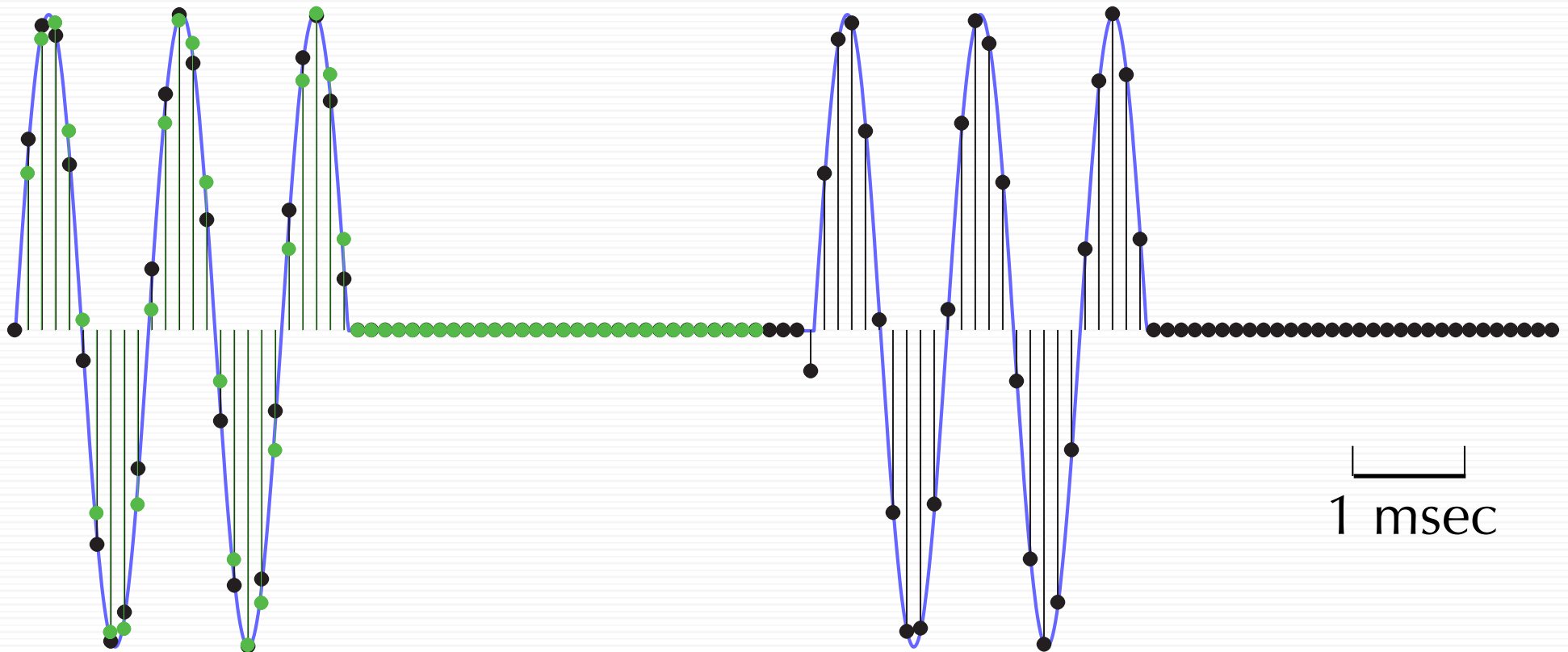
Sampling and Nyquist



Scanner Artifact (simulated)
Digital Sampling 5X Nyquist
Second Cycle - not Phase-Locked



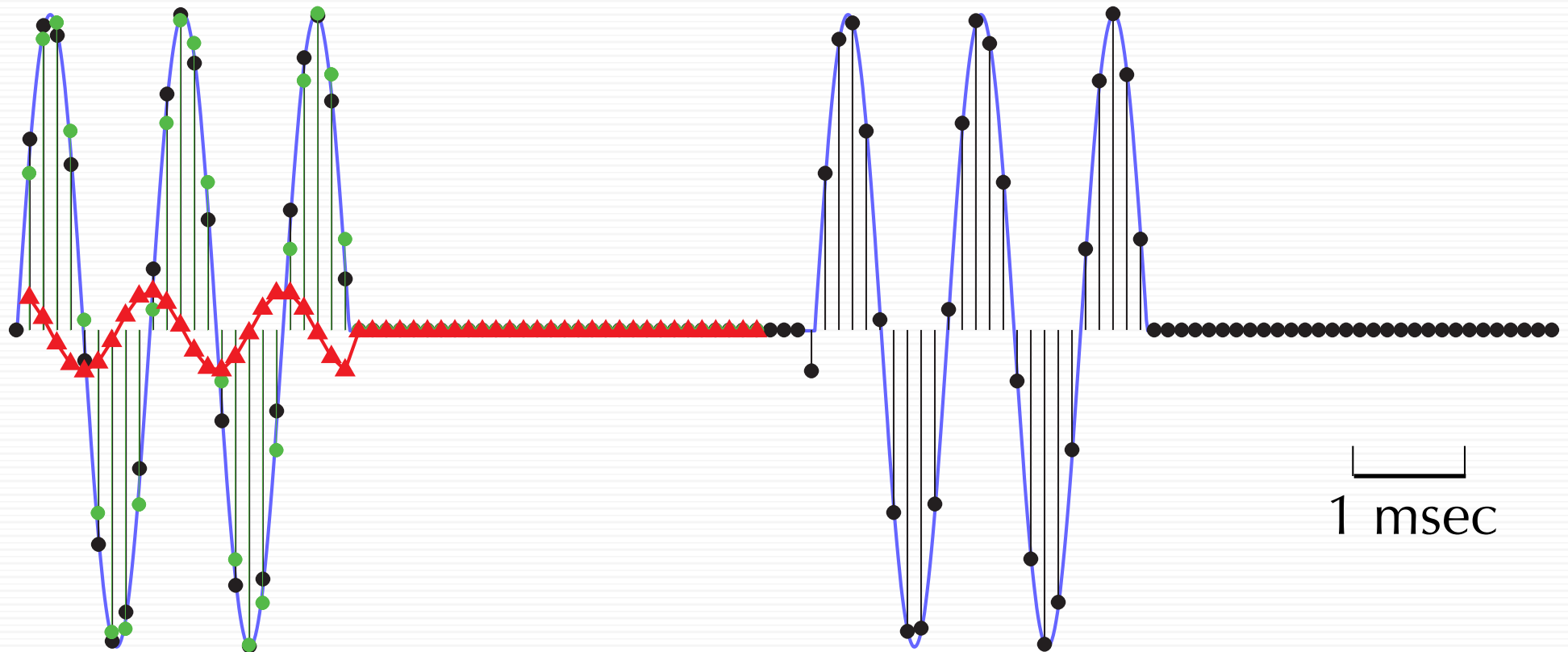
Sampling and Nyquist



Scanner Artifact (simulated)
Digital Sampling 5X Nyquist
Second Cycle - not Phase-Locked



Sampling and Nyquist



Scanner Artifact (simulated)

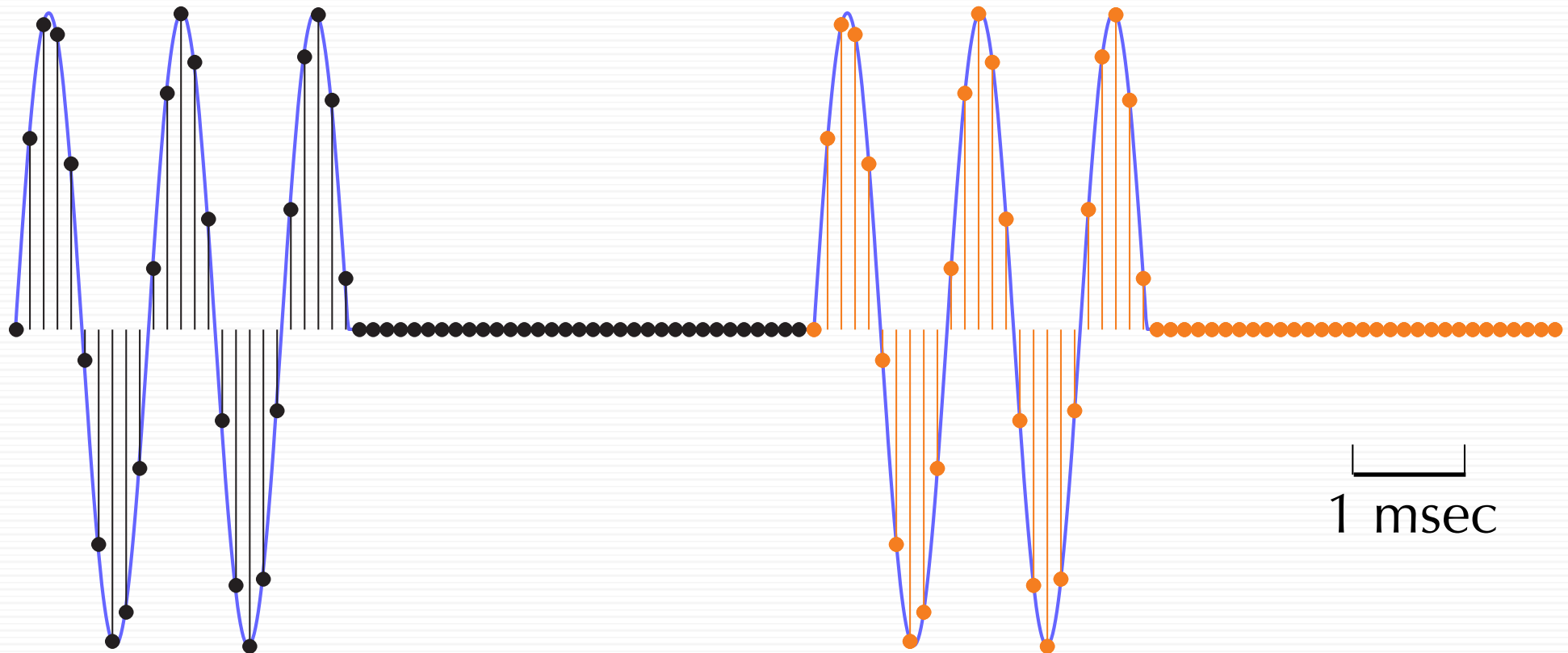
Digital Sampling 5X Nyquist

Second Cycle - not Phase-Locked

Error Difference Between Cycles



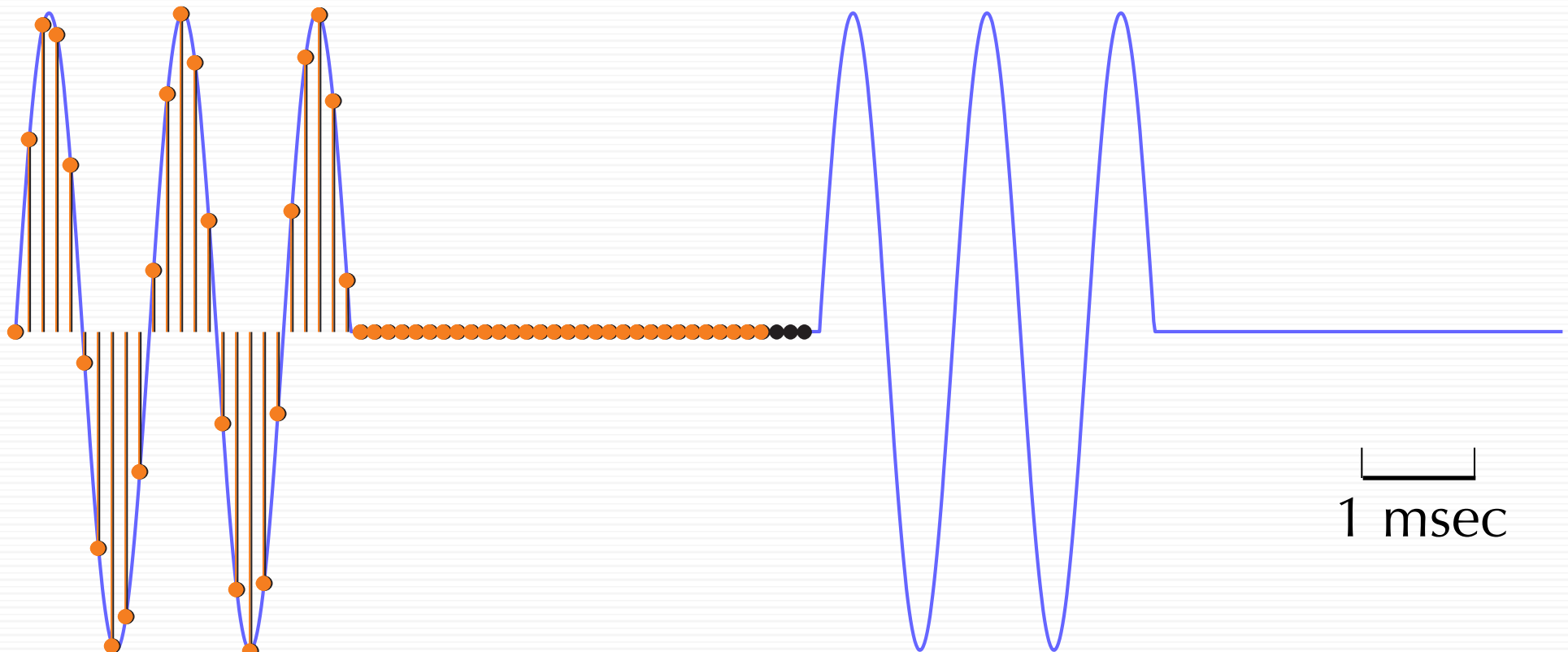
Synchronized Sampling



Scanner Artifact (simulated)
Digital Sampling 5X Nyquist
Second Cycle - Phase-Locked



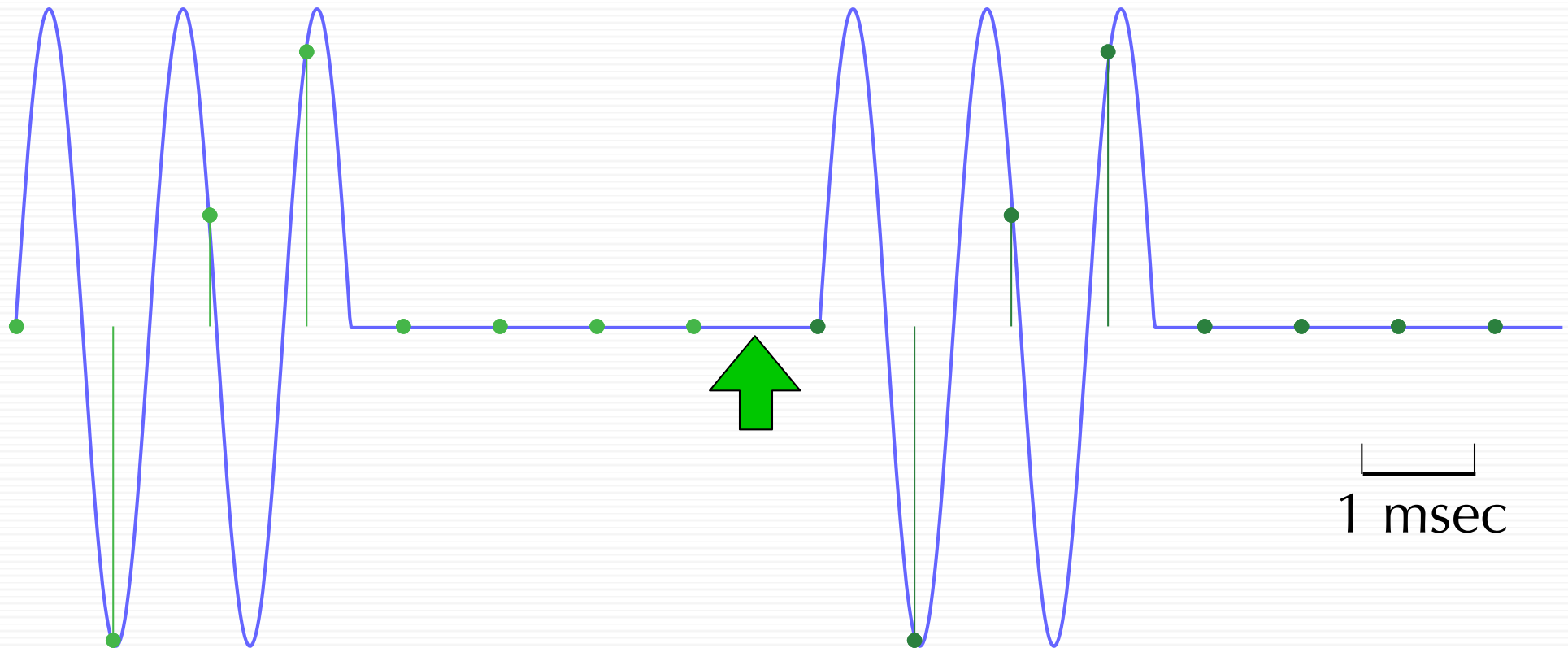
Synchronized Sampling



Scanner Artifact (simulated)
Digital Sampling 5X Nyquist
Second Cycle - Phase-Locked



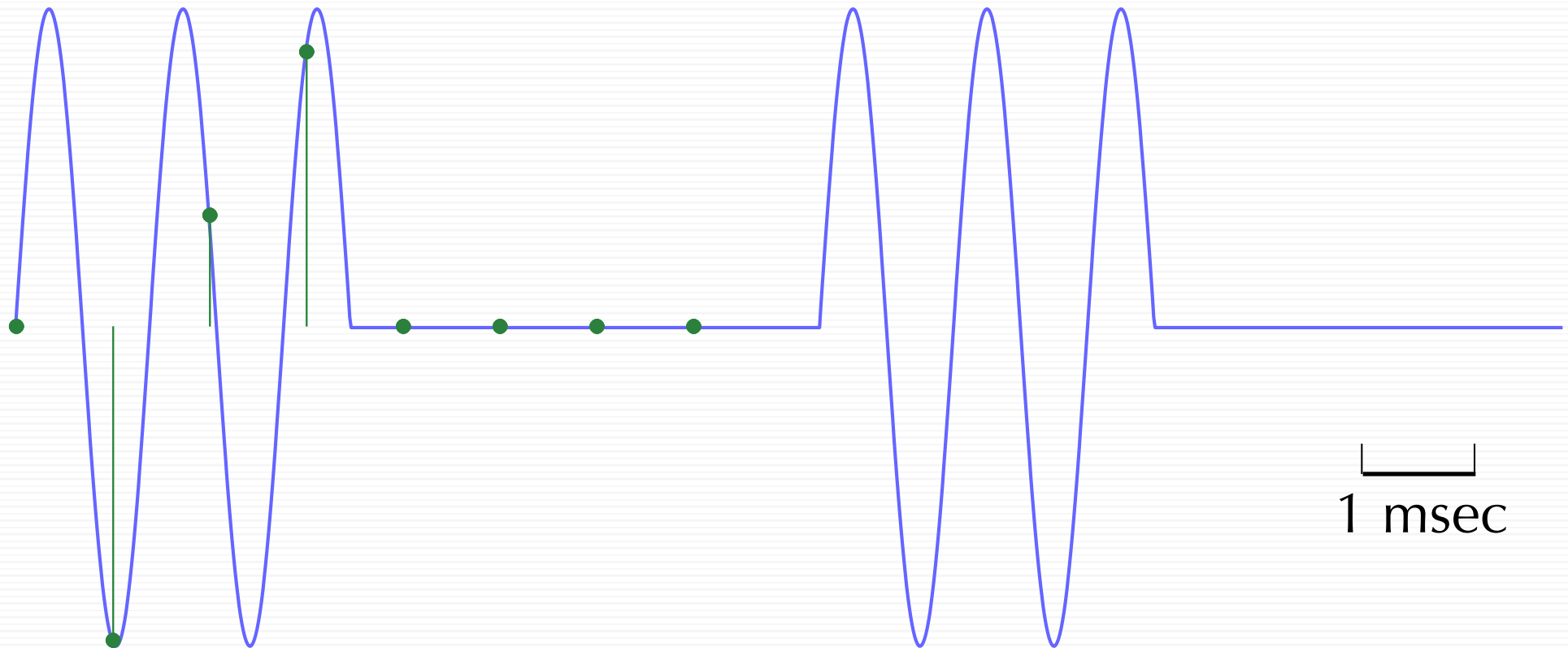
Synchronized Sampling



Scanner Artifact (simulated)
Sub-Nyquist Sampling



Synchronized Sampling



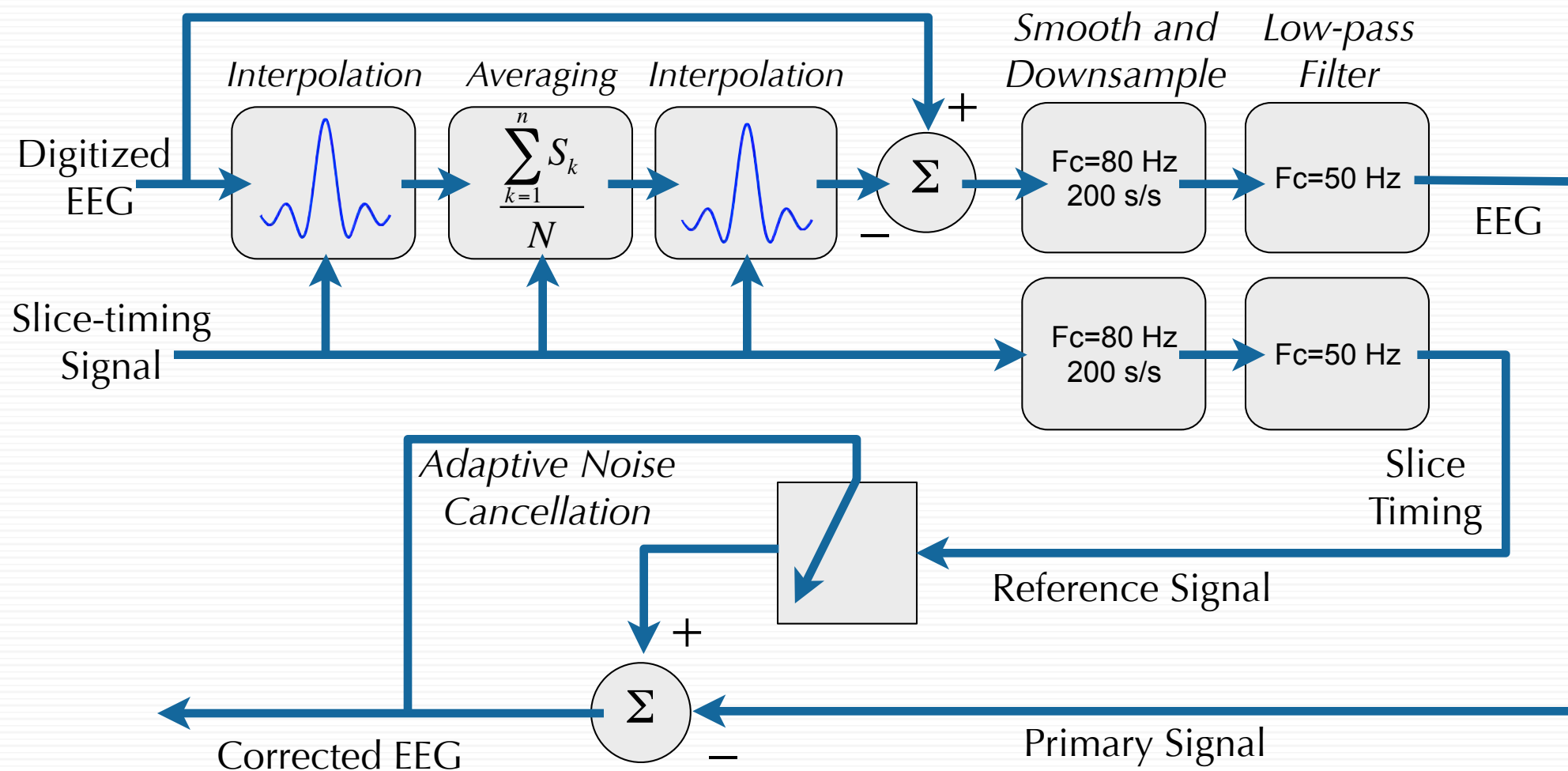
Scanner Artifact (simulated)

Sub-Nyquist Sampling

Error is Depends on **Phase Accuracy** -
Independent of Sampling Rate



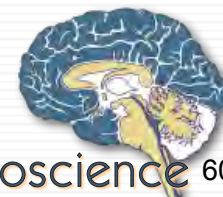
Allen Method



NeuroImage 12, 230–239 (2000)

A Method for Removing Imaging Artifact from Continuous EEG
Recorded during Functional MRI

Philip J. Allen,* Oliver Josephs,† and Robert Turner†



Residual Errors

$$\begin{aligned}\varepsilon &= \cos(2\pi ft) - \cos(2\pi ft - \varphi) \\ &= \cos(2\pi ft)\cos(\varphi - 1) - \sin(2\pi ft)\sin \varphi\end{aligned}$$

...where:

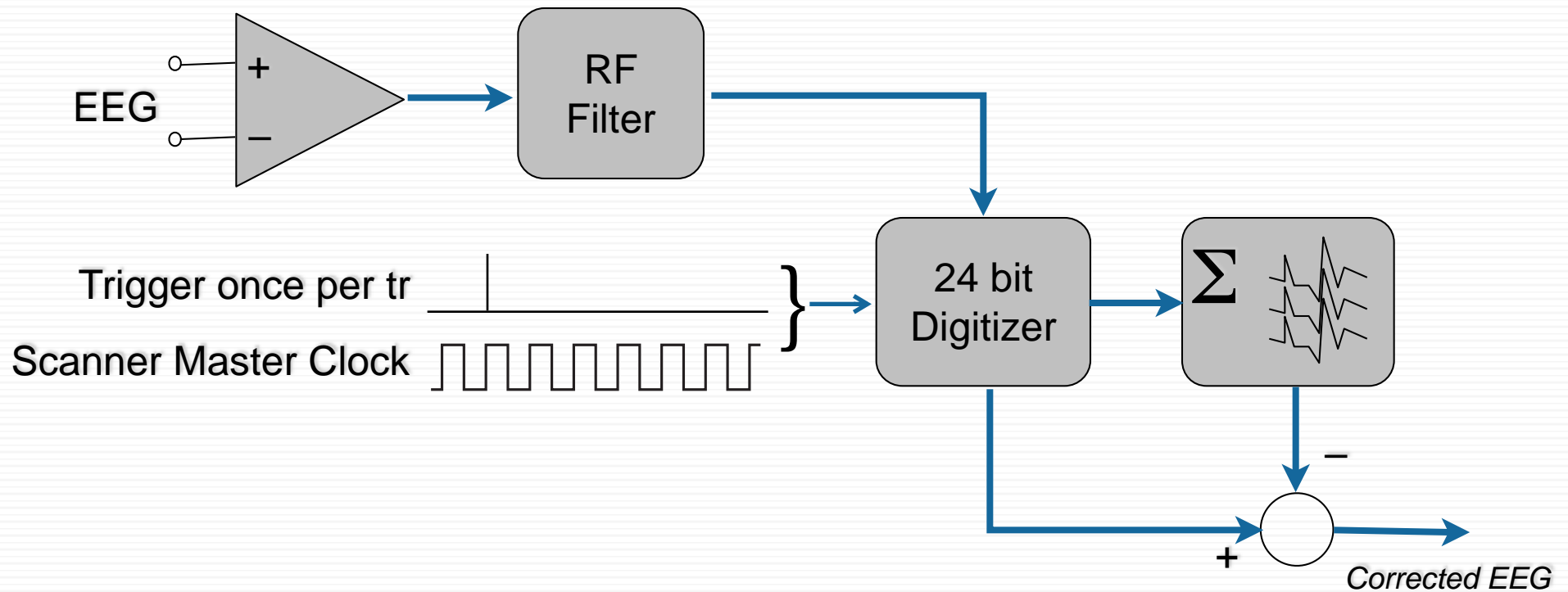
f is the frequency of the artifact
 φ is the phase error, equal to $2\pi f_0/f_s$,

- f_0 is the EPI readout frequency and
- f_s is the sampling frequency.

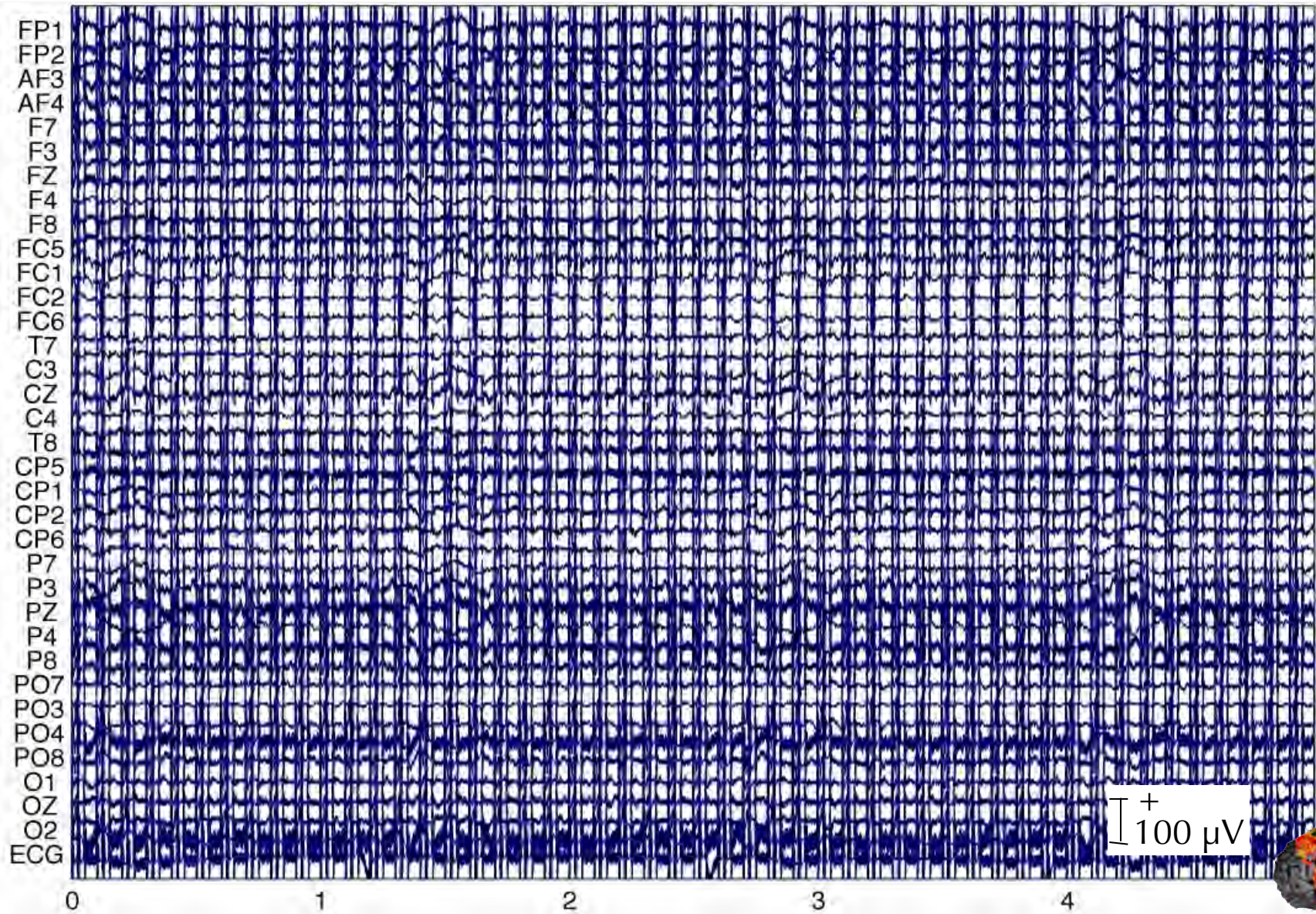
At high sampling frequency (small φ) the error, ε , is linearly proportional to the sampling frequency



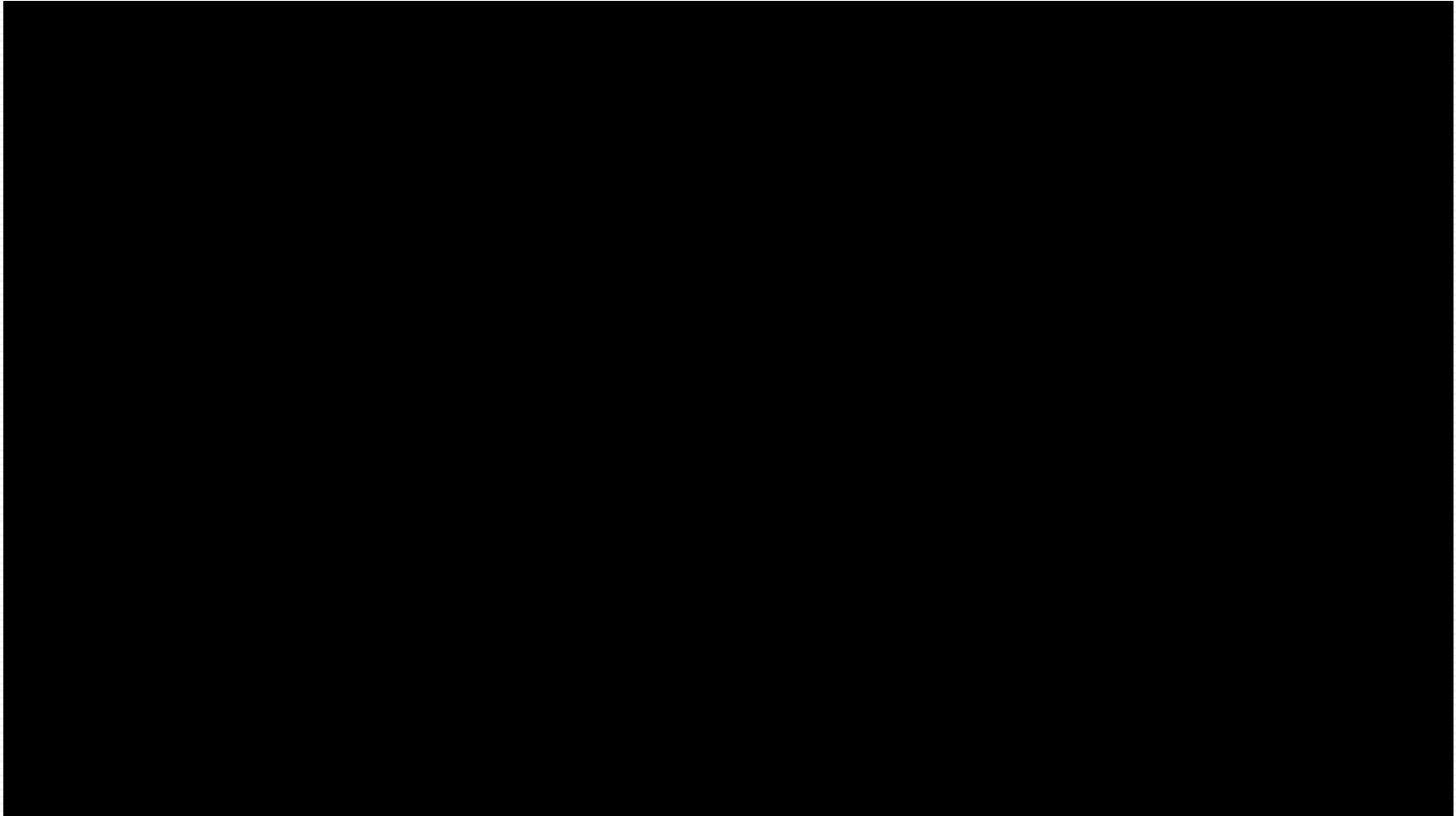
Synchronized Correction



Artifacts During Scanning



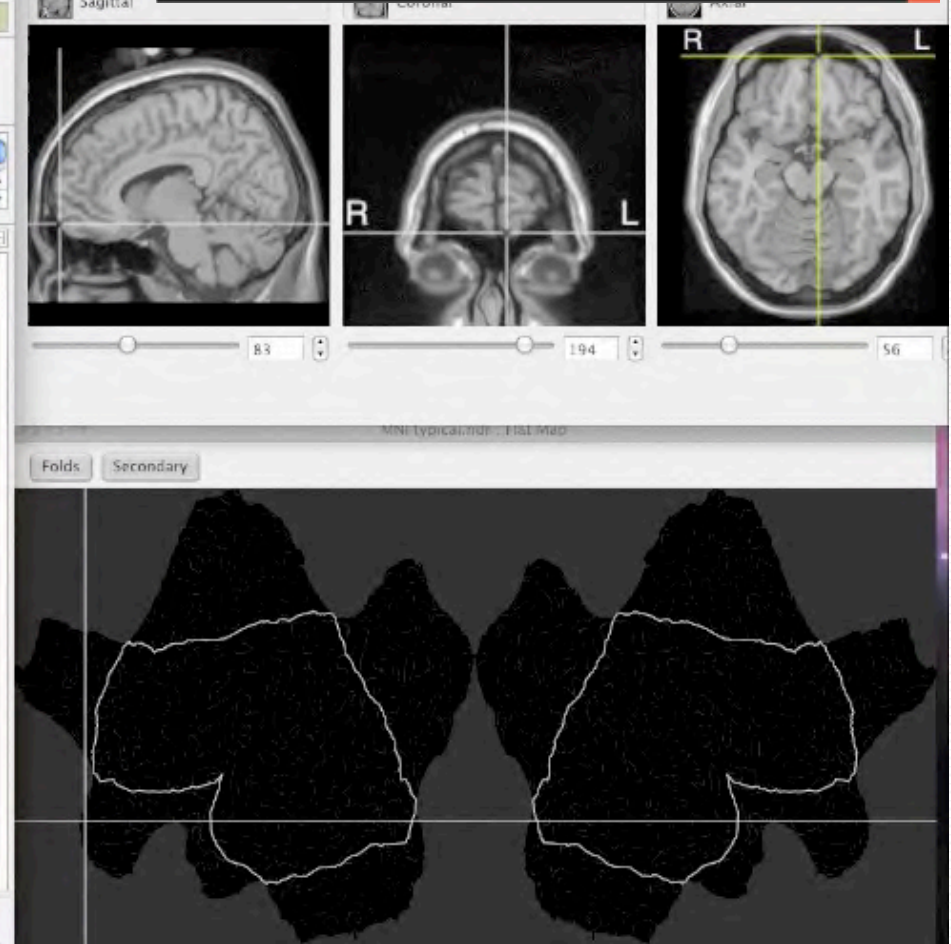
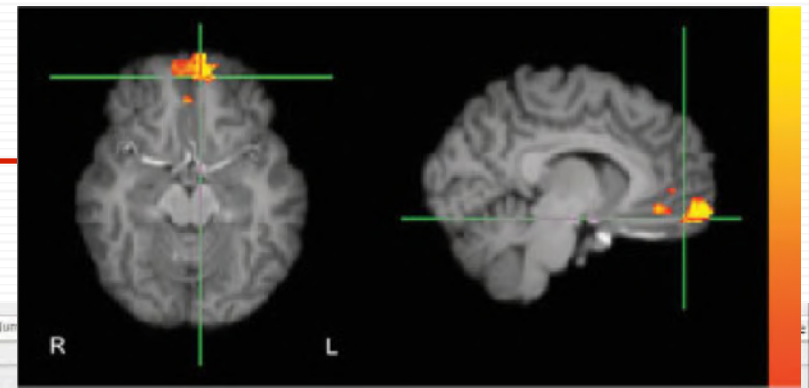
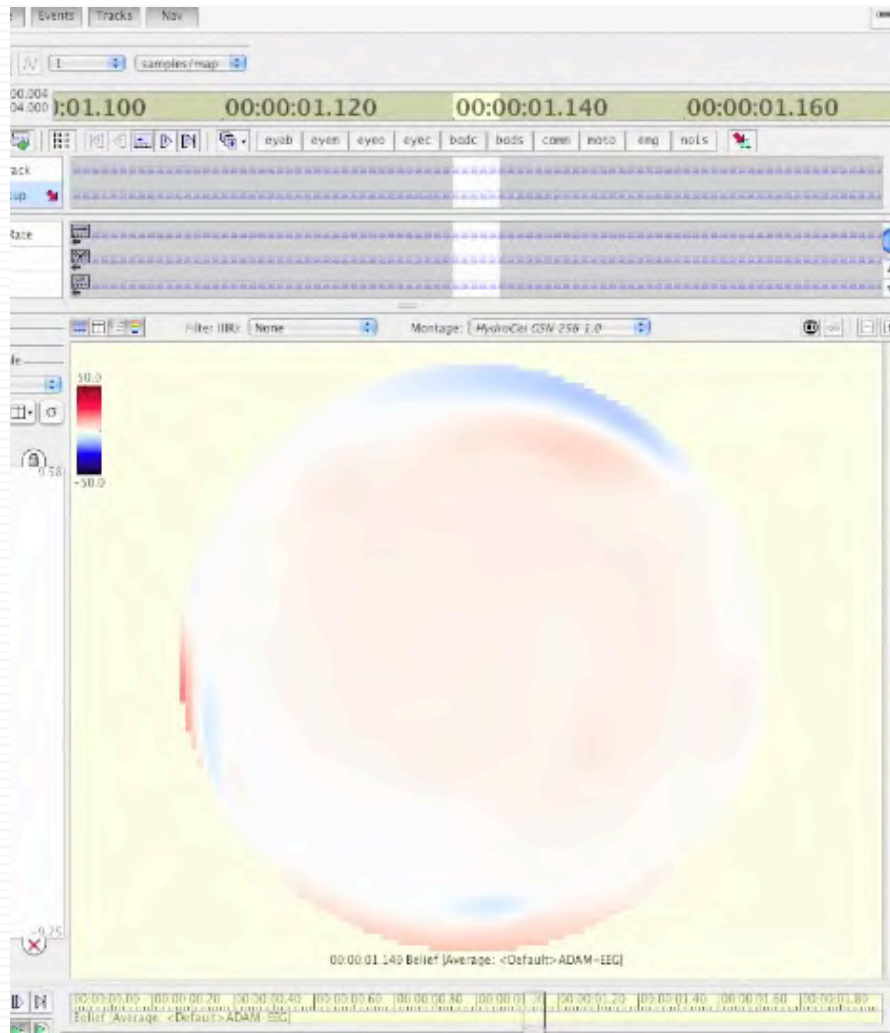
Simultaneous EEG & fMRI



Disclaimer: The author receives royalties on sales of the EGI instrument



Tomographic EEG Projection



Example: Epilepsy

Affects 0.5-1% of population (e.g., 1.5 million Americans)

Source: Merck, AAFP & NINDS, others

Up to 50% cannot be treated with medication

Source: AAFP, others

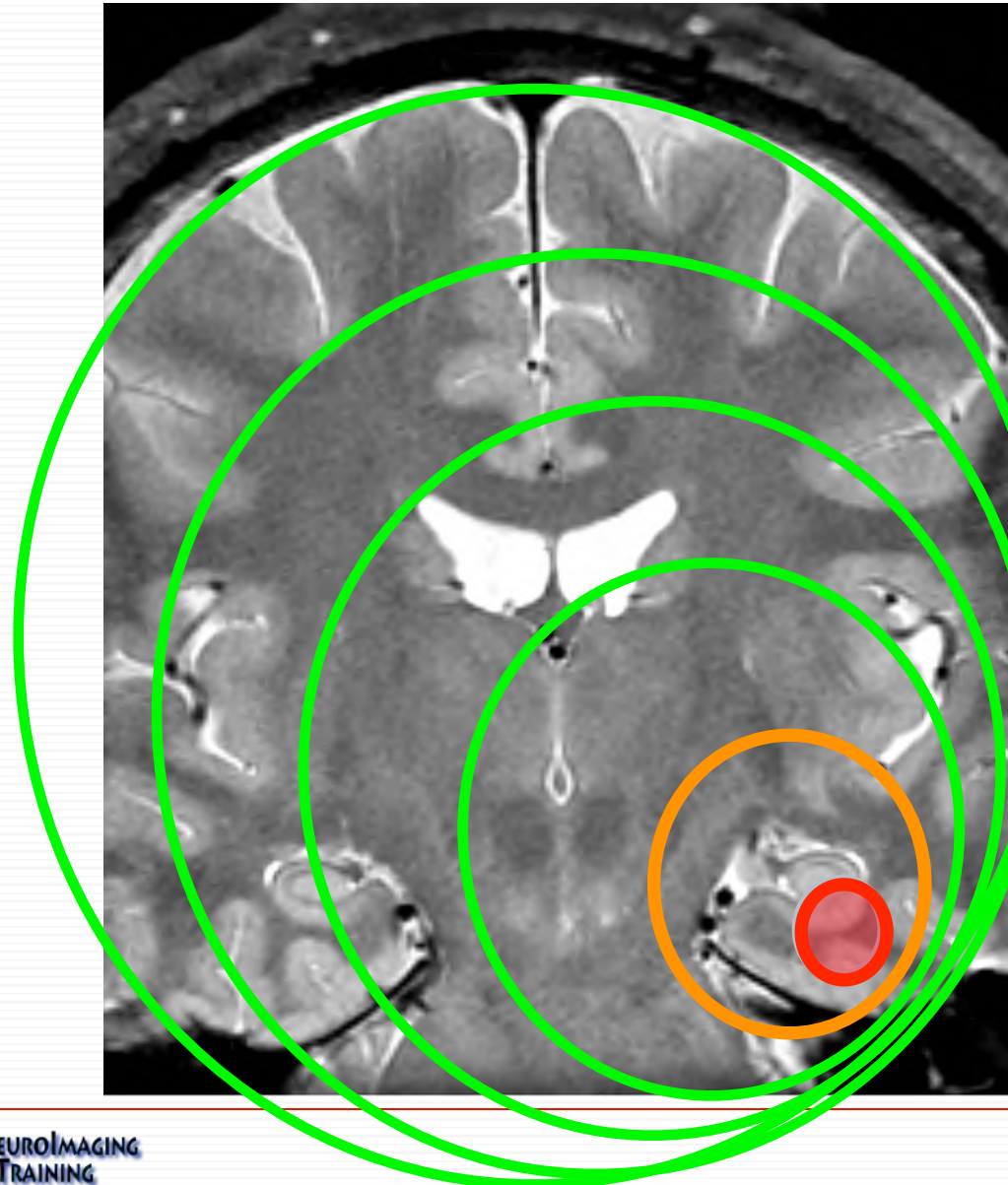
Surgical Treatment is probably the best first line treatment

Source: Wiebe, et al., NEJM, Engel (UCLA), others

Determination of Resectable Region is the Major Challenge!



Red and Green Spikes



Seizure Activity Spreads from an Irritative Zone

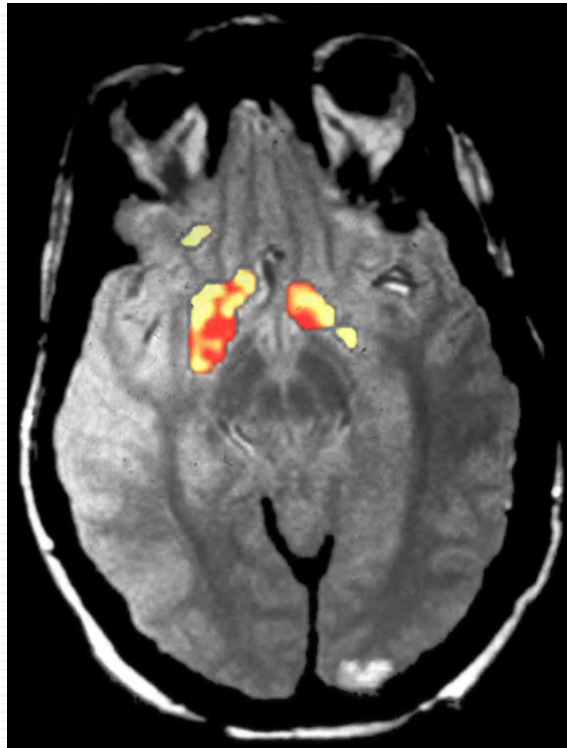
Hypotheses:

- Initial Event is Energetically Costly
- Spreading Depolarization is Not

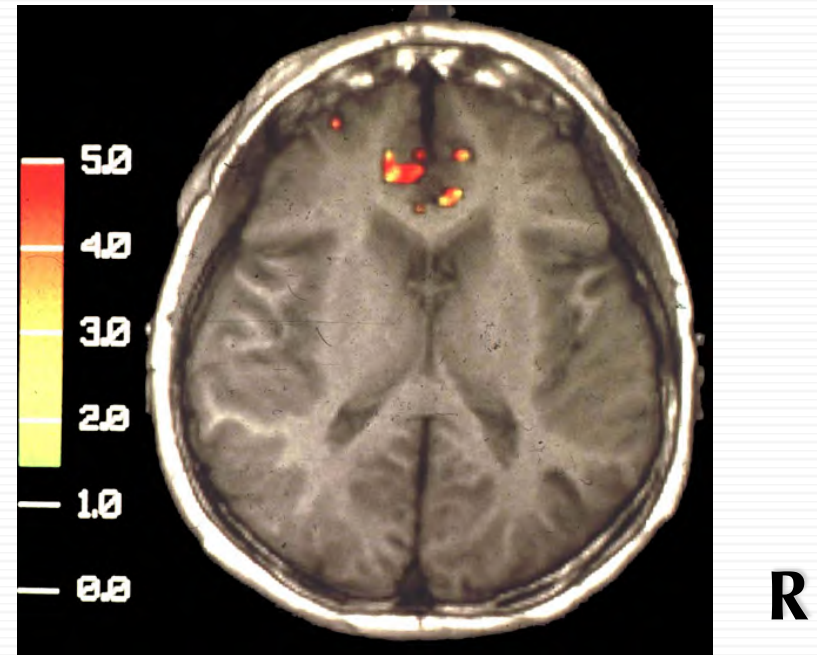
Functional MRI may be timed by Epileptiform Spikes



Spike-Triggered fMRI



- Complex partial seizures, rare generalization
- EEG: generalized interictal discharges, some with left temporal onset
- MRI: normal

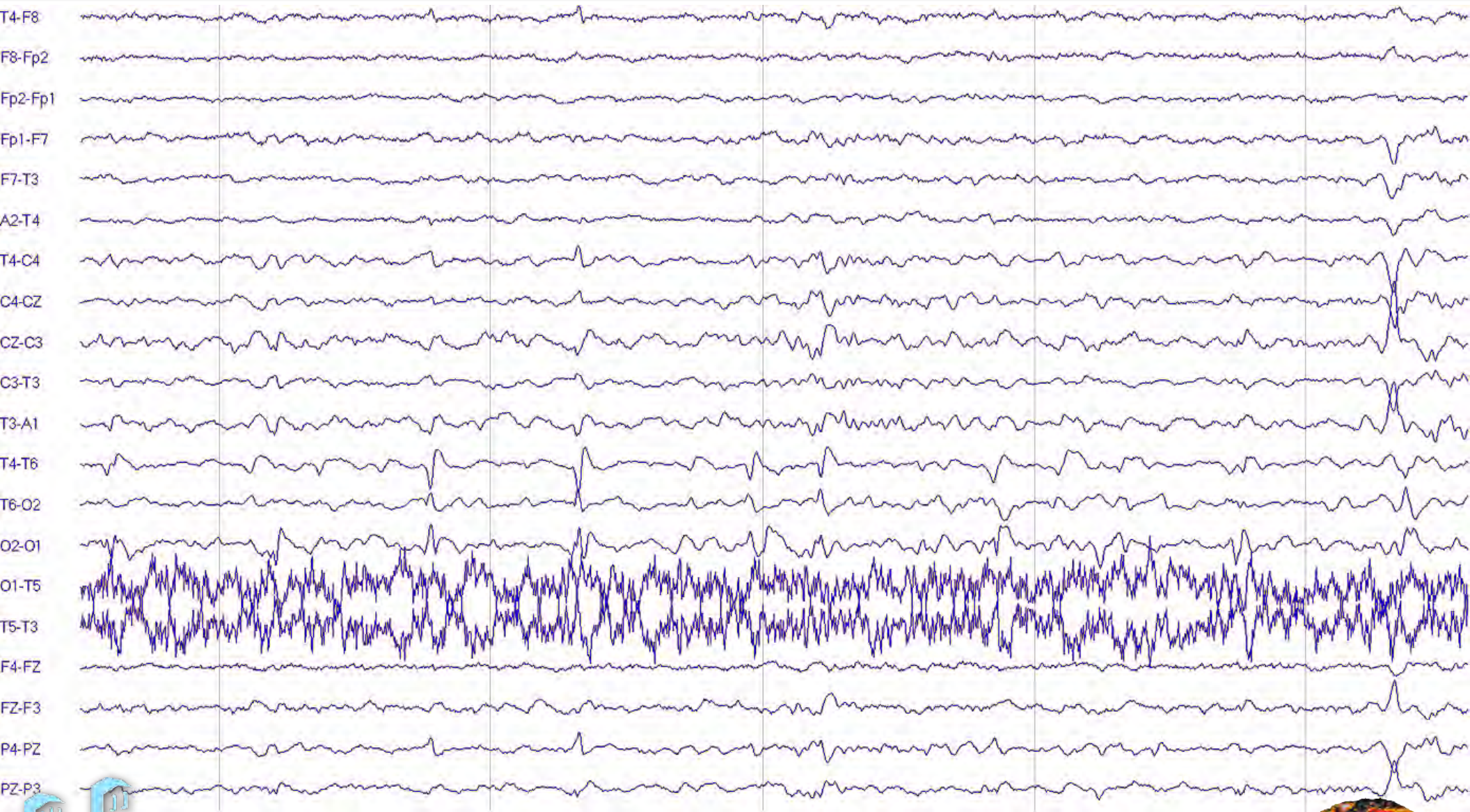


- Complex partial seizures, occasional generalization
- EEG: multifocal and generalized interictal discharges
- MRI: symmetric subependymal heterotopias

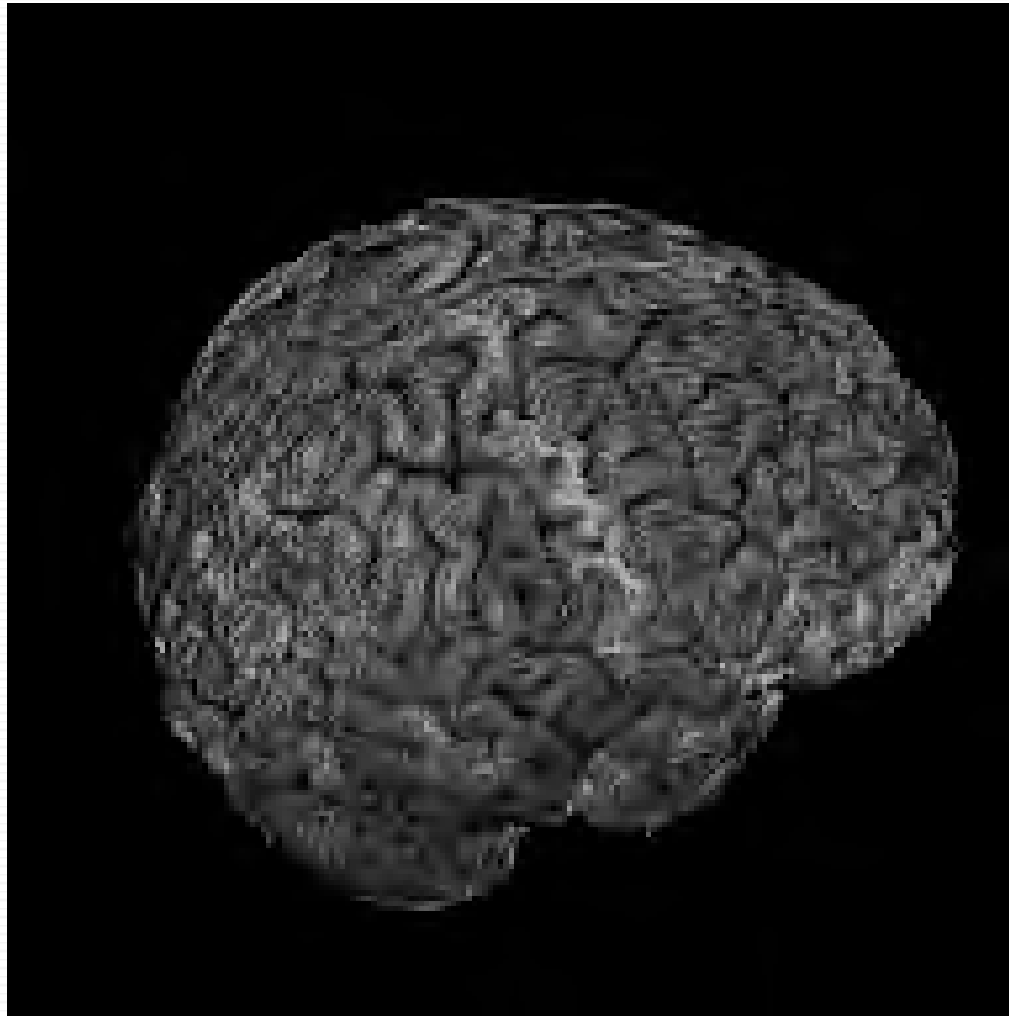
Warach, et al. (1996)



Interictal Discharge



IED Time Course



with
John Stern
Alex Korb
Manjar Tripathi
Massoud Akhtari



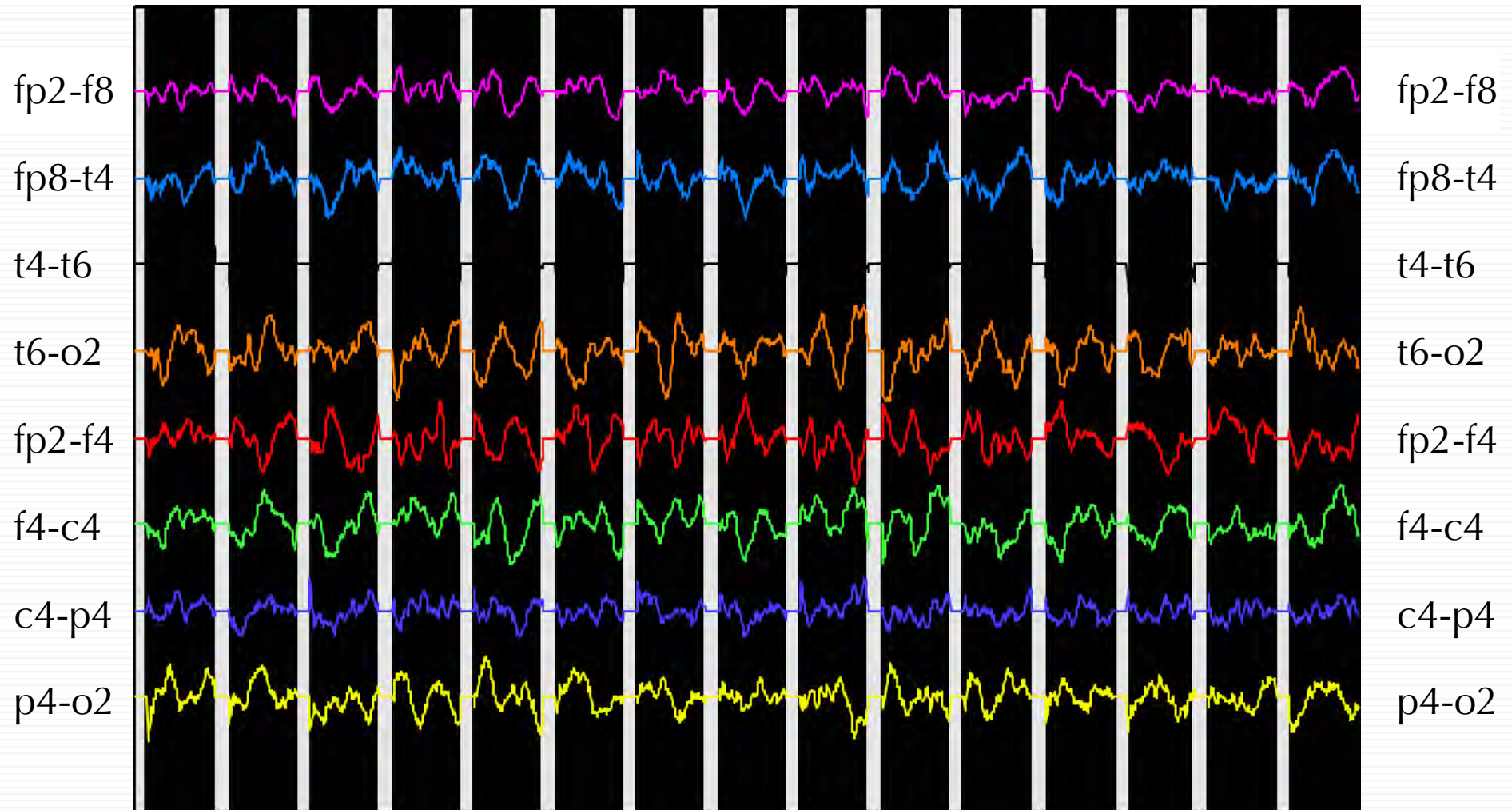
State Measurements

EEG may be the best available measure of state:

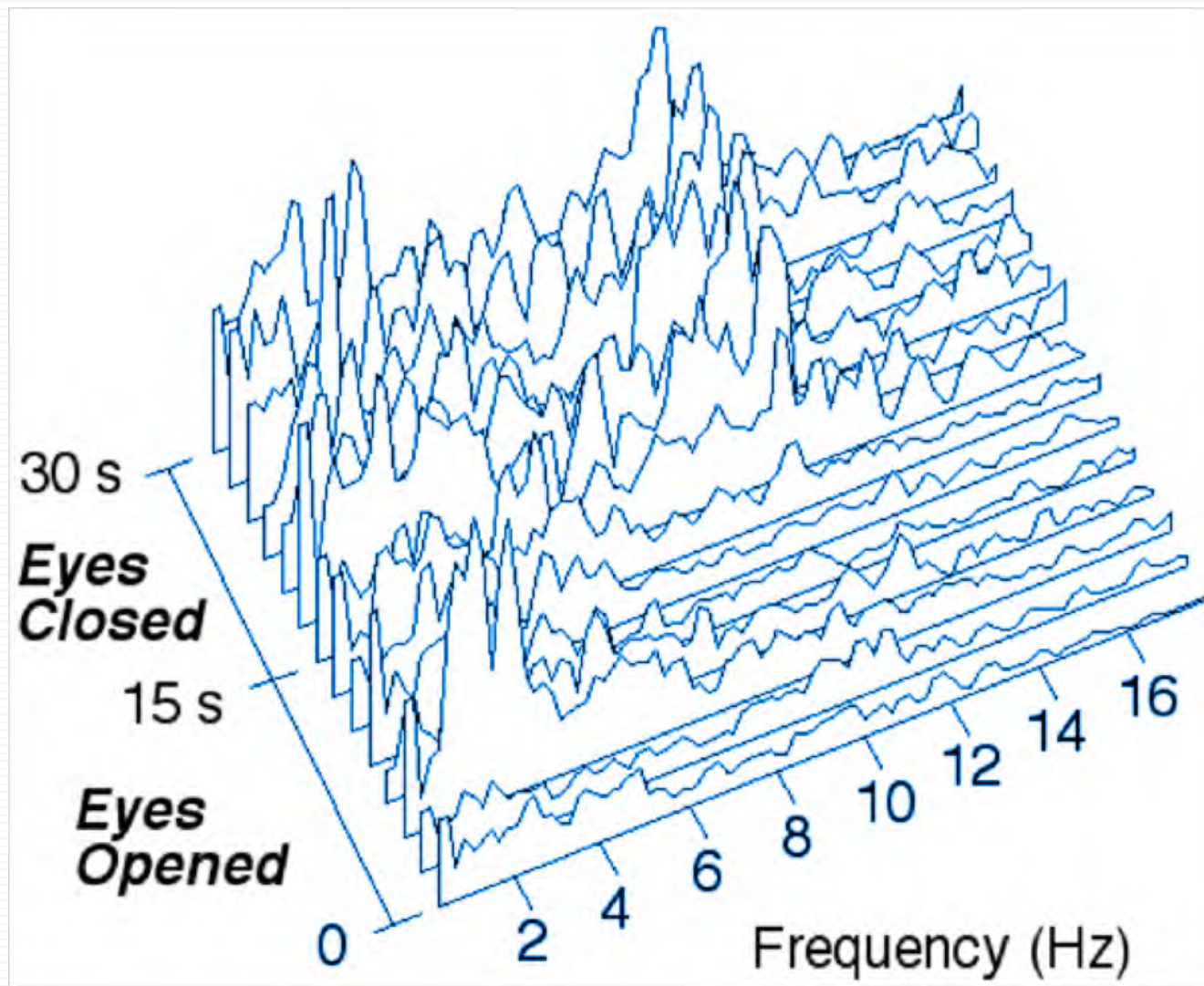
- ✓ Sleep
- ✓ Attentiveness
- ✓ Arousal
- ✓ Responsiveness



EEG during Sleep (corrected)



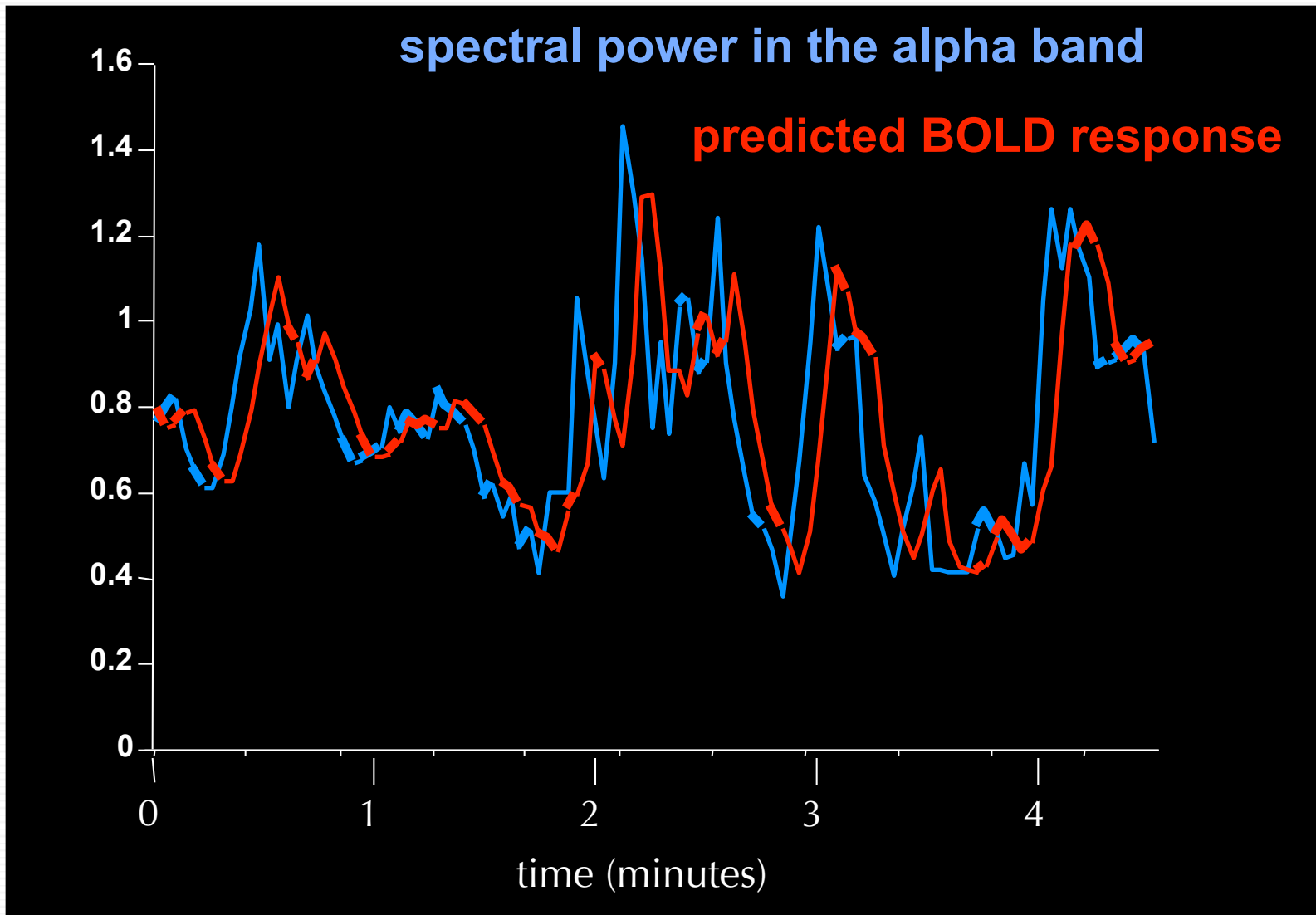
EEG Spectral Content



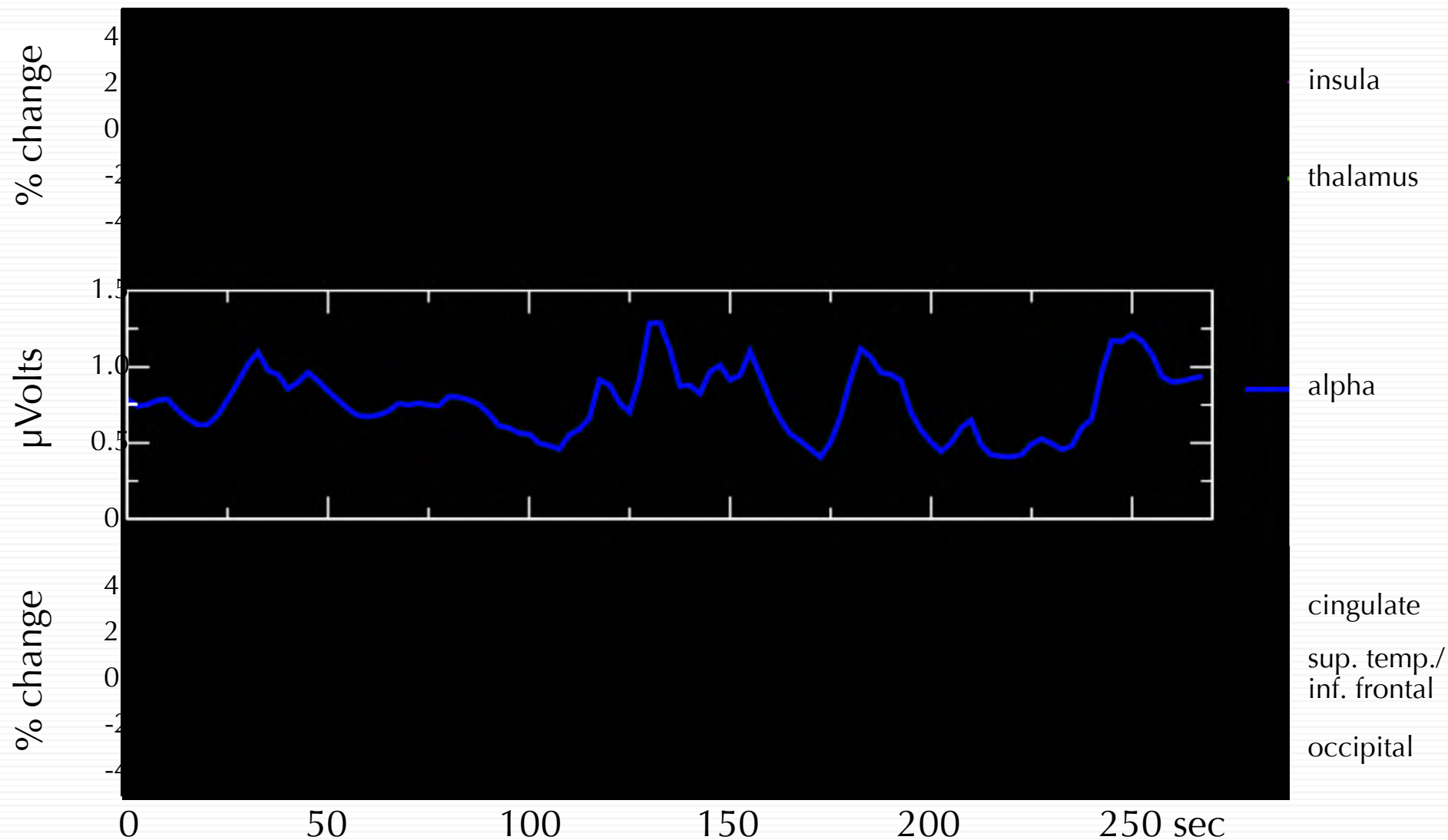
Goldman, et al., Clinical Neurophysiology, 2000



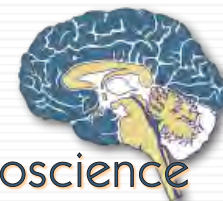
Alpha Mapping



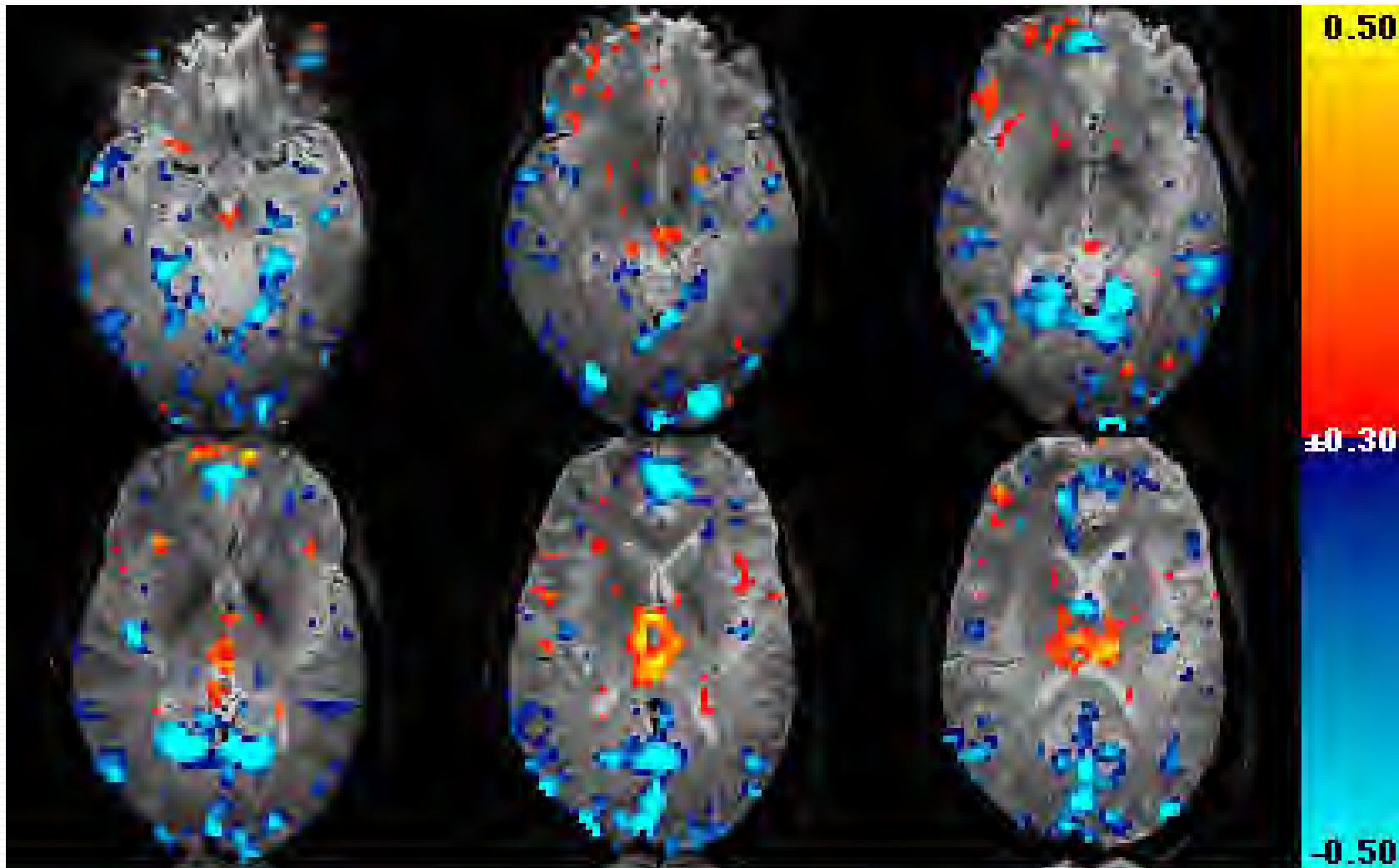
Alpha Rhythm and BOLD



Goldman (2002) NeuroReport
13(18):2487



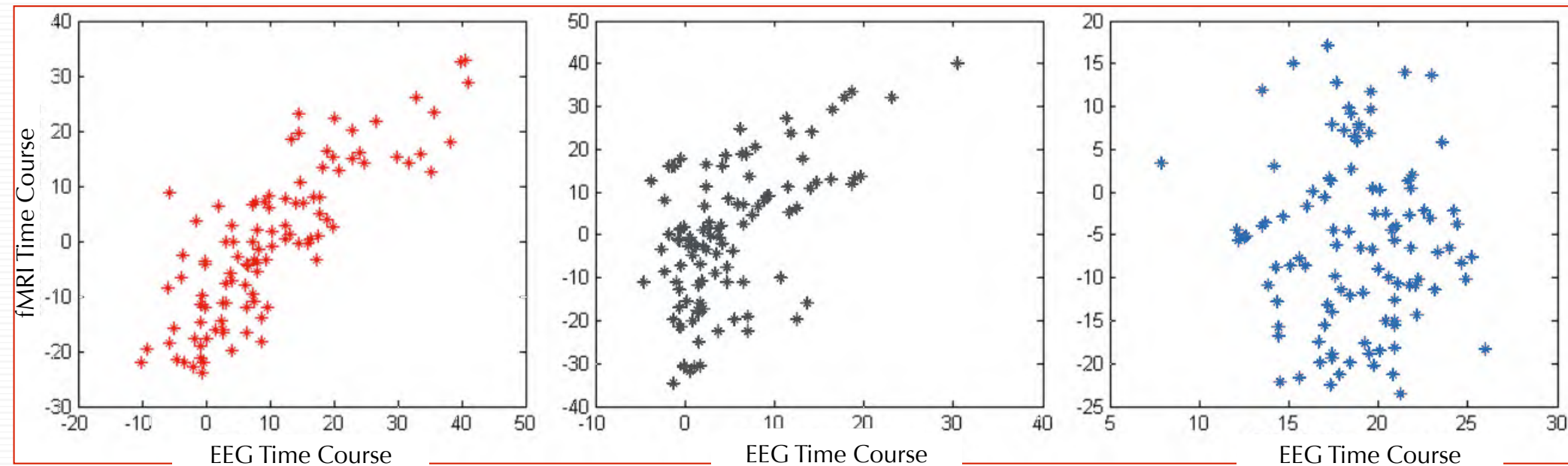
Alpha Tomograms



Goldman (2002) NeuroReport
13(18):2487



Correlation of EEG and fMRI data



Alpha

$$r^2 = 0.83$$

$$p < 0.05$$

Theta

$$r^2 = 0.56$$

$$p \approx 0.07$$

Gamma

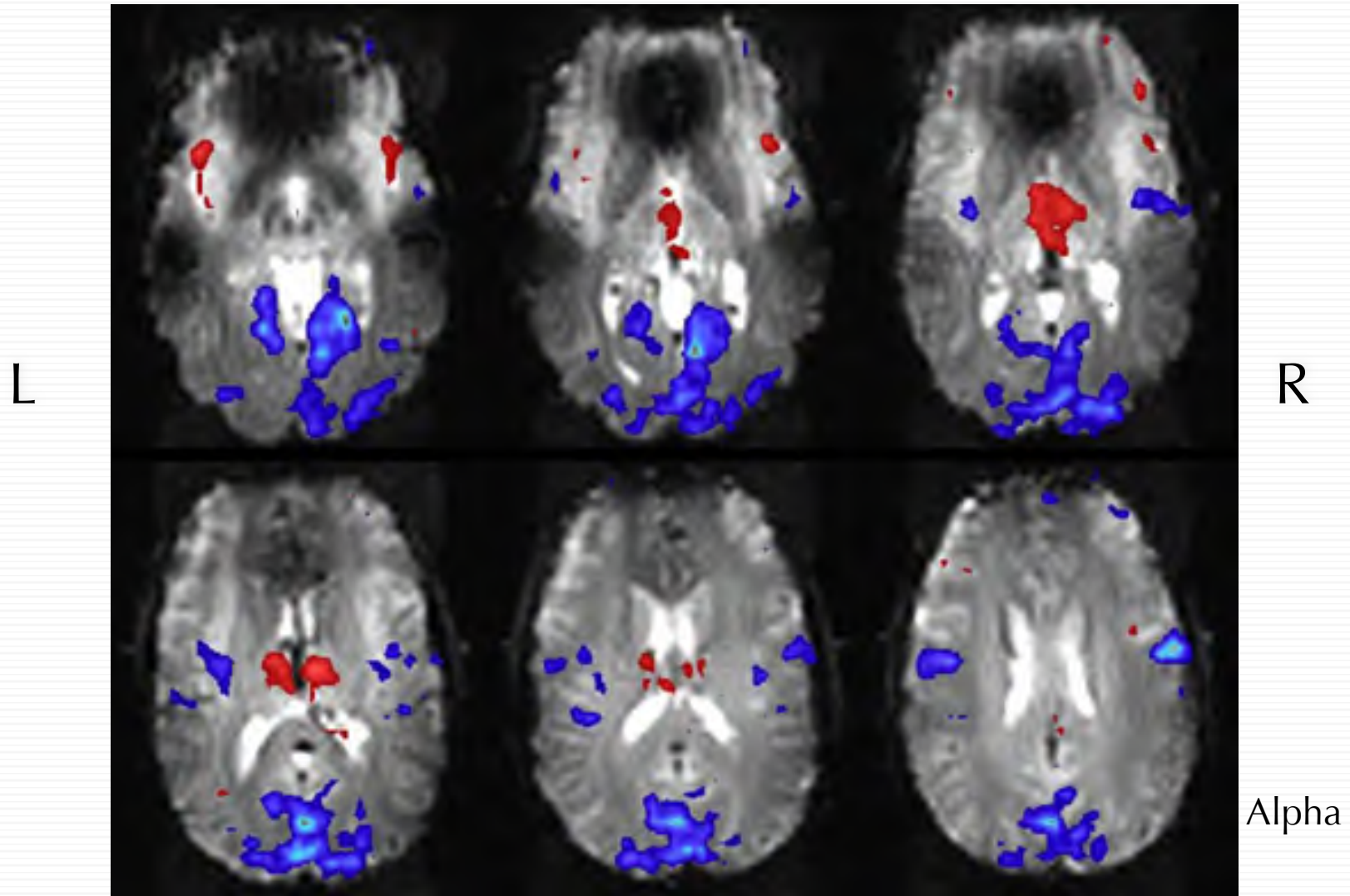
$$r^2 = -0.03$$

$$p = \text{n.s.}$$

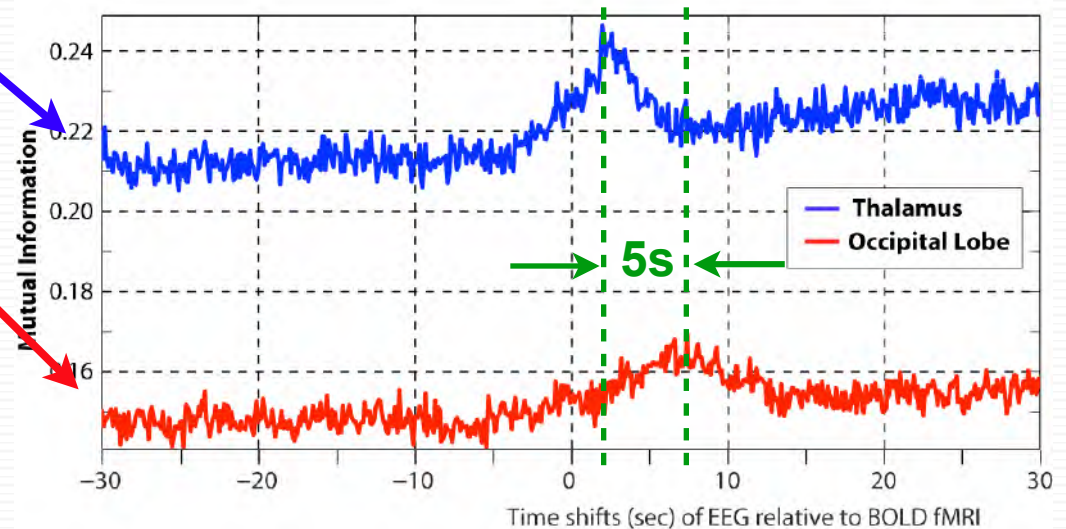
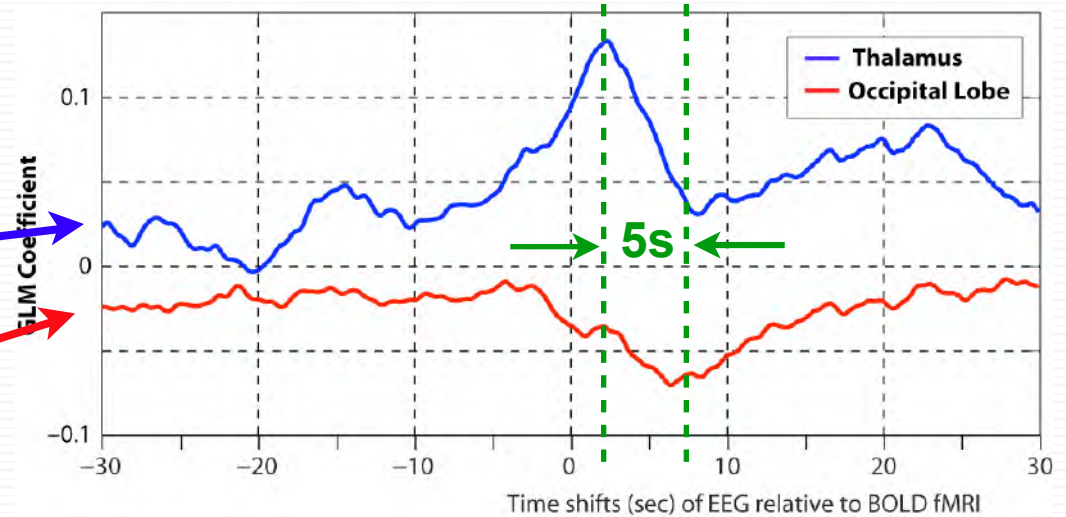
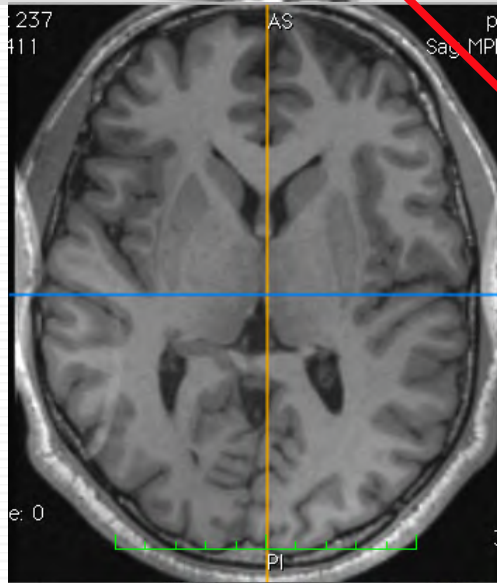
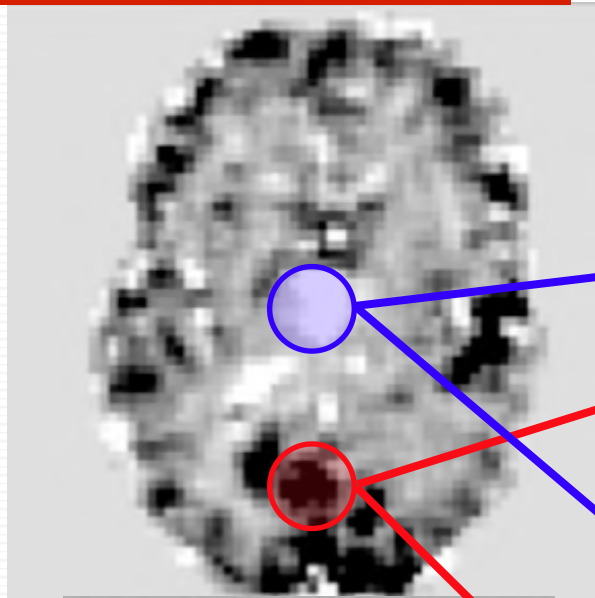
E. Martinez-Montes, et al., NeuroImage 22:1023-34, 2004



JackKnife pseudo t-image



EEG-fMRI Coupling - A Variety of Mechanisms?

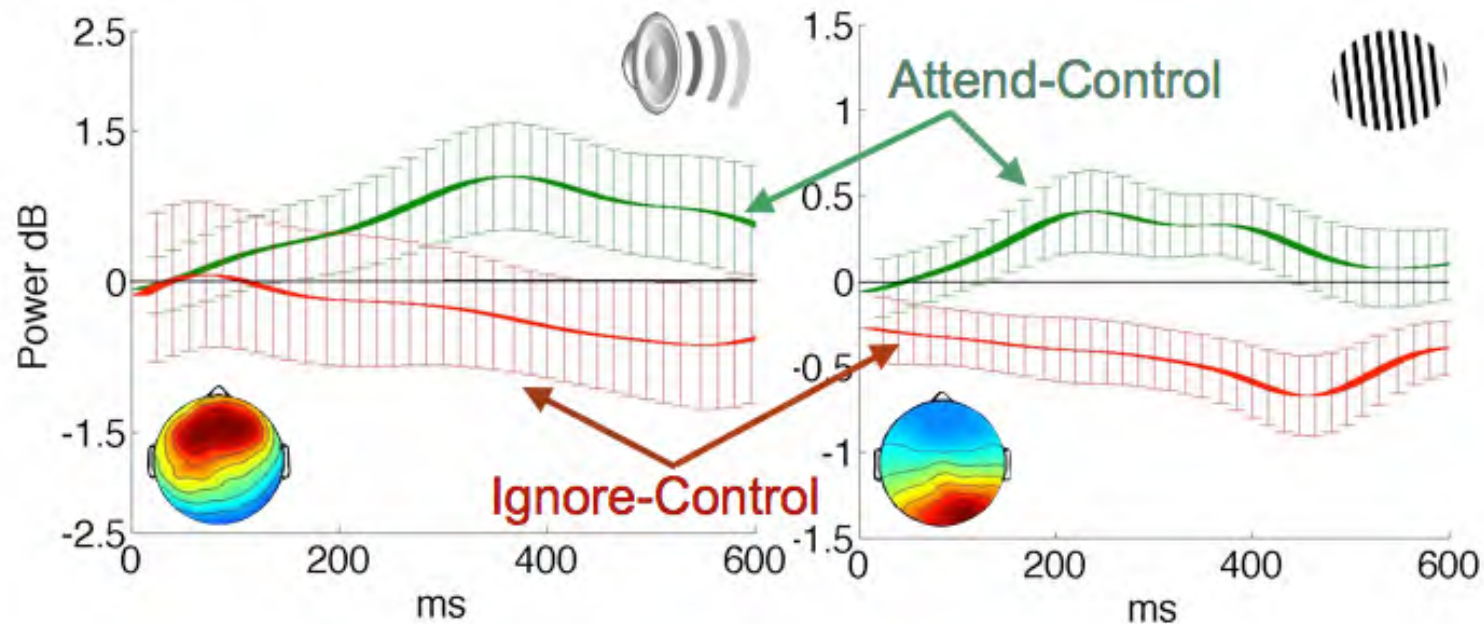


Xia Hongjing
Organization for Human Brain Mapping 2012



States of Attention

Theta (4-7Hz)



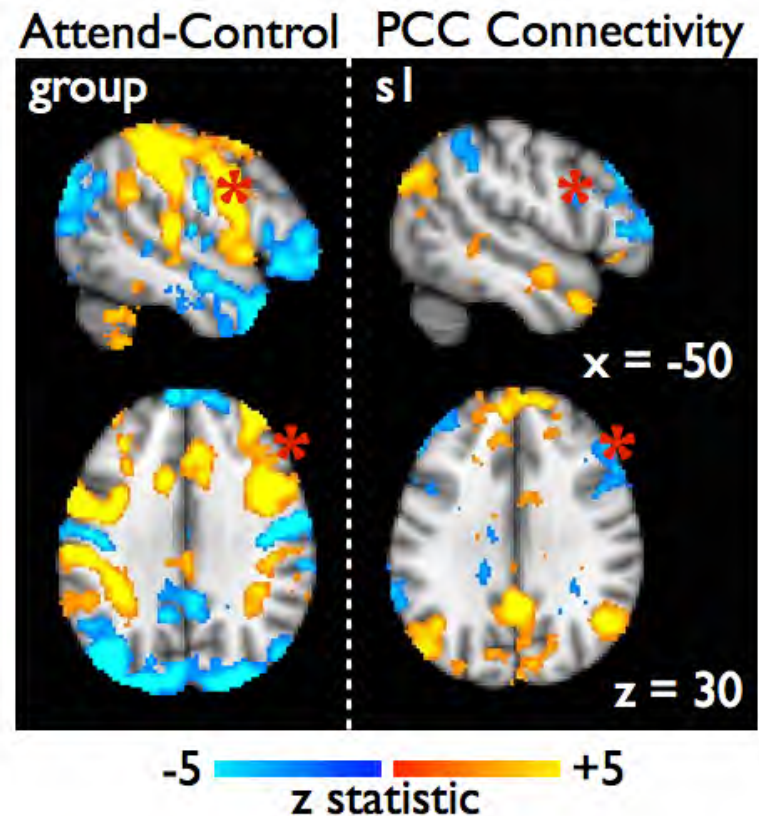
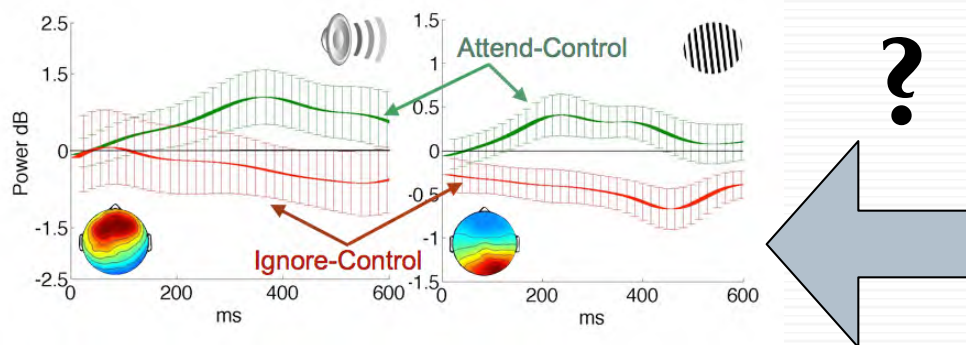
- attention comprises enhancement of attended signals and suppression of ignored signals
- spatio-temporally distinct EEG signatures can be calculated for attended and ignored signals in both auditory and visual modalities
- these can be tracked across trials to assess focus and distractibility

Agatha Lenartowicz
Work in Progress



States of Attention

- How are the EEG traces of attending and ignoring affected by activity in critical neural networks such as fronto-parietal (FPN) & default mode (DMN), and their interactions?

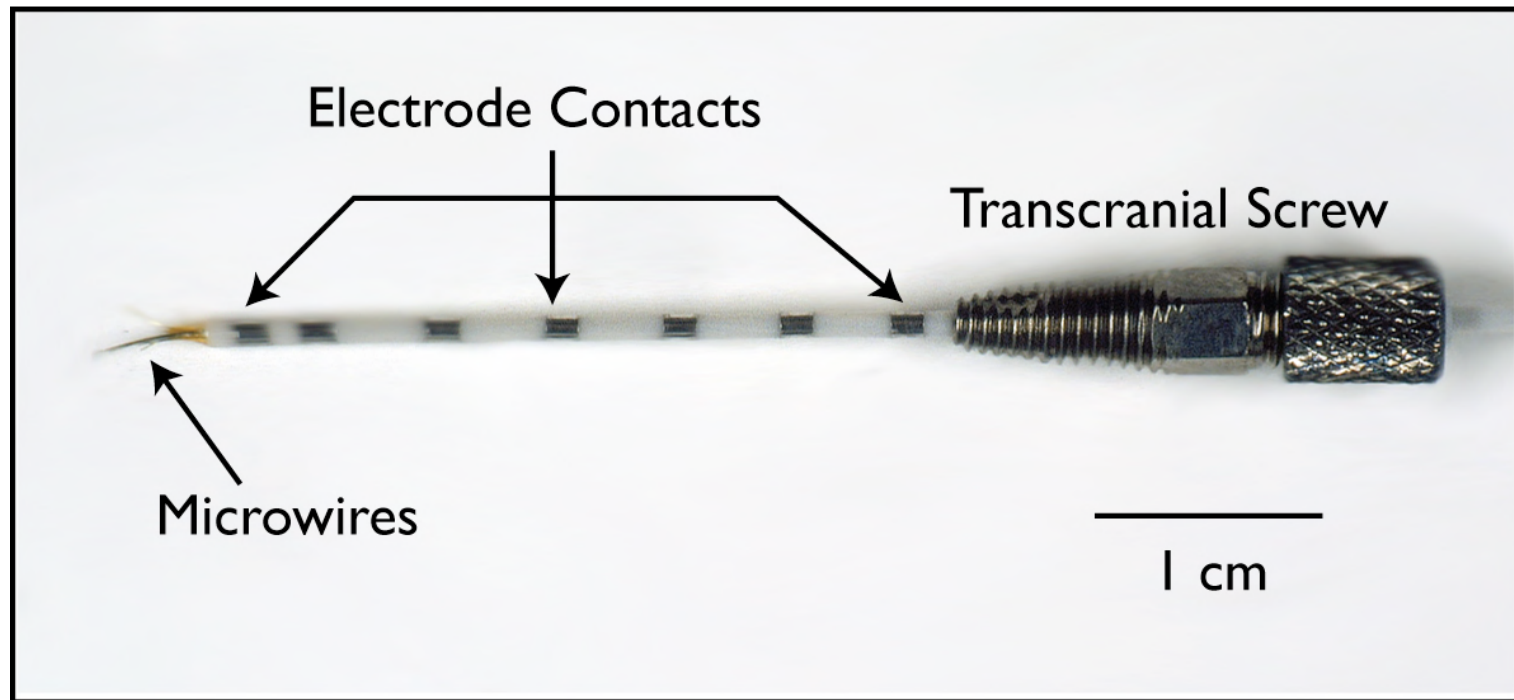


- Answering this question will allow us to neurally dissociate attention states - such as fatigue, distractibility and mind-wandering.

Agatha Lenartowicz
Work in Progress



Application

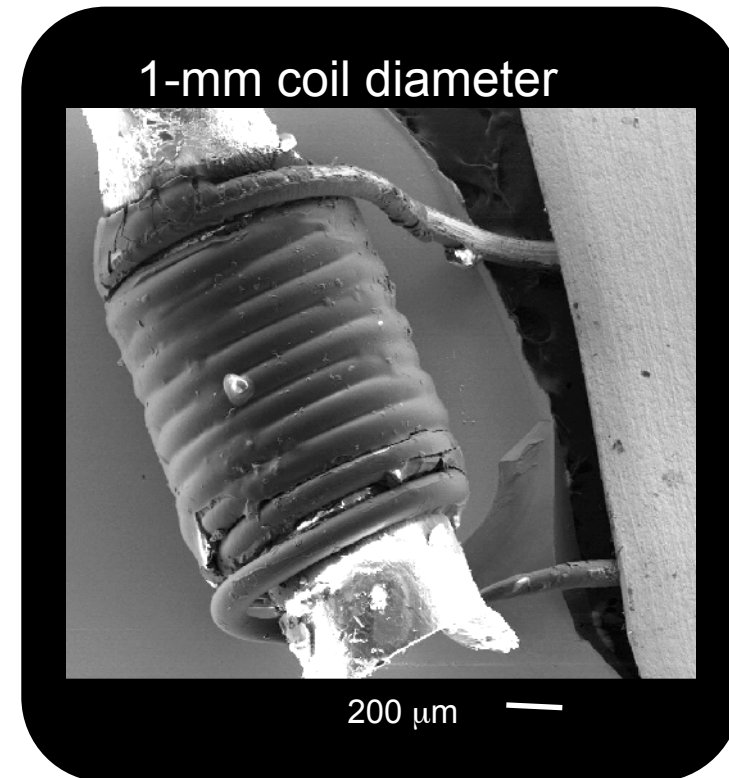


- **Temporal-Lobe Epilepsy Depth Electrode and Microwire Array**

Strick, *et al.*, *Society for Neuroscience*, 2007

Objectives

- **Design pick-up coil to integrate with depth electrode**
 - Potential:
 - Microscopic imaging
 - Small-volume spectroscopy
 - 1 mL → 1/1000 mL
- **Investigate depth electrodes**
 - Established heating experiments
 - Rare resonant-frequency characterization



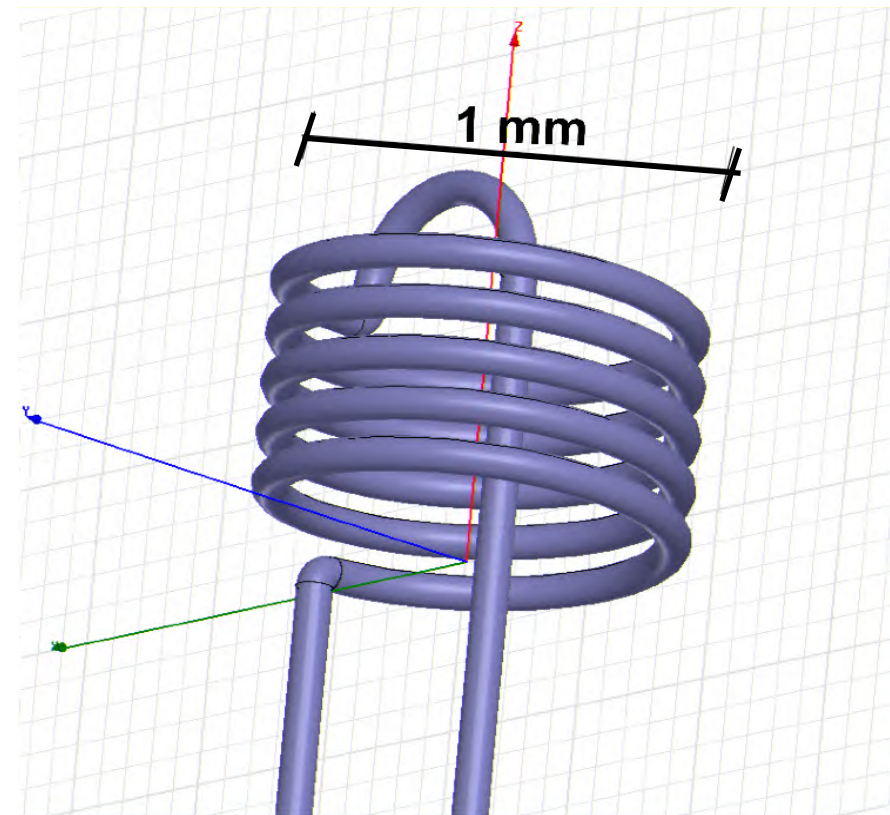
Strick, *et al.*, *Society for Neuroscience*, 2007

Novel Implantable Design

- Small diameter < 2 mm
- Prioritize homogeneity magnetic flux density
- Orthogonal to static magnetic field
- $f_{\text{coil}} > 3 \cdot f_{\text{operating}}$
- Maximize

$$Q = \frac{(2 \cdot \pi \cdot f_{\text{operating}}) \cdot L}{R}$$

f = frequency, L = inductance,
 R = resistance

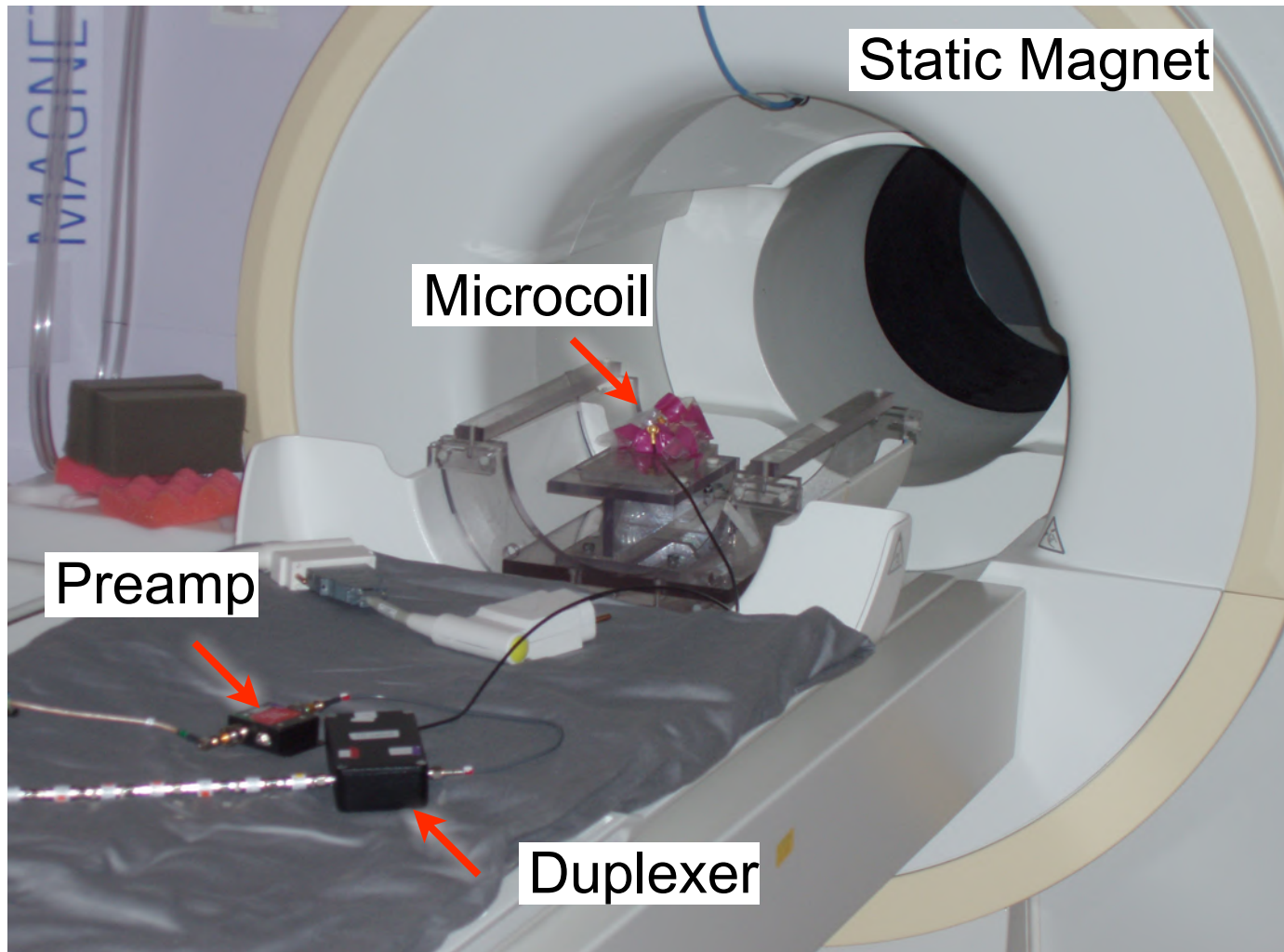


Transform NMR microcoil into implantable design

NOVEL: INTRACRANIAL MRI MICROCOIL

Strick, *et al.*, *Society for Neuroscience*, 2007

Imaging Set-up



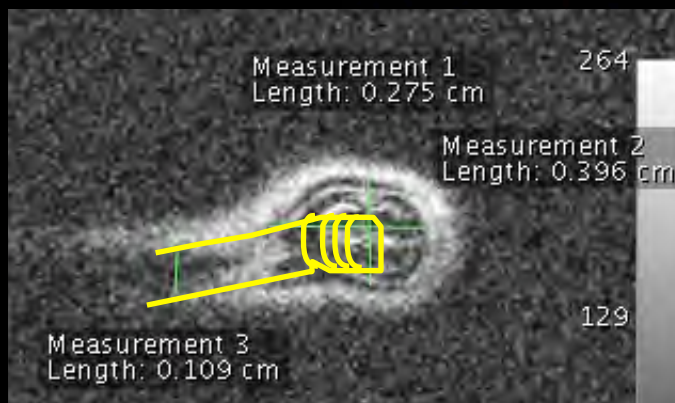
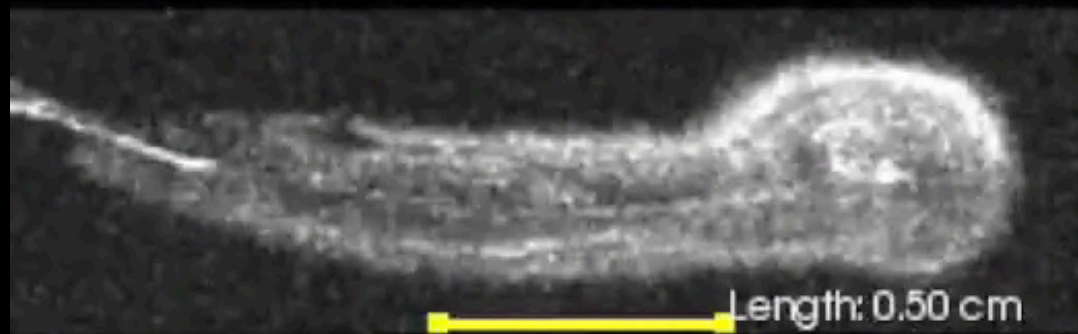
Lewis Center for Neuroimaging, University of Oregon

Strick, *et al.*, *Society for Neuroscience*, 2007

Experimental Results

3-Tesla Magnetom Allegra (Siemens, Erlangen, Germany)
Butcher-grade *Ovis aries*

Turbo Spin Echo, TR/TE 4000/22 ms, slice 0.4 mm, FOV 26 × 25 mm, 256 × 256



Strick, *et al.*, *Society for Neuroscience*, 2007

Experimental Results

Gradient Echo, TR/TE 123/48 ms, FOV 22 × 14 mm, 640 × 1024,
slice thickness 0.14 mm, NEX 4

3-Tesla Magnetom Allegra (Siemens, Erlangen, Germany)
Butcher-grade *Ovis aries*



Strick, *et al.*, *Society for Neuroscience*, 2007